國立臺灣大學生物資源暨農學院生物科技研究所

博士論文

Institute of Biotechnology
College of Bioresources and Agriculture
National Taiwan University

Doctoral Dissertation

幹細胞療法在肝臟疾病的應用

Stem Cell Therapy for Liver Diseases

黃郁蓁

Yu-Jen Huang

指導教授：李宣書 博士

吳耀銘 醫師

Advisor: Hsuan-Shu Lee, M.D./Ph.D.

Yao-Ming Wu, M.D.

中華民國 105 年 1 月

Jan 2016

國立臺灣大學博士學位論文
口試委員會審定書

幹細胞療法在肝臟疾病的應用
Stem Cell Therapy for Liver Diseases

本論文係黃郁蓁君（D98642004）在國立臺灣大學生物科技學系、所完成之博士學位論文，於民國 105 年 1 月 13 日承下列考試委員審查通過及口試及格，特此證明

口試委員：李宣書（簽名）

（指導教授）

誌謝

誠摯的感謝論文指導委員 林淑華老師、黃敏銓老師、宋麗英老師、李宣書老師、吳耀銘老師使本論文更趨於完善。感謝我的兩位指導老師李宣書老師與吳耀銘老師的教導。謝謝李宣書老師的悉心指導並不時給予幫助與關懷。在這七年多的日子裡，特別的感謝吳耀銘老師，老師提供了我科學研究的學習環境與知識和觀念上的啟發，同時也給予我思想與人生道路上的啟發，並且讓我可以在家庭與學業上可以兼顧，也因為有吳耀銘老師的協助與指導才能讓我完成我的博士學位。這麼長的日子來，感謝秀霞學姐在我緊急狀況下總是來幫我想法子，謝謝玉真不只在實驗上給我指引更是陪我話家常、謝謝亭喻在我煩悶時總是很理性分析並給我建議，謝謝心妤、惠宣、世紋不只實驗協助還有吃喝玩樂你們全包了，謝謝李志元醫師不間斷的給我寶貴的意見，謝謝陳博達醫師在我完成論文之前給予我英文上的協助，謝謝博士班的同學五百、佳佳、為芳、居凡、餃子學姐、小巫學長、鬍鬚學弟，脫線的我要謝謝你們總會提醒我並給予我幫助，雖然每次去上課車程總有一點點的小距離，但是每次去上課總可以讓我心情愉悅。感謝生我養我的爸爸媽媽，還有我最愛的兒子，你們是我生活上的一帖良藥。最後謝謝犧牲生命的老鼠，有你們才能完成科學的研究。

謝謝

郁蓁 105.01

摘要

細胞移植 (cell transplantation) 可以取代器官移植 (organ transplantation) 成為器官衰竭病人的第一治療選擇。不管在動物實驗或臨床上肝細胞移植 (hepatocyte transplantation) 已被證明可用來治療多種不同的肝臟疾病。然而肝細胞移植的發展仍需克服肝細胞來源短缺以及異體排斥的問題。幹細胞移植近年來被應用在許多疾病上並且具有治療的可行性。因此，幹細胞療法 (stem cell therapy) 有可能成為協助治療肝臟疾病的新選擇。目前幹細胞被應用於動物實驗與臨床試驗做為修補和組織再生之用途。本論文利用誘導性全能幹細胞 (induce pluripotent stem cells, iPSCs) 的分化潛能獲得具有功能性的肝細胞以及網膜脂肪幹細胞 (adipose stem cells, ASCs) 做為細胞移植的細胞來源，並分別移植到不同類型的肝臟疾病-第九凝血因子 (clotting factor IX, FIX) 剔除之B型血友病 (hemophilia B, HB) 的基因缺陷的疾病模式與乙醯胺酚 (acetaminophen, APAP) 引起的急性肝臟衰竭 (acute liver failure, ALF) 的動物模式分別探討其治療潛能性。誘導性全能幹細胞具有與胚胎幹細胞 (embryonic stem cells, ESCs) 相同特質，並且具有可分化成特定細胞的能力。在體外誘導條件下將誘導性全能幹細胞分化成具有功能性的肝細胞並進一步去探討其細胞對於基因缺陷肝臟疾病的治療效果。結果顯示來自誘導性全能幹細胞分化而成的肝細胞具有肝臟的主要功能，包含合成血清白蛋白 (albumin) 與尿素 (uric acid)、代謝功能並儲存肝醣 (glycogen) 能力。將此細胞移植到第九凝血因子剔除之B型血友病小鼠後可在宿主的血清中偵測到第九凝血因子活性並改善凝血能力且可嵌入 (engraftment) 宿主的肝臟組織中。因此，來自於誘導性全能幹細胞所分化的肝細胞可提供做為細胞移植的細胞來源並做為基因缺陷肝臟疾病的新治療選擇。再者，從網膜脂肪組織去提取脂肪幹細胞並探討其細胞對於急性肝衰竭的治療潛力。網膜脂肪幹細胞做為細胞移植的來源可以明顯改善急性肝衰竭動物的死亡率並且抑制細胞色素P450 (cytochrome P450) 表現，進而減少硝基酪氨酸 (nitrotyrosine)的堆積並同時提高NF-E2-related factor 2 (Nrf2)的表現進而減低乙醯胺酚的毒性傷害達到保護肝臟。綜合上述實驗結果顯示幹細胞療法提供肝臟疾病治療的新契機。

關鍵詞: 細胞移植、器官移植幹、幹細胞療法、誘導性全能幹細胞、網膜脂肪幹細胞、第九凝血因子、血友病B型、乙醯胺酚、急性肝臟衰竭。

Abstract

Cell transplantation are expected to replace the whole organ transplantation as the first therapeutic choice for patients with organ failure. Hepatocyte transplantation has been proved with the ability of treating a wide variety of liver disease in both animal experiments and clinical studies. However, the hepatocytes shortage and allograft rejection remained unsolved during the development of hepatocyte transplantation. On the other hand, stem cell therapy has been shown to have the therapeutic potential in many kinds of diseases, and the autograft of stem cell is suggested as the key of organ shortage and allograft rejection. Therefore, the stem cell transplantation is gathering the attention with the potential of being the next therapeutic strategy for liver diseases. For the reason, various cell types have been tried, whether in animal models or in clinical trials, to repair or regenerate the damage tissue. In this dissertation, we allowed hepatocyte-like cell derived from induce pluripotent stem cells (iPSCs) and adipose stem cells (ASCs) generated from omentum adipose tissue as the candidates, and addressed their therapeutic potential in inherited diseases-hemophilia B and acute liver failure (ALF) induced by acetaminophen (APAP), respectively. iPSCs, shared some characteristics with the ESCs, have been demonstrated with the capability of differentiating into different somatic cells. However, whether hepatocytes differentiated from iPSCs is functioning with the therapeutic efficiency of genetic liver disease, the hemophilia B disease (factor IX knockout mice model), has never been proved. Our data showed that iPSCs derived hepatocytes shared many characteristics with hepatocytes, including albumin synthesis, metabolic capacity, glycogen storage, and ureagenesis. In fact, iPSCs-derived hepatocytes transplantation led to increased coagulation factor IX activity, improved thrombus generation, and better hemostasis parameters, moreover, the transferred cells were localized in the liver in recipient HB mice. As a result, hepatocyte-like cells derived from iPSCs is suggested to be a potential cell source for cell-based therapy in the treatment of HB. Another study is about the therapeutic potential of omentum derived adipose stem cells in APAP-induced ALF. We successfully acquired

the ASCs from omentum adipose tissue, and proved the antioxidant activity of the candidate. Our data showed that ASCs transplantation significantly improved the survival rate of mice with ALF, and attenuated the severity of APAP-induced liver damage by suppressing cytochrome P450 activity. Following the activity, the cell reduced the accumulation of toxic nitrotyrosine and the upregulation of NF-E2-related factor 2 (Nrf2) expression, and in sequential resulted in the increase of antioxidant activity. Taken together, our results suggested the stem cell therapy is an opportunity to open up entirely new perspectives for treatment of severe liver diseases.

Key words: Cell transplantation, Organ transplantation, Stem cell therapy, induce pluripotent stem cells, Omentum adipose stem cells, Clotting factor IX, Acetaminophen, Acute liver failure

CONTENTS

List of Tables

List of Figures

Abbreviations

Acetaminophen, APAP

Acute liver failure, ALF

Adipose derived stem cells, ASC

Carbon tetrachloride, CCl4

Clotting factor IX, FIX

Clotting factor VIII, FVIII

Coagulation index, CI

Cytochrome P450 subfamily 2E1, CYP2E1

Dulbecco's modified Eagle's Medium, DMEM

Embryonic stem cell, ESC

Fetal bovine serum, FBS

Glucuronosyltransferase 1A1, UGT1A1

Glutathione peroxidase, GPx

Glutathione, GSH

Hank's balanced salt solution, HBSS

Hemophilia A, HA

Hemophilia B, HB

Hepatocyte growth factor, HGF

Hydroxyl radicals, OH·

Indocyanine green, ICG

Induced pluripotent stem cell, iPSC

Insulin–transferrin–selenium, ITS

Iscove's modified Dulbecco's Medium, IMDM

Leukemia inhibitory factor, LIF

Mesenchymal stem cell, MSC

Mesenchymal stem cells, MSCs

Monocrotaline, MCT

N-acetyl-p-benzoquinoneimine, NAPQI

Periodic acid–Schiff, PAS

Reactive oxygen species, ROS

Real-time quantitative PCR, QPCR

Reverse transcription-polymerase chain reaction, RT-PCR

Superoxide dismutase, SOD

Superoxide, O_2^-

Thromboelastography, TEG

Chapter 1

Literature Review

1-1 Introduction

Liver is one of largest and most complex organs in human body, with responsibility of detoxification, protein synthesis, and regulation of glycogen storage. Liver failure is defined as the loss of liver function with the life-threating condition. Although liver transplantation is an effective choice for end-stage liver disease, organ shortage remained the greatest challenge in nowadays. For this reason, many studies have been tried to use cell therapy as an alternative strategy to replace or bridge organ transplantation. In this study, we summarize historical, current and future of cell therapy and liver transplantation in animal and clinical.

1-2 Liver transplantation

In 1963, Starzl tried the first human liver transplantation for a 3-years-old with biliary atresia, however, the patient died of coagulation disorder and uncontrolled bleeding during the surgery (Starzl TE, 1963). Until 1967, Starzl and Colorado succeed their first case for a patient with hepatocellular cancer, and helped the patient surviving more than 1 year with preserved liver function before passing with the malignancy recurrence (Starzl TE, 1968). For the increasing number of patients on the waiting list, transplantation of partial liver from living-related donors was established by Broelsch, and then performed successfully by Strong in 1990 (Strong RW, 1990). However, graft rejection remained a main problem after liver transplantation without immunosuppression agents. The survival rate increased dramatically from 30% to 50% since the cyclosporine-A was discovered (Calne RY, 1979). After the immunosuppressant, more than 1,000,000 liver transplantations have been performed in the world during the past 40 years (Meirelles Júnior RF, 2015).

Liver transplantation is an effective therapy for end-stage liver disease. The surgical procedure is to remove the dysfunctional liver and replace it with a healthy orthostatic or partial liver from another person. Although most donated livers come from decreased donors, the

living-related liver transplantation is accommodated as an alternative procedure in realizing that the graft liver can regenerate with normal size and function in recipient and the remaining liver can recovers in donor. However, the willing of donation is confined with immunologic matching, and the donor hepatectomy is a complex surgery with high risks and complications for a healthy candidate. Many people in need of liver transplantation would expire while waiting on the list. Despite the improvement of surgical technique and immunosuppression treatment, the gap of donor shortage and need of liver transplantation remained wide. Therefore, we are eager to have the resolution of organ shortage and the high waiting list mortality rate.

1-3 Cell therapy

Cell therapy is promising to treat and alter course of diseases, in which the living cell was used as therapeutic agent to improve or repair the damage organ. Cell therapy is considered as first-line treatment to replace organ transplantation for end-stage liver failure disease, or as bridge therapy to prolong waiting time on waiting list. Most cell therapies are in the experimental stage, and only hematopoietic stem cell transplantation has become the routine clinical procedure for bone marrow regeneration. Over the past decade, multiple candidate cell types have been tried in liver diseases, including hepatocytes, embryonic stem cells (ESCs), induced pluripotent stem cells (iPSCs), adult stem cell, and hepactocyte-like cells. Although an ideal cell source for cell therapy are not emerged, considerations should be taken as follows: (1) Safe, (2) improve or repair organ function, (3) integrated in recipient organ, (4) minimally invasive delivery method for clinical application, (5) be “off the shelf” available as a standardized reagent, (6) be tolerated by the immune system, (7) no ethical concerns (Malliaras K and Marbán E, 2011).

1-3-1 Hepatocyte transplantation

Hepatocyte transplantation is a promising alternative therapy for the liver diseases. A number

of animal and clinical experiments have shown that the hepatocyte transplantation could replace damage hepatocyte and improve liver function. In 1970, first hepatocyte transplantation was performed by Rugsta. He transplanted the hepatoma cell line to rare inborn metabolic disease, the deficiency of the hepatic enzyme uridine diphosphoglucuronate glucuronosyltransferase 1A1 (UGT1A1), and then demonstrated UGT1A1 enzyme activity was expressed in the recipient rat and functioned with improving hyperbilirubinemia. (Rugsta HE, et al., 1970). In 1976, Matas et al further demonstrated primary hepatocyte transplantation can ameliorate metabolic liver disease in Gunn model. (Matas AJ et al., 1976). Finally in 1977, the true first hepatocyte transplantation was performed by Groth et al, which resulted in 40 % decrease of serum bilirubin by only 0.2% liver mass transplantation (Groth CG et al., 1977). The first successful clinical hepatocyte transplantation in child with Crigler-Najjar disease was performed by Fox et al. (Fox IJ et al., 1998). Thereafter, hepatocyte transplantation has been expected for regeneration of the unhealthy liver and prolongation of waiting time for a suitable liver donation. Hepatocyte transplantation has less invasive and lower morbidity and mortality compared to organ transplantation. More importantly, with hepatocyte transplantation, one donated liver can provide enough cells for several patients. However, hepatocyte transplantation still has some obstacle, such as the cells number was varied, quality, metabolic, and functional activity. Nevertheless, isolated hepatocytes can be cryopreserved for emergency transplantation, it highly susceptible to the freeze-thaw process, and reduced functional activity after cryopreservation. (Yagi T et al., 2001). Admittedly, optimal cryopreservation technique and new cell source are needed to supplement for cell therapy on liver diseases.

1-3-2 Stem cell therapy

Stem cell therapy is a promising alternative of cell therapy and has great potential to treat liver diseases. Stem cells, based on their high proliferative potential and ability of differentiating into any

cell type, led to repair or improvement of damage organ. Moreover, stem cell has been proposed as an ideal cell source for generating unlimited numbers of hepatocytes. Stem cells can be derived from different sources. According to the potency, they are classified into totipotency, pluripotency, and multipotency. Totipotent cells have the ability of developing into a complete organism or differentiating into all type of cells or tissues, such as zygotes and early cleavage stage blastomeres (Condic ML, 2014). Pluripotent stem cells have the potential to differentiate into all kinds of cells in the body, including ESC and iPSC. When totipotent cells start to specialize and form a blastocyst, the inner cell mass with pluripotency will differentiate into three-embryonic germ layers, including ectoderm, mesoderm, and endoderm. These pluripotent stem cells are different form totipotent stem cells because they don't develop into a complete organism. Multipotent stem cells have the basic properties of all stem cells but only differentiate into limited cell types.

1-4 Stem cells source for liver diseases

1-4-1 Pluripotent stem cells

Pluripotent stem cells have the potential to differentiate into specialized cells of the human body, but they can't be developed into complete organism. ESC and iPSC, as one of the pluripotent stem cells, are able to perform self-renewal and differentiate into all types of cell. ESC, as derived from the inner cell mass of embryo, may arise a significant ethical concern for their undifferentiated state with tumor-genesis problem. In addition, clinical applications of ESC are also limited due to the allogeneic rejection by the host immune system. The considerations mentioned above are overcame after iPSC was emerged in 2006. First, iPSCs are generated from somatic cell without ethical concern. Yamanaka et al. reported that somatic cell would reprogram into pluripotency through the introduction of transcription factor, including Oct4, Sox2, c-Myc and Klf4 (Takahashi, K and Yamanaka, S, 2016). These cells have similar great therapeutic potential as ESC, because they can be derived from patient's somatic cells to overcome the immune-rejection problem. Second,

although the pluripotentcy of iPSCs might result in tetratomas formation in host, modern research has shed significant light on cell therapy, disease modeling, personalized medicine, and drug toxicity screening (de Lázaro I et al., 2014; Robinton DA et al., 2012). Third, considerable evidences has been established to support the therapeutic potential of iPSCs in regenerative medicine, and numerous publications have been devoted to the study of iPS technology. In fact, with their wide differentiation potential, iPSCs have been used to generate somatic cells to treat several diseases (Fox IJ et al., 2012; Inoue H et al., 2014), including Parkinson's disease, Alzheimer's disease, sickle cell anemia and heart disease.

1-4-2 Multipotent stem cells

Multipotent stem cells have stem cell features and exist in almost all tissues. They can be isolated from bone marrow, umbilical cord blood, placenta, adipose tissue, muscle and fetal liver, and then be expanded in vitro. These multipotent mesenchymal stem cells (MSCs) could get rid of the major problem with pluripotentcy including tumorigenic and ethical issue. Currently, MSCs have great potential in treating degenerative diseases and performing tissue repair. Although the details of therapeutic mechanism are not completely understood, the evidences of the differentiation, homing, immunomodulation, and trophic factors are getting revealed. MSCs have differentiation ability to a variety of cell types, and they have been indicated with the ability of differentiating into tissue-specific cells in vivo (Caplan AI et al., 2001). When MSCs are delivered to animal or human, they can target the damaged tissue sites as the 'homing' manner. MSCs homing property has been demonstrated with chemokines, adhesion molecules (Wynn RF, 2004; Belema-Bedada F, 2008), and matrix metalloproteinases (Ries C, 2007; Ding Y, 2009). Besides, engraftment efficiency is responsible for inflammation state of host (Shi M, 2007; Ren G, 2010), and it is realized that the therapeutic benefits of MSCs are dependent on its trophic factors. After MSCs were delivered and homing to damage tissue site, they would produce trophic factor for tissue regeneration during

repair process. Meanwhile, recent literatures show that MSCs are able to suppress immune response, as IFNγ-pretreated MSCs protected 100% of mice from GvHD-induced death (Chanr Z, 2008).

1-4-3 Hepatocyte-like cells

Hepatocyte-like cells is an alternative cell source for cell therapy on liver diseases. Recent studies suggested that various stem cells have the differentiation capacity toward hepatocyte-like cells, and these cells functioned as primary hepatocyte. Several studies indicated that multipotent stem cells, such as bone marrow MSCs and adipose MSCs, can rapidly expand and perform allogenic transplantation properties, and become a more suitable source for stem cell therapy (Yu Y, 2012). Another promising source of hepatocyte-like cells is iPSCs. Because iPSCs can bypass ethical concerns and potential issues of allogenic rejection, iPSCs are more ideal to produce patient-specific and disease-specific adult cell for future clinical applications. Moreover, data also reveals hepatocyte-like cells derived from iPSCs have the ability of synthesizing albumin and secreting urea, and expressing cytochrome P450 enzymes. Transplantation of hepatocytes derived from human iPSCs could improve liver function and correction of genetic disorders (Si-Tayeb K, 2010; Rashid ST, 2010).

1-5 Cell therapy for liver diseases

Liver is one of largest and most complex organs in human body, with important roles of detoxification, protein synthesis, and regulation of glycogen storage. Liver failure is the condition when liver become damaged and no longer functioning, and the condition is classified into acute liver failure, inherited metabolic liver disease, and end-stage liver disease.

1-5-1 Acute liver failure

Acute liver failure is the rapid loss of hepatocellular function with high mortality. The most

common causes of acute liver failure are virus and drug. Compared to the rare cases of virus-caused acute liver failure, including hepatitis A, B, and E, drug-induced liver injury accounts for the most acute liver failure cases in the world. The most important drug is acetaminophen, especially with single large dose (Bernal W, 2013). The liver organ transplantation is an efficient therapy strategy for acute liver failure but organ shortage is an obstacle. Cell therapy for acute liver failure might support liver function rapidly and recover the damage hepatocytes steadily. Pareja et al. demonstrated that hepatocyte transplantation might reduce the mortality and prevent death from acute liver failure (Pareja E, 2010). In addition, result of bone marrow mononuclear for cell therapy on acute liver failure, combined with hepatocyte growth factor (HGF), showed improved liver function with liver recovery in mouse model (Jin SZ, 2011). Moreover, Parekkadan et al. demonstrated that MSCs-derived condition medium exerted immunomodulation ability and altered leukocyte migration in rat with acute liver failure (Parekkadan B, 200). Nevertheless, beyond those positive results, the study control remained difficult for the course of acute liver failure is full of variation and complexity.

1-5-2 Inherited metabolic liver disease

Inherited metabolic liver disease is characterized by deficiency of a hepatic enzyme or protein, which might result in the life-threatening condition. At present, liver organ transplantation is the only treatment strategy. However, the shortage of organ resource limited the clinical application. This explained that why most treatment strategy still relied on support therapy. With the evidences from animal and clinical experiment, cell therapy is a promising therapy and may replace organ liver transplantation or make a bridge to liver organ transplantation for patients with inherited metabolic liver disease. Hepatocyte transplantation or stem cell transplantation are expected to make up the partial missing function without the replacement of the whole organ. Related literature has showsn that hepatocyte transplantation provides therapeutic potential in the inherited metabolic liver disease,

including familial hypercholesterolemia, Crigler-najjar syndrome type I, glycogen storage disease type 1a, urea cycle defects, and a coagulation factor deficiency (Jorns C, 2012). Moreover, iPSCs are providing a unique approach to the creation of patient- and disease-specific treatments for inherited metabolic liver disease. Rashid et al. stated that iPSCs can be derived from the skin fibroblasts from the patients with lpha-1 anti-trypsin deficiency, glycogen storage disease type 1a and familial hypercholesterolemia, and then differentiate into hepatocyte in vitro (Rashid ST, 2010). Although iPSCs therapy was only proved with efficacy in animals, it is encouraging that multiple approaches to cell therapy for the clinical liver disease might be developed.

1-5-3 End-stage liver disease (cirrhosis)

Cirrhosis is a slowly progressing disease with chronic liver failure, in which liver tissue is replaced with scar tissue, and the condition eventually result in liver dysfunction. On the contratry of acute liver failure, the most common cause of liver cirrhosis is hepatitis virus. From animal and clinical studies, it has been shown that MSCs transplantation increase liver function with anti-fibrotic. Infuse the MSCs through the tail vein of animal mode of carbon tetrachloride (CCl_4) induced liver fibrosis was proved with significantly increased survival rate and reduced liver fibrosis. In the clinical study, autologous MSCs via the peripheral vein also slowed the progress of fibrosis significantly (Takami T, 2012). In other words, the autologous stem cell has been proved with efficacy and safety by the clinical study.

1-6 Delivery route for cell therapy

The route of cell administration is important in cell therapy. A safe and effective cell delivery method is needed to increase the therapeutic efficacy, and each route has its own pros and cons. Although cell administration has been performed by systemic delivery and site-directed, the intravenous route remained the most common method with the advantages of easy, convenient, and

less invasive. Beyond the report of distribution of donor cell in lungs, evidence has been accumulated to show that stem cells are able to homing to injure liver. In animal model, donor cells were found mostly in lymphoid after 24 hours after tail vein injection. Among them, 10% donor cells were found in spleen and 5% in lymph nodes (Kurtz A, 2008). Site-directed delivery has been shown with the benefit increased engraftment efficiency without homing requirement, and donor cells could be detected within these sites. For repopulating in the liver, donor cells via intrahepatic injection are favored, but the procedure is hesitated with its invasiveness. Another major route of site-directed delivery is intrasplenic injection (Xu YQ, 2004). Spleen has rich blood supply with accessibility of hepatic portal circulation, which helped the translocation of the transplanted cells to the hepatic sinusoids. Gupta et al. indicated that about 8% delivered cell would reach liver, 20% went to lungs, and less than 1% remained in spleen after hepatocytes transplantation via intrasplenic injection (Gupta S, 1994). Although most of cells will migrate to the liver via to portal vein system, they might complicate with portal vein embolism (Rosenthal RJ, 1996; Wilhelm A, 2004). For engraftment, very few cells engraft in the liver with the systemic delivery, in more depth, only 1~5 % of transplanted cells engraft within target site. Instead, more engraft cells could reach target site through direct injection. However, site-directed delivery used in basic research may be not applicable in clinical condition. Therefore, the safe and efficient systemic delivery is more suitable for clinical studies.

1.7 Hypothesis and aims

In modern era, organ shortage is the greatest challenge while facing the field of liver transplantation because the waiting list for liver transplantation is growing at an alarming rate. Therefore, cell therapy is the rising hope for end-stage liver disease, by introducing healthy cell to repair or regenerate damage cells. Stem cells are ideal cell source of cell therapy in liver disease because it’s high proliferation and differentiation ability. This dissertation was focused on stem cell

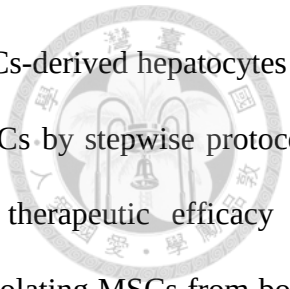

therapy for liver diseases. First, to address the therapeutic potential of iPSCs-derived hepatocytes in genetic liver disease, I attempt to obtain functional hepatocytes from iPSCs by stepwise protocol, and use hemophilia B mice disease model to assess the in vivo therapeutic efficacy of iPSCs-derived hepatocytes. Second, beyond the most popular method of isolating MSCs from bone marrow and subcutaneous adipose tissue, I obtain MSCs from the mice omentum adipose tissues, which have not been described. We hypothesize that omentum adipose-derived stem cells (ASC) has antioxidant and anti-inflammation properties to protect hepatocytes against toxicity damage, and then prove the therapeutic potential of ometum ASCs in acetaminophen (APAP)-induced acute liver failure model. These results would help us to open up entirely new perspectives in treatment of severe hepatic disease.

Chapter 2

Therapeutic Potential of iPSCs Derived Hepatocytes in Genetic Liver Disease

2.1 Summary

Cell therapy is being developed as an alternative to orthotopic liver transplantation, the only effective therapy for many liver diseases. Hepatocytes transplantation has been employed in animal models and clinical study in attempts to correct genetic deficiencies. Our laboratory also demonstrated that genetically modified donor cells could improve the therapeutic efficiency of hepatocyte transplantation in treatment of genetic liver disease. Unfortunately, this method is limited by the availability of useful cells. iPSCs is a potential source for cell therapy for genetic liver diseases. In this dissertation, I proved the ability of differentiation of iPSCs to be the acquired functional hepatocytes, and transplant them into hemophilia B disease, an inherited deficiency in coagulation factor IX (FIX) that leads to prolonged bleeding after injury. With the hypothesis that hepatocyte-like cells derived from iPS cells would have therapeutic efficiency in a mouse model of HB, our results showed iPSCs undergo stepwise protocol would appear hepatocyte morphology, express hepatocyte-specific marker, and perform hepatocytes function, including albumin synthesis, metabolic capacity, glycogen storage, ureagenesis and cytochrome P450 2E1 activity. Moreover, iPSCs-derived hepatocyte transplantation led to increased coagulation factor IX activity, improved thrombus generation and better hemostasis parameters, with the evidence that the transferred cells were localized in the liver in recipient HB mice. In conclusion, our results clearly demonstrated that hepatocyte-like cells derived from iPSCs is a potential cell source for cell-based therapy in the treatment of HB.

2.2 Introduction

Hemophilia is an X-linked inherited bleeding disorder caused by lack of functional coagulation factor. There are two most common types; lack of clotting factor VIII (FVIII) results in hemophilia A (HA) and lack of clotting factor IX (FIX) results in hemophilia B (HB) (Bolton-Maggs PH and Pasi KJ 2003). The deficiency of these clotting factors will disrupt the clotting process, and fail to form blood clots when stop bleeding is needed. Normal clotting factor is between 50% and 150%. According to the amount of the clotting factor, the hemophilia is classified into mild (6% ~ 49%), moderate (1% ~ 5%) and severe (<1%). A FIX activity level of 1% results in severe disease and possible death, while improvement to a level of approximately 5% is sufficient to prevent spontaneous and life-threatening bleeding events (Burlina AB 2004). FIX is a vitamin K-dependent single-chain glycoprotein, which is synthesized firstly by the hepatocyte as a precursor protein. Under the posttranslational modification, including gamma-carboxylation, β-hydroxylation, removal of the signal peptide and propeptides, addition of carbohydrates, sulfation and phosphorylation, the FIX would mature and be secreted into the blood. There is no cure for hemophilia, and current treatments are clotting factor replacement and gene therapy. Clotting factor replacement therapy is a kind of component therapy with clotting factor to stop or prevent bleeding by raising the patients' factor level, but the patient with the treatment need frequent transfusions. Thus, clotting factor replacement therapy is not completely efficient, and some issues remain unresolved, including high cost, high risk of anaphylaxis and life-threatening hemorrhagic complications. On the other hand, gene therapy is bringing a hope for patients, by inserting functioning clotting factor genes into the cell of hemophilia patients to produce their own clotting factor (FVIII or FIX), and subsequently reduce frequency of transfusion. However, gene therapy is also limited by host immune tolerance and the long-term expression of therapeutic gene products (Bigger BW et al., 2006; Peyvandi F et al., 2006). Therefore, it is important to develop another available strategy for hemophilia disease.

Induced pluripotent stem cells (iPSCs) are ideal cell source for cell therapy because of their

stem cell properties for self-renewal and differentiation. The somatic cells were introduced with a set of reprogramming factors (Oct4, Klf4, c-Myc, Sox2) to obtain the iPSCs. (Yamanaka S, 2006) Many studies have demonstrated that iPCs shared high similarity with ESCs in molecular and genetic level, morphology and functions (Lowry et al., 2008; Chin et al., 2010). As derived from somatic cells, iPSCs are bounded to no ethical issue, and can be derived from patient to creat patient- or disease-specific cell line for autologous transplantation. However, a problem still unsolved is that iPSCs were generated by insertion of genes using viruses, which carried the risk of transformation. Nevertheless, iPSCs represent a novel hope for regeneration medicine. In animal studies, it have shown that differentiated iPS cells can be used to rescue a disease phenotype, including sickle cell disease, (Hanna J et al., 2007) parkinson's disease, (Wernig M et al., 2008) and hemophilia A (Xu D et al., 2009). Hepatocyte-like cells that derived from iPS cells have been shown with the ability of secreting human albumin, synthesizing urea and expressing cytochrome P450 enzymes, as a very promising cell population for future therapeutic transplantation (Si-Tayeb K et al., 2010). Thus, iPSCs-derived hepatocyte-like cells might have therapeutic potential for metabolic liver disease.

Our previous data demonstrated that hepatocyte transplantation would provide in concept the protection in hemophilia B disease mice model. Although primary hepatocytes are suitable cell source for hemophilia B disease mice, the shortage of the cells remain an obstacle. To overcome this problem, provide unlimited source of hepatocytes from iPSCs is in consideration. Hence, we planned to acquire the hepatocytes form iPSCs through differentiation ability of its stem cell properties. Further, to assess the therapeutic potential, iPSCs-derived hepatocyte is studied in hemophilia B disease mice model.

2.3 Materials and Methods

2.3.1 Animal

All mouse experiments were approved by the institutional animal care and use committee at National Taiwan University. The HB mice deficient in FIX (male, 6 to 8 weeks old) used as recipient mice and obtained from Professor Lin SW. C57BL/6 mice were purchased from National Laboratory Animal Center, Taipei, Taiwan. C57BL/6 mice were used to acquire normal hepatocytes.

2.3.2 iPSCs and hepatocyte differentiation

Mouse iPSCs were obtained from Yamanaka S. The iPSCs were cultured and expanded from mouse embryonic fibroblasts with mytomycin C (Sigma-Aldrich, St Louis, MO) treatment in Dulbecco's modified Eagle's Medium (DMEM; Gibco, Grand Island, NY) supplemented with 10% fetal bovine serum (FBS, Hyclone Laboratories, Logan, UT), 0.3% leukemia inhibitory factor (LIF; Millipore, Bedford, MA), 1 mM L-glutamine, 1% nonessential amino acid and 0.1 mM β-mercaptoethanol (all were purchased from Gibco, Grand Island, NY). Derivation of hepatocytes from iPSCs was performed according to the protocols described and modified by Song Z et al. (Song Z et al., 2009). The iPSCs were cultured on low-attachment dishes (Corning Life Science, NY) to form embryonic bodies, which were cultured in Iscove's modified Dulbecco's Medium (IMDM; Gibco, Grand Island, NY) supplemented with 1% FBS and 100 ng/ml activin A (ProSpec, Israel) for 1 day. On the following days, 0.1% insulin–transferrin–selenium (ITS; Sigma-Aldrich, St Louis, MO) was added to this medium, and 1% ITS was added 1 day later. After endoderm induction, the cells were cultured in IMDM supplemented with 10% FBS, 30 ng/ml FGF4 and 20 ng/ml BMP2 for 5 days (all were purchased from ProSpec, Israel). Next, the cells were incubated in IMDM supplemented with 10% FBS, 10 ng/ml HGF (ProSpec, Israel), 10 ng/ml oncostatin M (ProSpec, Israel) and 0.1 μM dexamethasone (Sigma-Aldrich, St Louis, MO) for 5 days (Fig. 1A).

2.3.3 Primary hepatocytes

Mouse hepatocytes were isolated using a two-step collagenase perfusion method. The liver was perfused with Hank's balanced salt solution (HBSS, Gibco, Grand Island, NY) containing 0.1mM EGTA at 37℃for 10 minutes at the rate of 3 mL/minutes. Then, perfusion with 0.025% of collagense type IV prepare in HBSS containing 5 mM $CaCl_2$ for 10 minutes at 2 mL/minutes. After enzyme digestion, the liver was dissected out, hepatocytes were released and filtered through a 70μm cell strainer. After centrifugation at 50 xg for 3 minutes, pellet was washed with HBSS containing 5 mM $CaCl_2$ and cultured in hepatocyte culture medium supplement 10% FBS.

2.3.4 Cell transplantation and preconditioned animal model

For cell transplantation, hepatocyte-like cells derived from iPSCs (at 13 day induction) and primary hepatocytes were transplant into hemophilia B mice via intrasplenic injection with 100 μl of 5×10^5 cells per mice. Before transplantation of thirty minutes, HB mice were received 100 IU/kg recombinant FIX protein (Bene FIX®; Wyeth Pharmaceuticals, PA, USA) via intravenous injection. For precondition animal model, we allow the immunosuppress drug to disrupt the endothelial cells for improve transplant cell engraft in recipient's liver. Rifampicin (Sigma-Aldrich, St Louis, MO) was dissolved in 20 M sodium hydroxide (NaOH; Sigma-Aldrich, St Louis, MO), and monocrotaline (MCT; Sigma-Aldrich, St Louis, MO) was dissolved in normal saline at a pH of 7.4. HB mice received 75 mg/kg rifampicin intraperitoneally daily for 2 days. MCT was administered intraperitoneally as a single 200 mg/kg dose on the third day. Cells were transplanted on the fourth day. (Fig. 2.1B).

2.3.5 Engraftment assay

The differentiated cells or primary hepatocytes were stained with PKH26 fluorescent dye

(Sigma-Aldrich, St Louis, MO) according to the manufacturer's instructions. After fluorescent staining, the cells were transplanted into HB mice. At 1 and 4 weeks after transplantation, the recipient mice were sacrificed, and the liver tissue was embedded in TissueTek OCT (Sakura Fintek, Torrance, CA) for immunocytochemistry. For quantitation assay, number of PKH positive cells was examined under x 200 magnification and counted by 20 continuous fields per liver lobule for three individual mice.

2.3.6 Reverse transcription-polymerase chain reaction (RT-PCR)

Total RNA was extracted using RNeasy mini kits (Qiagen Ltd, Crawley, UK), and RT-PCR was performed using a Fast-RunTM Hotstart RT-PCR kit (Protech Technology, Taiwan) according to the manufacturer's instructions. The PCR program consisted of 35 cycles of 94°C for 30 s, 72°C for 1 min and extension at 72°C for 5 min. All PCR primers are shown in Table 2.1.

2.3.7 Functional assay for hepatocyte-like derived from iPSCs

Periodic acid–Schiff (PAS) staining was performed to identify glycogen storage. Cells were fixed in 4% paraformaldehyde (Sigma-Aldrich, St Louis, MO) for 20 min and then stained with PAS (Sigma-Aldrich, St Louis, MO). Cellular uptake and indocyanine green (ICG; Sigma-Aldrich, St Louis, MO) release were measured. ICG (1 mg/ml) was added to the culture medium for 30 min at 37°C, and ICG release was measured after 6 h. During cell differentiation, albumin and uric acid were secreted into the culture medium. The albumin concentration was quantified using a mouse albumin enzyme linked immunosorbent assay (ELISA) kit (Bethyl Laboratories, Montgomery, TX). The total protein content was determined using a BCA protein assay kit (Pierce, Rockford, IL). The albumin content was normalized to the total cellular protein level. The uric acid levels were measured using a uric acid assay kit (BioVision, CA, USA) according to the manufacturer's protocol. The cytochrome P450 2B activity assay was performed according to the manufacture's

protocol (Cytochrome P450 2B fluorescent detection kit, Sigma-Aldrich, St Louis, MO). Before the assay, the differentiated cells were treated with 200 μg/ml phenobarbital (Sigma-Aldrich, St Louis, MO) for 3 days. The cells were homogenized with sonication and according to the manufacturer's instructions. We measured the fluorescence (Ex 530nm/Em 585nm) with BioTek Multi-Detection Microplate Reader, using Gene5 software.

2.3.8 Immunofluorescence

Cells were fixed in 4% paraformaldehyde for 20 min, permeabilized in 0.1% Triton X-100 (Sigma-Aldrich, St Louis, MO) for 20 min and blocked in 3% bovine serum albumin (BSA; Sigma-Aldrich, St Louis, MO) for 1 h. The cells were then incubated with the primary antibody at 4°C overnight. The mouse anti-α-fetoprotein (Cell Signaling Technology, Beverly, MA), rabbit anti-albumin (Abcam, Cambridge, UK), rabbit anti-cytokeratin 7 (Abcam, Cambridge, UK), anti-cytokeratin 18(Abcam, Cambridge, UK) and sheep anti-FIX (Molecular innovations, Michigan, USA) primary antibodies were used at a dilution of 1:100, and the rabbit anti-cytokeratin 19 (Abcam, Cambridge, UK) primary antibody was used at a dilution of 1:1,000. After washing with PBS-0.02% Tween-20 (Sigma-Aldrich, St Louis, MO), cells were incubated with FITC- or PE-conjugated secondary antibody (Invitrogen, Carlsbad, CA) diluted to 1:200 for 2 h and then stained with DAPI (Biogenex, San Ramon, CA) to stain the cell nuclei.

2.3.9 FIX clotting activity assay

FIX clotting activity was determined using the APTT reagent (Actin® FSL; Dade Behring, Newark, DE) as the activator in a semi-automated blood coagulation analyzer according to the manufacturer's instructions (CA-50; Sysmex, Kobe, Japan). Pooled mouse plasma was obtained from inbred C57BL/6 male mice (n = 18) to generate standard curves for the quantification of test samples. FIX clotting activity in the standard was assumed to be 100%. The test samples were

diluted 1:5 in imidazole buffer prior to analysis. A one-stage clotting assay was performed by incubating 50 μl of the test sample with 50 μl of human FIX-deficient plasma (American Diagnostica, Stamford, CT, USA) for 1 min at 37°C, after which 50 μl of activator was added for 3 min at 37°C. Next, 50 μl of 25 mM calcium chloride (CaCl2; Sigma-Aldrich, St Louis, MO) was added, and the time required for clotting was measured. Each value was reported after subtracting the mean baseline level in HB mice.

2.3.10 Hemostatic function assay

Whole blood mixed with a one-tenth volume of 3.2% sodium citrate (Sigma-Aldrich, St Louis, MO) was assayed by thromboelastography (TEG® analyzer; Haemoscope, Braintree, MA, USA) using the citrated-kaolin mode. Analyses for the variables were conducted according to the manufacturer's instructions.

2.3.11 Statistical analysis

Values are presented as means ± SEM. Student's paired t-test or one-way ANOVA followed by Tukey's test was used for between-group comparisons of the means. The survival analysis was assessed with the SigmaStat software, version 3.5 (Chicago, IL, USA); other analyses were performed with the GraphPad InStat software, version 3 (San Diego, CA, USA). All directional P values were 2-tailed, and a value of .05 or less was considered significant for all tests.

2.4 Result

2.4.1 Generation and characterization of hepatocytes from mouse iPSCs

Following stepwise differentiation protocol, iPSCs (Fig. 2-1A) were through the endoderm induction by Activin A induced, toward hepatoblast stage by BMP2 and FGF4 (at day 7, Fig. 2-1B), and differentiation to early hepatocyte stage by HGF induction (at day 13, Fig 2-1C) then finally

differentiation to hepatocyte-like cell by OSM/Dex (at day 20, Fig. 2-1D). During the differentiation, the cells morphology was changed from colonial to polygonal. We checked the mRNA expression at day 18 in hepatocyte expression. RT-PCR result demonstrated these expression hepatocyte markers, including AFP, ALB, HNF4, G6P, TAT, CK18, Cyp3A11, Cyp7A, and Cyp7B (Fig. 2-3). Further, to detect protein expression by immunofluoresencent staining. AFP was expressed in immature hepatocyte and detected at day 10, ALB and CK7 were expressed at day 15, and more differentiated cells expression CK18 and CK19 at day 20 (Fig. 2-4). Importantly, the RT-PCR and immunofluorescence results confirmed that the iPSCs-derived hepatocytes expressed FIX mRNA (Fig. 2-3) and protein (first detected at day 10, Fig. 2-4). Taken together, these data show that hepatocytes can be derived from iPSCs using our differentiation procedure. We further examined the functionality of the hepatocyte-like cells derived from iPSCs. PAS staining demonstrated the ability of the derived cells to store glycogen start at 13 day (Fig. 2-5C) and monitored for 18 days (Fig. 2-5D). For metabolism ability, performed with ICG analysis shows their capacity to accumulate and excrete compounds (Fig. 2-5A and 2-5B). Protein synthesis is another characteristic of functional hepatocytes, which can be monitored by the secretion of proteins into the culture medium. Thus, we monitored the concentration of albumin during the period of differentiation. Albumin production was first detected after 13 days of differentiation, and reaching the maximum level on 21 days of differentiation (1.51 ± 0.65 ng/mg protein/day) (Fig. 2-5E). Although these cells could synthesize ALB, concentration was lower than primary hepatocytes and AML cells (mice hepatocyte cell line) (Fig. 2-5F). Moreover, after 18 days of differentiation, the uric acid production level was 4.45 ± 0.48 nmole/ml/day (Fig. 2-5G). Cytochrome P450 enzymes also hepatocyte specific function to metabolize toxic, RT-PCR assay shows cytochrome P450 gene (CYP3A11, CYP7A, CYp7B) were expressed in hepatocyte-like cells (Fig. 2-3). The cytochrome P450 enzyme activity was detected at maturation induction. The activity of CYP2E1 was increased to approximately one fold compare with untreated phenobarital in hepatocyte-like cells and primary

hepatocytes (Fig. 2-5H). These results revealed that the generated iPSCs-derived hepatocytes exhibited hepatic functionality and potential to as a drug screen model.

2.4.2 Transplantation of iPSCs-derived hepatocytes in HB mice

Next, we assessed the therapeutic efficacy of iPSCs-derived hepatocytes in the HB mouse model. The HB mice were divide into two groups, one that received normal hepatocyte transplantation (as positive control) and the other iPSCs-derived hepatocytes transplantation, and the circulating FIX activity was monitored for 4 weeks of transplantation. Our data showed iPSCs-derived hepatocytes enhanced FIX clotting activity by 2–3%, and the circulating FIX activity were stable for up to 1 month (Fig. 2-6A). These results reflected a substantial improvement in disease in HB mice. Because the clotting test could not fully reflect the in vivo hemostatic response, we utilized the TEG assay to further examine the in vivo hemostatic state. Moreover, we used transplantation to improve the therapeutic efficacy. For this purpose, HB mice underwent a second intrasplenic transplantation (separated by 1 week) of iPSCs-derived hepatocytes or normal hepatocytes, and we assessed hemostasis in whole blood 7 days after the second transplantation. The peak level of thrombin generation progressively decreased, and the time of thrombus generation was 43 min in HB mice. However, repeated normal hepatocyte transplantation improved the peak thrombin level and reduced the time of thrombus generation to 14 min. In addition, the effects of repeated iPSCs-derived hepatocytes transplantation were similar to the effects of repeated normal hepatocyte transplantation (Fig. 2-6A). Moreover, repeated iPSCs-derived hepatocytes transplantation improved both the reaction time and strength of thrombus generation and the coagulation index (CI) value, which is another hemostatic parameter that reflects the overall coagulability of blood. The CI value of mice after repeated iPSCs-derived hepatocytes transplantation improved to -6.4 (the value before transplantation was -32.3; Table 2). Taken together, these results indicate that iPSCs-derived hepatocytes transplantation markedly improved

hemostasis, suggesting that iPSCs-derived hepatocytes could be used to treat HB.

2.4.3 Engraftment of iPSCs-derived hepatocytes

Finally, to investigate whether the iPSCs-derived hepatocytes were retained in the liver parenchyma, we utilized immunofluorescence to trace the grafted cells in recipient mice. Before transplantation, the differentiated cells were stained with PKH26 fluorescent dye, and liver sections were examined at 1 week after transplantation. The immunofluorescence staining showed that PKH26-positive cells were localized in the livers of recipient mice, thus indicating that the transplanted cells were engrafted (Fig. 2-6C and 2-6D). To improve the engraftment efficiency, we adopted a preconditioned model that included immunosuppression (MCT and rifampicin). For iPSCs-derived hepatocytes engraftment in the livers of preconditioned animals 1 week after transplantation, the number of engrafted cells was similar to the value observed in non-preconditioned mice (Fig. 2-6F), whereas more PKH26-positive cells were detected at 4 weeks after transplantation (Fig. 2-6E). These results indicated that the transplantation of iPSCs-derived hepatocytes into the livers of preconditioned mice could enhance the efficiency of engraftment. Additionally, we assessed hemostasis in the preconditioned animal model with iPSCs-derived hepatocytes transplantation. The TEG assay revealed that the time of thrombin generation for iPSCs-derived hepatocytes transplantation was similar to the result for normal hepatocyte transplantation, with a shorter time of thrombus generation. Meanwhile, iPSCs-derived hepatocyte transplantation resulted in improved CI values and hemostasis parameters in the preconditioned model, compared with the normal hepatocyte transplantation group. Therefore, iPSCs-derived hepatocytes possess therapeutic potential in HB mice.

2.5 Discussion

Hepatocyte transplantation has been demonstrated with therapeutic efficacy in animal model and clinical study. Our laboratory has demonstrated the therapeutic efficacy of hepatocyte transplantation in the HB mouse model, yet the shortage of hepatocyte source is a big problem. Therefore, another cell source is urgently needed for cell therapy. iPSCs has revolutionized the field of regenerative medicine and have been shown to represent a novel source of hepatocytes for drug development and cell therapy (Choi SM, 2011;Wu SM, 2011). I utilized the ability of iPSCs to obtain functional hepatocytes in stepwise protocol, and then transplanted these cells into HB mice to assess their therapeutic potential. Results showed that iPSCs differentiated into functional hepatocytes in our optimized culture conditions, and transplantation resulted in enhanced FIX clotting activity and improved hemostasis.

iPSCs technology is bringing great hope to treat various diseases, for iPSCs can be obtained from somatic cells, and they subsequently differentiate into cells at affected sites, including neuron, hepatocytes and cardiomyocytes. Numerous reports have indicated that iPSCs therapy could improve liver function in disease models. Specifically, Xu et al. reported that the transplantation of iPSCs-derived endothelial cells to a hemophilia A mouse model resulted in factor VIII expression, provided a proof-of-concept for genetic disorder treatment (Xu D, 2009). Moreover, iPSCs-derived hepatocytes can improve liver function and prevent oxidative stress-induced damage on lethal acute hepatic failure mice model induced by thioacetamide, a hepatotoxin that causes the production of reactive oxygen species and alleviated acute hepatitis (Li HY, 2011). Besides, iPSCs-derived hepatocyte improved survival and protected against liver injury induced by CCL_4 (Chen YF, 2012). In my study, iPSCs-derived hepatocyte transplantation in HB mice resulted in increased FIX clotting activity and improved hemostasis. Similar effects of transplantation have been reported for other disease, for example, the combination of iPSCs therapy and gene therapy has been reported for therapeutic applications in sickle cell anemia (Sebastiano V, 2011). It is exactly on such grounds

that we believe that gene therapy combined with iPSCs therapy holds promise for treating HB in the future (Kaji EH, 2001).

The repopulation capacity of grafted cells may limit the efficiency of cell therapy. However, 2–5% replacement has been shown to sufficiently improve the liver function (Sancho-Bru P, 2009). To examine this aspect, we adopted a preconditioned model (Wu YM, 2008) and repeated transplantation to improve the engraftment efficiency. Results revealed that repeated transplantation can improve hemostasis in HB mice, with similar results of normal hepatocyte transplantation. Further experiments showed that the engraftment efficiency of iPSCs-derived hepatocytes transplantation was further improved in the preconditioned model, and the transplanted cells were engrafted in the liver parenchyma. Although the time of thrombus generation was shortened, the strength of thrombus was insufficient, partly because the differentiated cells did not fully acquire hepatic function. This problem will hinder clinical application, for undifferentiated cells can induce tumorigenicity. Currently, no definite strategy is established for fully separating differentiated cells from heterogeneous cell populations to eliminate the risk of teratoma formation. However, some evidences suggest that undifferentiated ES cells highly express onco-fetal genes (Blum B, 2009). The asialoglycoprotein receptor is an endocytotic cell surface receptor expressed by hepatocytes that can be used to purify cells by flow cytometry (Basma H. 2009), as a promising strategy for separating cell populations. Nevertheless, additional technologies are needed. When differentiating iPSCs into hepatocyte-like cells under optimal in vitro culture conditions, we could clearly see that these cells not only expressed hepatic genes and proteins and performed hepatocyte functions, including albumin synthesis, glycogen storage, and ureagenesis and ICG uptake. Most importantly, iPSCs-derived hepatocytes exhibit Cyp 2B enzyme activity and stand with a suitable metabolic activity for drug screening and discovery. In conclusion, functional hepatocytes can be derived from iPS cells via a stepwise differentiation protocol, and the therapeutic potential of iPSCs-derived hepatocytes in an HB mouse model is well demonstrated. Hence, iPSCs-derived hepatocytes

provide a promising modality for genetic disorders, and this strategy should contribute to the development of tailored drug and cell therapies.

Table 2-1. Primer sequence

Primer	Sequence (5′→ 3′)
CK 18, Forward	CCATGGACTCCGCAAGGT
CK18, Reverse	CTTCCTTGAGTGCCTCGATTTCT
ALB, Forward	GACAAGGAAAGCTGCCTGAC
ALB, Reverse	TTCTGCAAAGTCAGCATTGG
G6P, Forward	GCCTCCGGAAGTATTGTCTCATC
G6P, Reverse	CACCCCTAGCCCTTTTAGTAGCA
TAT, Forward	CGAGCCATTGTGGACAACAT
TAT, Reverse	GGTCCCCAATTGACAGAGAGAT
AFP, Forward	CACTGCTGCAACTCTTCGTA
AFP, Reverse	CTTTGGACCCTCTTCTGTGA
HNF4, Forward	GAGGCTCCCCTGAGAATAGACA
HNF4, Reverse	TGTTTGGTGTGAAGGTCATGATTAG
Cyp3a11, Forward	TCTAAGCAGAAGCACCGAGT
Cyp3a11, Reverse	ACAAGGCTGGAAGGAGAAGT
Cyp7a,Forward	CAACGACACACTCTCCACCTT
Cyp7a, Reverse	GGCTCTCTACAAGCTCCAGTTC
Cyp7b, Forward	CCAGCTATGTTCTGGGCAAT
Cyp7b, Reverse	CTTCAGCCTCTTCCCTCCTT
Factor IX, Forward	GGAAGCAGTATGTTGATGG
Factor IX, Reverse	ACCAGAAGTCCTGTGAACCA
β-actin, Forward	ACGGCCAGGTCATCACTATTG
β-actin, Reverse	CAAGAAGGAAGGCTGGAAAAGA

CK18, cytokeratin 18; ALB, albumin; G6P, glucose6-phosphate; TAT, tyrosine aminotransferase; AFP, α-fetoprotein; HNF4, hepatocyte nuclear factor 4; Cyp3a11, cytochrome P450 3a11; Cyp7a, cytochrome P450 7A; Cyp7b, cytochrome P450 7B, FIX, clotting factor IX.

Table 2-2. Effects of transplantation on whole blood hemostasis in HB recipient mice

	B6	HB	B6 repeated	iPS repeated	Precondition
R (min)	4.10 ± 0.84	43.88 ± 4.39	14.43 ± 4.98**	15.45 ± 7.73**	2.20 ± 0.67*
K (min)	1.20 ± 0.18	14.13 ± 2.17	2.80 ± 0.52**	4.65 ± 2.31**	7.13 ± 1.13*
Angle(deg)	73.83 ± 2.28	18.73 ± 2.95	58.20 ± 5.57**	54.1 ± 10.66**	35.80 ± 3.40***
MA (mm)	67.65 ± 0.63	65.53 ± 7.57	71.27 ± 5.24	74.38 ± 2.92	55.30 ± 9.10
CI	2.95 ± 0.67	−32.30 ± 4.28	−5.1 ± 3.46**	−6.40 ± 6.50**	−2.43 ± 1.31*
MRTG	19.20 ± 2.87	2.08 ± 0.39	9.24 ± 1.99	10.10 ± 3.07	3.34 ± 0.28*
TMRTG	5.27 ± 0.75	52.81 ± 4.70	17.42 ± 5.59**	19.48 ± 8.63**	4.17 ± 1.86*

B6, inbred C57BL/6 mice; HB, hemophilia B mice; R (reaction time), the time to initial fibrin formation; K, the speed to reach a specific level of clot strength; Angle, the rapidity of fibrin build-up and cross-linking; MA (maximum amplitude), the reflection of clot strength contributed by platelets and fibrin; CI (coagulation index), overall assessment of coagulability; MRTG, maximum rate of thrombus generation; TTG, total thrombus generation. Data are expressed as the mean ± SEM, $n \geq 3$. Compared with the HB group, $^{**}p < 0.01$

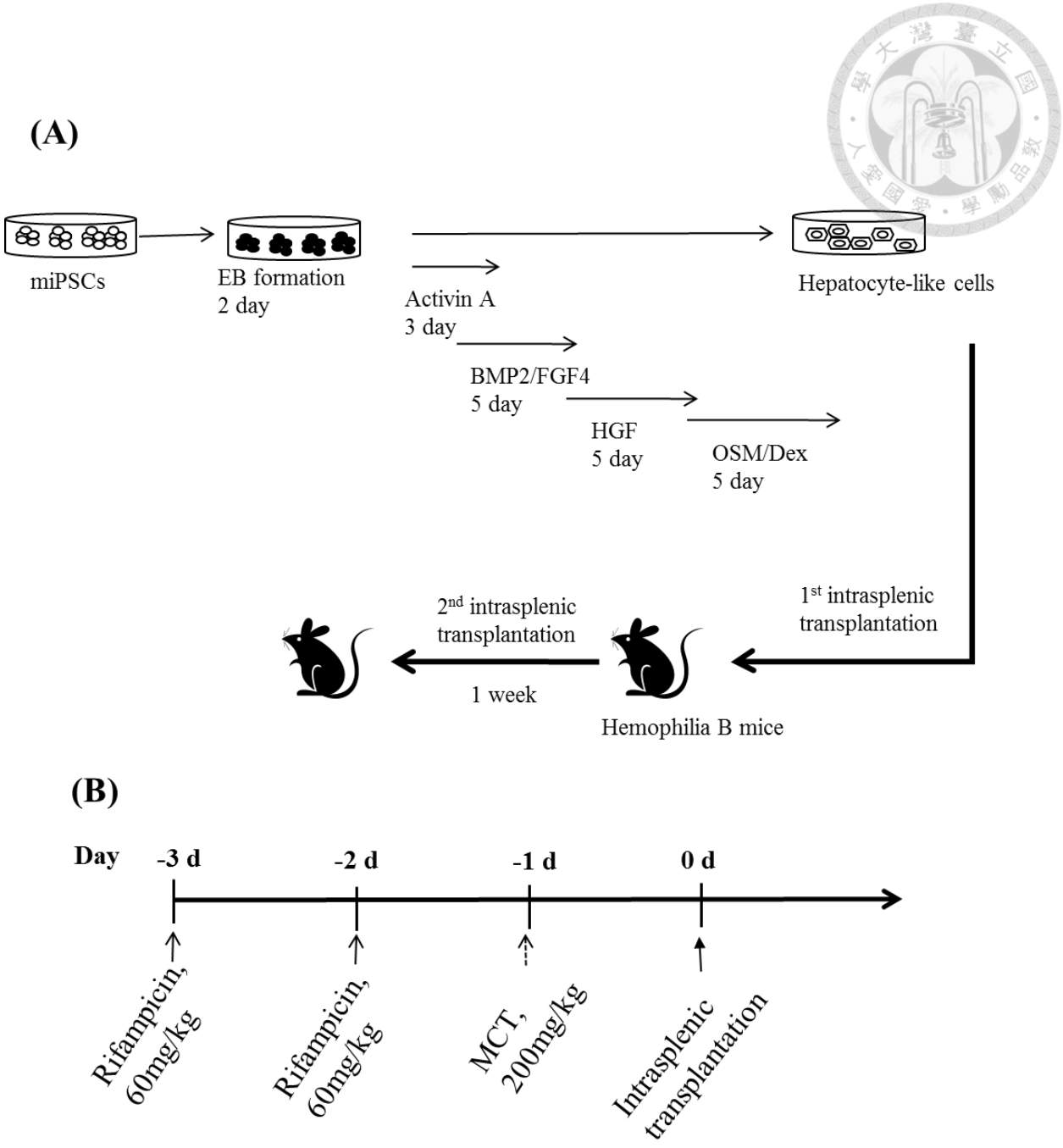

Figure 2-1 Experimental design. (A) Flow chart showing the hepatocyte-like cells from iPSCs via stepwise protocols and to assess the therapeutic potential in hemophilia B mice. (B) Precondition model was established by rifampicin and MCT to disrupt the liver endothelial cells in hemophilia B mice. iPSCs, induced pluripotent stem cells; EB, embryonic body; BMP2, bone morphogenetic proteins; FGF4, fibroblast growth factor 4; HGF, hepatocte growth factor; OSM, oncostatin M; Dex, dexamethasone.

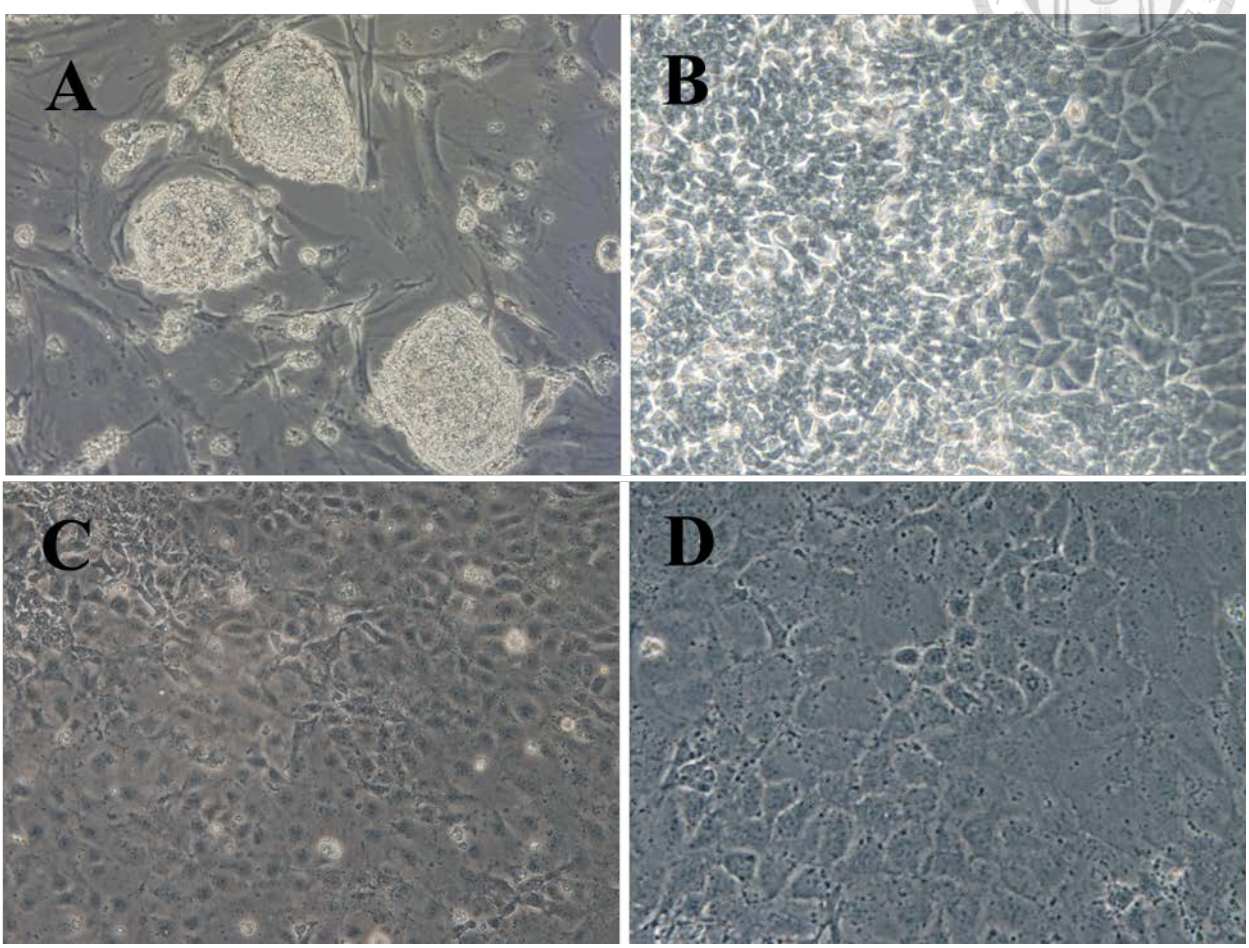

Figure 2-2 Generation of hepatocyte-like from iPSCs. Morphological was changes at differentiation stages. iPSCs (A) appeared colony morphology. Undergo induction at 7 day, cells were enter the hepatic specification (B), subsequent induction at 13 day toward early hepatocytes (C) , and mature at 20 day (D). Magnification, x100.

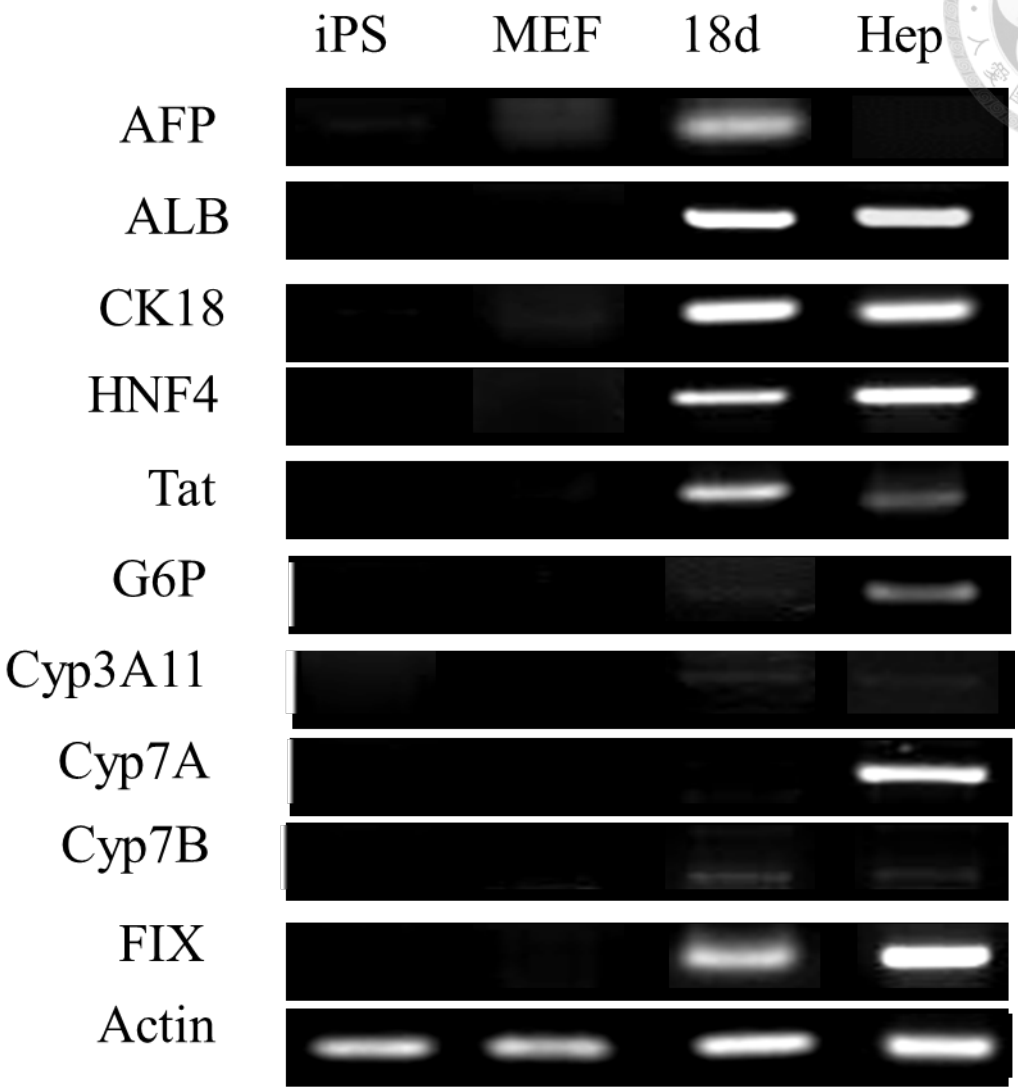

Figure 2-3 Expression of hepatocyte-specific gene in hepatocyte-like cells. To detect hepatocyte-specific gene (AFP, ALB, CK18, HNF4, Tat, G6P, Cyp3a11, Cyp7A, Cyp7B, FIX) in iPSCs, MEF, hepatocyte-like cells, and primary hepatocytes by RT-PCR. MEF, mouse embryonic fibroblast cells; Hep, hepatocyte; CK18, cytokeratin 18; ALB, albumin; G6P, glucose6-phosphate; TAT, tyrosine aminotransferase; AFP, α-fetoprotein; HNF4, hepatocyte nuclear factor 4; Cyp3a11, cytochrome P450 3a11; Cyp7a, cytochrome P450 7A; Cyp7b, cytochrome P450 7B, FIX, clotting factor IX.

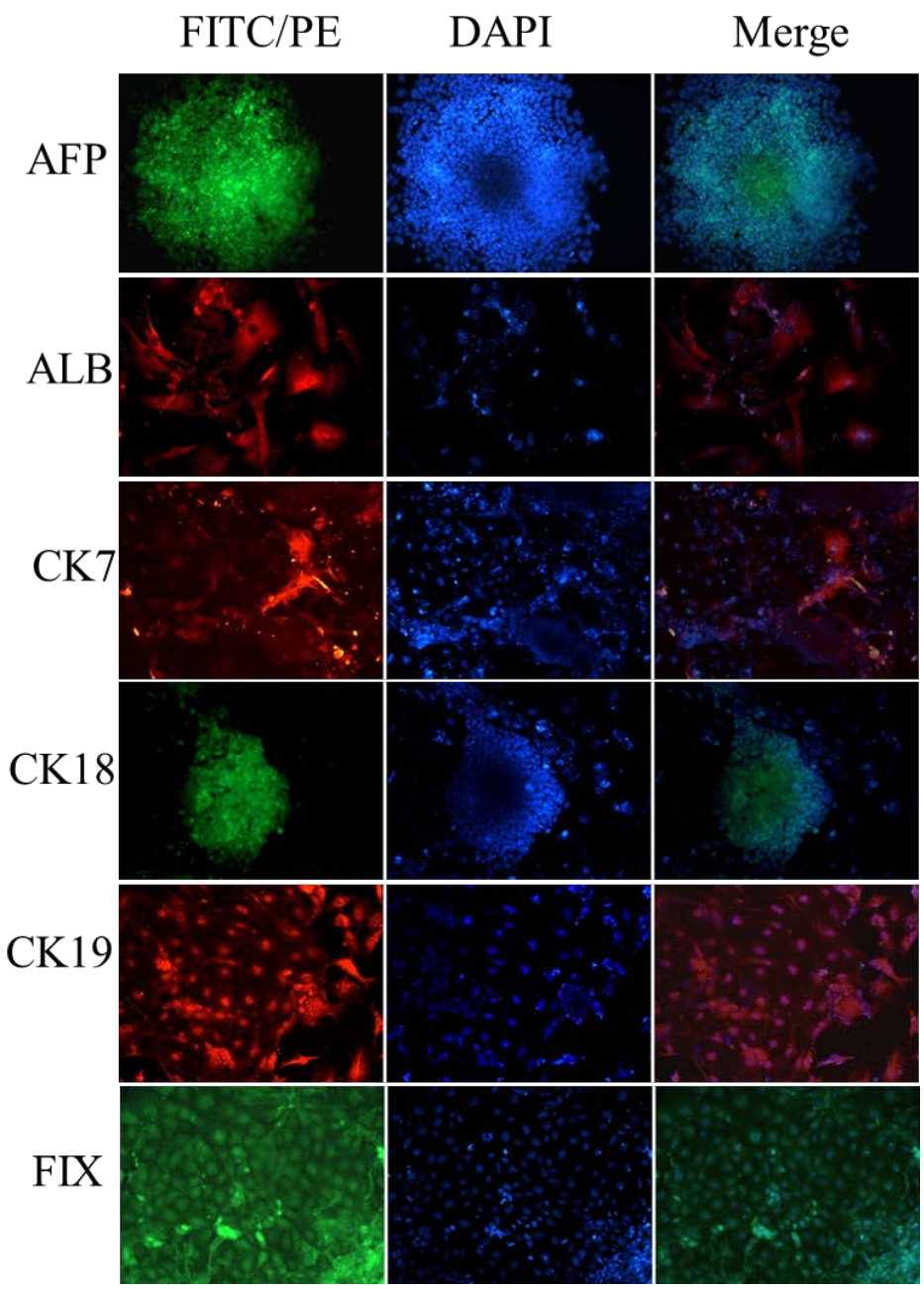

Figure 2-4 Immunostaining analysis. Expression of AFP and FIX in day 10-induced differentiated cells. ALB and CK7 were expressed in day 15-induced differentiated cells CK20 and CK19 were expressed in day 20-day induced differentiated cells. Magnification, 100x (AFP, CK7, and CK18), 200x (ALB, CK19, and FIX). AFP, α-fetoprotein; ALB, albumin; CK7, cytokeratin 7; CK18, cytokeratin 18; CK19, cytokeratin 19; FIX, clotting factor IX.

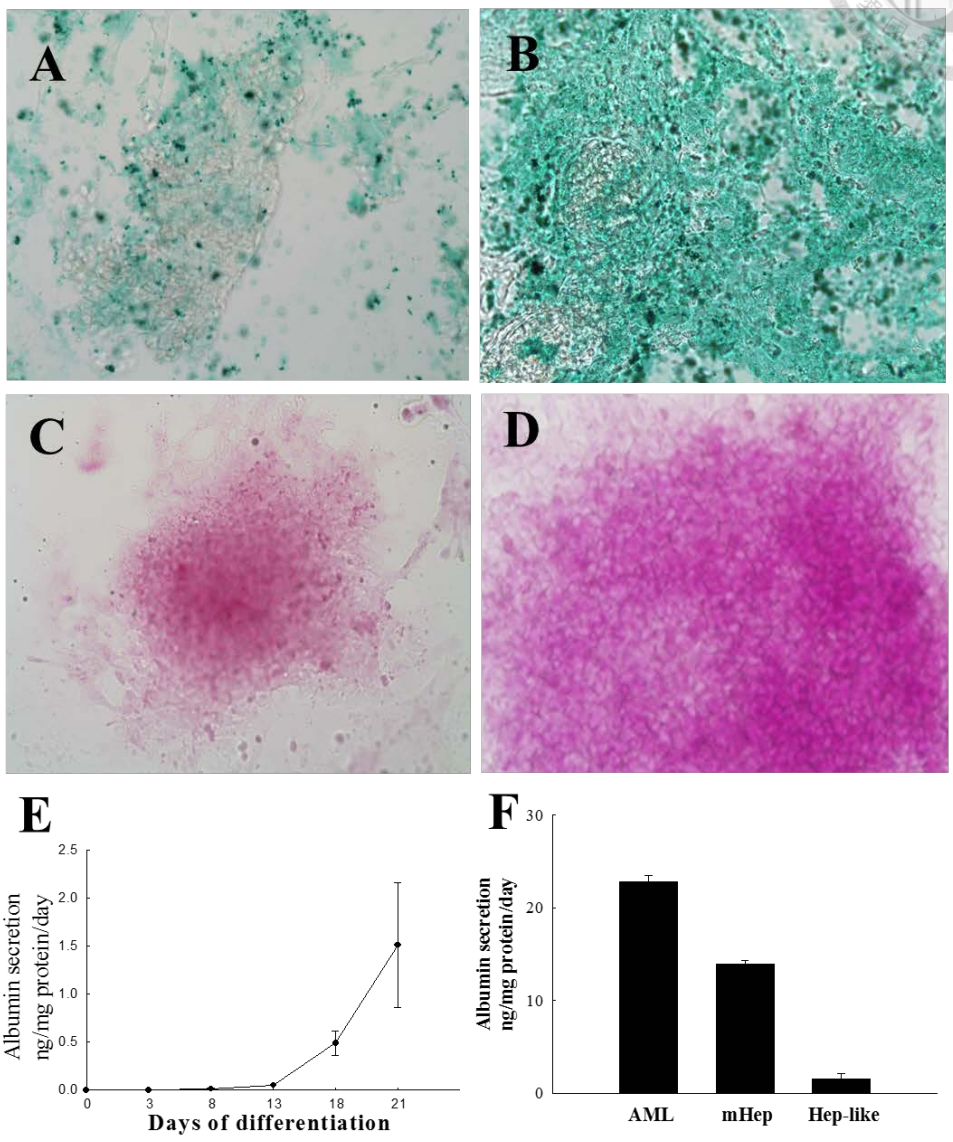
A
B
C
D
E
Albumin secretion ng/mg protein/day
2.5
2.0
1.5
1.0
0.5
0.0
0
3
8
13
18
21
Days of differentiation
F
Albumin secretion ng/mg protein/day
30
20
10
0
AML
mHep
Hep-like
G
Uric acid, nmole/ml/day
8
6
4
2
0
Hep
iPS-Hep
H
Cyp450 2B, pmole/ml/min
40
30
20
10
0
-phenobarbital
+phenobarbital
Hep
iPS-Hep

Figure 2-5 Functional assay of hepatocyte-like from iPSCs. The ability to uptake substances was assessed by ICG dye at day 13 (A) and day 18 (B). Glycogen deposition was tested by PAS staining at day 13(C) and day 18(D). Magnification, 100x. Albumin secretion was measured using ELISA during differentiation process (E). Albumin concentration in AML (mouse hepatocyte cells line), primary hepatocyes, and hepatocyte-like cells derived from iPSCs (F). Uric acid release was measured at day 18 differentiaiton and compare with primary hepatocytes (G). Cytochrome P450 2El activity was assessed after phenobarbital sodium induction. Primary hepatocytes were as a positive control. ICG, Indocyanine green; PAS, periodic acid schiff.

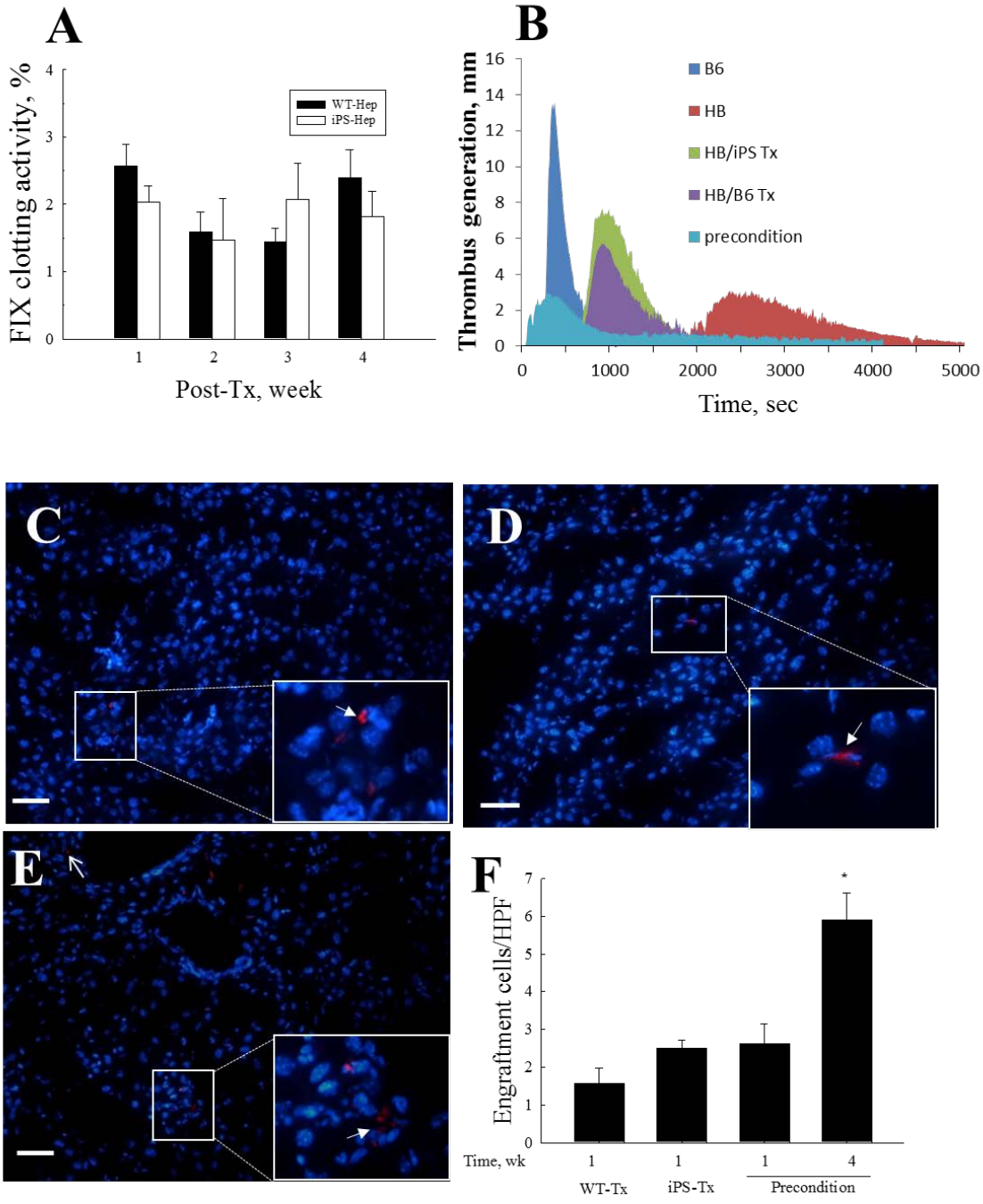
A
FIX clotting activity, %
WT-Hep
iPS-Hep
Post-Tx, week
B
Thrombus generation, mm
B6
HB
HB/iPS Tx
HB/B6 Tx
precondition
Time, sec
C
D
E
F
Engraftment cells/HPF
Time, wk
WT-Tx
iPS-Tx
Precondition

Figure 2-6 Transplanted with hepatocyte-like cells derived iPSCs in hemophilia B mouse model. (A) FIX clotting activity was monitored sequentially at 1, 2, 3, and 4 week after transplantation with hepatocyte-like cells (iPS-Hep) and primary hepatocytes (WT-Hep). Data were expressed as mean ± SEM. (B) Hepatocyte-like cells had a greater thrombus generation. Cell localization after transplatated with primary hepatocytes (C) and hepatocyte-like cells (D) at 1wk, (E) precondition (F) Quantification of hepatocyte-like cells engraftment in the HB mice. The arrow indicated the transplantated cell. Red: PKH 26; blue: DAPI. Magnification, 200x.

Chapter 3

Therapeutic Potential of Omentum Adipose Derived Stem Cells in Acute Liver Failure

3.1 Summary

Acute liver failure (ALF) is the most dramatic clinical situation and has high mortality. For the disease, the liver transplantation is only effective treatment but the shortage of donor organ limits the application. Therefore, cell therapy is expected to be a bridge therapy for helping patient to sustain longer waiting time for transplantation. Mesenchymal stem cells (MSCs) have properties of high proliferation rate, differentiation capacity and proper immunomodulation, and they are grow in popularity derived from the bone marrow and subcutaneous adipose tissues. Omentum adipose tissue is an alternative cell source of MSCs for cell therapy. In this dissertation, I isolate and culture adipose stem cells (ASCs) from mice omentum adipose tissues. These cells express MSCs properties, including fibroblast-like morphology, surface marker and differentiation ability. The hypothesized antioxidant effect of omentum ASCs to savage excessive reactive oxygen species (ROS) and protect hepatocytes against toxicity induced by acetaminophen (APAP) were examined. Results showed the transplantation of omentum ASCs is able to improve significantly the survivals of mice with APAP-induced acute liver failure, and these cells can scavenge ROS generation through downregulation of Nrf2 activation, and decrease toxic peroxynitrite formation by suppressing CYP2E1 expression. Moreover, the omentum ASCs can attenuate the subsequent inflammatory response and MAPK signal activation to protect APAP-induced hepatocyte death.

3.2 Introduction

Acute liver failure (ALF) is severe liver dysfunction with rapid progression and high mortality, which is mainly developed due to viral infection or medication overdose. Inflammation is a common feature of ALF, which is associated with a more rapid progression of hepatic encephalopathy and intracranial hypertension. Acetaminophen, originally developed as an effective analgesic and antipyretic, was documented to cause severe liver damage severe liver damage and accounted for the most common cause of ALF (Larsen A et al., 2007). APAP toxicity is controlled by cytochrome P450, particularly cytochrome P450 subfamily 2E1 (CYP2E1), through the formation of N-acetyl-p-benzoquinoneimine (NAPQI), a highly reactive intermediary and toxic metabolite. This compound subsequently induces oxidative stress and covalently binds to liver proteins, causing cell death and dysfunction. At therapeutic doses, NAPQI conjugates with intracellular glutathione (GSH), and is excreted from the kidney. However, the overdose of APAP leads to increased NAPQI production, the rapid depletion of GSH and peroxynitrite formation (James LP et al., 2003). Excessive NAPQI formation can trigger cell damage via an imbalanced oxidative stress with high levels of reactive oxygen species (ROS), such as superoxide (O_2^-), hydroxyl radicals (OH·) and peroxynitrite, and low levels of antioxidant enzymes, such as superoxide dismutase (SOD), glutathione peroxidase (GPx) and catalase. Antioxidant defenses can scavenge the excess ROS. For example, SOD can convert O_2^- into H_2O_2 and then further convert H_2O_2 into H_2O and O_2 by GPx and catalase (Jorge LP et al., 2009). Consequently, GSH can prevent the covalent binding of toxic metabolites and suppress oxidative stress, which is a potential approach to attenuate APAP toxicity and promote tissue repair/regeneration. Currently, liver transplantation is an effective therapy but organ shortage is a big problem. Therefore, it is urgent to develop an effective treatment strategies for ALF treatment.

MSCs are multipotent stem cells with stem cell properties, including self-renewal and differentiation ability. The cells are mostly isolated from bone marrow. However, the adipose tissue, as an alternative source, can provide the MSCs by a less invasive method and in larger quantities than bone marrow. Based on this, adipose tissues have recently been considered as a potential ideal source of MSCs for clinical application because the adipose tissue could be collected by minimally invasive procedures, with the ability to harvest large quantities and their higher potential immunomodulation and anti-inflammatory functions compared with those of other sources (Banas A et al., 2008). First isolated adipose stem cell was performed from subcutaneous approach in 2001. These cells are very similar to mesenchymal stem cells (MSCs) form bone marrow in cell surface marker, including positive for CD29, CD90, CD44, negative for CD31, CD34, and differentiation ability (Zuk PA et al. 2002). In addition, ASCs exert protective effects and antioxidant properties, and enhance tissue repair and regeneration in animal models of kidney (Chen YT et al., 2011) and liver failure (Salomone F et al., 2013). However, the underlying mechanisms of the antioxidant effects and the potential survival benefits are not fully understood. The omentum is the primary and largest intraperitoneal reservoir of adipose tissue. This tissue can be harvested easily during abdominal surgery, and it is available through a minimally invasive surgery approach. Therefore, omentum may be candidate for stem cell source.

In this study, we hypothesized that omentum is a source of multipotent stem cells, and have therapeutic potential in ALF. For this purpose, we isolate and characterize ASC from mice omentum adipose tissue, then to assess therapeutic potential of omentum-derived ASCs in mice with APAP-induced ALF.

3.3 Material and Methods

3.3.1 Animal

All mouse experiments were approved by the institutional animal care and use committee at National Taiwan University. C57BL/6 mice were purchased from National Laboratory Animal Center, Taipei, Taiwan. C57BL/6 mice were used to acquire normal hepatocytes, adipose stem cells, and establish ALF model.

3.3.2 Hepatocyte

Mouse hepatocytes were isolated using a two-step collagenase perfusion method. The liver was perfused with Hank's balanced salt solution (HBSS, Gibco, Grand Island, NY) containing 0.1mM EGTA at 37℃for 10 minutes at the rate of 3 mL/minutes. Then, perfusion with 0.025% of collagense type IV prepare in HBSS containing 5 mM $CaCl_2$ for 10 minutes at 2 mL/minutes. After enzyme digestion, the liver was dissected out, hepatocytes were released and filtered through a 70μm cell strainer. After centrifugation at 50 xg for 3 minutes, pellet was washed with HBSS containing 5 mM $CaCl_2$ and cultured in hepatocyte culture medium supplement 10% FBS.

3.3.3 Isolation and characterization of omentum ASCs

ASCs were isolated from mouse omentum adipose tissue, which was cut into small pieces and digested in 0.5 units/ml of collagenase type I (Life Technologies, Paisley, UK) for one hour at 37 °C. After centrifugation at 1500 rpm for 5 minutes, the pellet was resuspended with PBS (Corning, NY, USA) and seeded into minimum essential medium eagle-alpha modification (α-MEM) supplemented with 1 x antibiotic (Invitrogen, NY, USA) and 10% fetal bovine serum (FBS, SBI Biological Industries, Belt Haemak, Israel). After 24 hours of incubation, the cells were washed with phosphate-buffered saline (PBS), and then the medium was replaced with fresh medium. For all experiments, the cells were used after 3-7 passages and the medium was changed every 3 days.

For ASC characterization, the cells were stained with CD31-PE-CY7, CD34-FITC, CD44-PE, CD90-PE (BD Pharmingen, San Diego, CA, USA), CD105-PE (eBioscience, San Diego, CA, USA), and CD29-FITC (BioLegend, San Diego, CA, USA) and then analyzed by flow cytometry (all antibodies were diluted 1:100 with PBS containing 2% FBS). To evaluate the cell differentiation ability, adipogenic and osteogenic assays were modified according to Sotiropoulon et al. [9]. To evaluate hepatogenic differentiation, the cells were cultured in α-MEM containing 20 ng/ml epidermal growth factor (EGF) and 10 ng/ml fibroblast growth factor (FGF; PeproTech, Rocky Hill, NJ, USA) for two days; the medium was then replaced with α-MEM containing 20 ng/ml hepatocyte growth factore (HGF; PeproTech) and 4.9 mM nicotinamine (Sigma-Aldrich, St Louis, MO, USA) for one week, followed by treatment with 20 ng/ml oncostatin M (PeproTech), 1 μmol/L dexamethasone (Sigma-Aldrich), and 50 mg/mL insulin-transferrin-selenium (ITS; Gibco, Paisley, UK) that was prepared in α-MEM for one week. Glycogen storage was measured by periodic acid-Schiff (PAS) staining (Sigma-Aldrich).

3.3.4 ALF model and omentum ASC transplantation

ALF was induced in 8-week-old male C57BL/6 mice. APAP (Sigma-Aldrich) was prepared in saline at 70 °C and maintained in a water bath at 37 °C. Mice were fasted overnight and treated with APAP (600 mg/ kg, intraperitoneally) then randomly divided into two groups: one group was infused with PBS (100 μl/mouse), and the other group was infused with omentum ASCs (10^6/100 μl/mouse) via tail vein injection at 30 minutes after APAP treated. For survival, the mice were monitored by 168 hours (20 mice/group); At 6 hours and 24 hours after omentum-derived ASCs with/without infusion (10 mice/group), liver tissue and serum were collected and stored at -80 °C. The liver enzyme (glutamate-oxaloacetate transaminase, GOT; glutamic-pyruvic transaminase, GPT) were evaluated by the Laboratory Animal Center of National Taiwan University Medicine (Fig. 3-1B).

3.3.5 Real-time quantitative PCR (QPCR)

For real-time quantitative PCR (QPCR), total RNA was extracted from liver tissue with a Direct-Xol™ RNA MiniPrep kit (Zymo Research, CA, USA). Reverse transcription was performed with an iScript™ cDNA Synthesis kit (Bio-Rad). Q-PCR was performed by using an iCycler real-time detection system and SYBR Green Supermix system (Bio-Rad) according to the manufacturer's protocol. The primer sequences are provided in Table 3.1. The relative mRNA levels were determined by Q-PCR and normalized to GAPDH.

3.3.6 Immunohistology

The sections were stained with hematoxylin and eosin (H&E; Sigma-Aldrich) for histology, and the necrosis grade was evaluated in 20 random 100 x images per animal, as described by Liu et al. as follows: "0" indicated normal; "1" indicated necrotic cells in the first cell layer adjacent to the central vein; "2" indicated necrotic cells extending two to three cell layers from the central vein; "3" indicated necrotic cells extending three to six layers from the central vein; "4" indicated necrotic cells extending three to six layers and from one central vein to another; and "5" indicated necrotic cells throughout the section. The sections were deparaffinized and dehydrated for immunohistology, and the endogenous peroxide was inactivated with 3% hydrogen peroxidase (Sigma-Aldrich). The sections were then blocked with 3% normal goat serum (DAKO, Glostrup, Denmark) for one hour, stained with primary antibodies against cytochrome P450 subfamily 2E1 (1:200), 4-hydroxynonenal (1:200, Abcam, Cambridge, MA, USA), or nitrotyrosine (1:50, clone 2A8.2, Millipore, Bedford, MA, USA) for one hour at 37 °C and then incubated with an horseradish peroxidase (HRP)-detection kit (REAL™ EnVision, DAKO) according to the manufacturer's protocol.

3.3.7 Antioxidant enzyme activity assay and GSH content measurement

The activity of the antioxidant enzymes (SOD, GPx, and catalase) and the GSH content were measured according to the manufacturer's protocol (BioVision, Palo Alto, CA, USA). In brief, the liver tissues from the APAP treatment and the omentum-derived ASC transplantation groups were lysed in PBS by sonication, and the supernatants were collected by centrifugation. For the in vitro experiments, hepatocytes (10^5) that had been treated with 15 mM APAP were grown in the lower chambers of a six-transwell plate (0.4 μm pore size; BD, Bioscience, San Jose, CA, USA), and omentum-derived ASCs (10^5) were added to the upper chambers. Twenty-four hours later, the hepatocytes were washed and lysed, and the lysate was collected by centrifugation.

3.3.8 Western blot

Total proteins were extracted in lysis buffer (300 mM NaCl, 50 mM HEPES pH 7.6, 1.5 mM $MgCl_2$, 10% glycerol, 1% Triton X-100, 10 mM $NaPyrPO_4$, 20 mM NaF, 1 mM EGTA, 0.1 mM EDTA, 1 mM DTT, 1 mM PMSF, and 1 mM Na_4VO_3) containing phosphatase inhibitors (all were purchased from Sigma-Aldrich), quantified by protein assay (Bio-Rad, Hercules, CA, USA), separated by 10% SDS-PAGE (Bio-Rad) and transferred to PVDF membranes (Millipore). After being blocked with 5% bovine serum albumin (Sigma-Aldrich) in TBS buffer (50 mM Tris-HCl, 150 mM NaCl pH 7.2) with 0.1% Tween (Sigma-Aldrich) overnight, the membrane was incubated with primary antibody overnight at 4 °C (JNK, phospho-JNK, ERK, phospho-ERK, p38, and phospho-p38 were purchased from Cell Signaling Technology, Danvers, MA, USA 1:2000; cytochrome P450 subfamily 2E1 and 4-hydroxynonenal were purchased from Abcam, 1:1000; and nitrotyrosine and actin were purchased from Millipore at 1:500 and 1:3000, respectively), followed by HRP-conjugated secondary antibody (1:10000, Jackson ImmunoResearch Laboratories, West Grove, PA, USA) for one hour at room temperature. The protein intensity was detected with electrochemiluminescence (ECL) reagent (Millipore) according to the manufacturer's protocol. The

western blot band intensity was quantified with the ImageJ software according to the manufacturer's instructions.

3.3.9 ROS, viability and LDH assays

For the ROS assays, the primary hepatocytes were seeded in a 96-well plate (Corning) and treated with various concentrations of APAP (0, 5, 10, 15, 20, and 40 mM) for 24 hours. CellROX Deep Red reagent (Life Technologies) was added 30 minutes before the end point and then washed out with PBS. The ROS intensities were determined by using an ELISA reader (Ex/Em: 644/655 nm, BioTek, Instruments, Inc., Winooski, VT). Cell viability was assessed by the MTT assay (Sigma-Aldrich). Cytotoxicity was determined using the LDH activity assay (BioVision) according to the manufacturer's instructions.

3.3.10 Statistical analysis

Values are presented as means ± SEM. Student's paired t-test or one-way ANOVA followed by Tukey's test was used for between-group comparisons of the means. The survival analysis was assessed with the SigmaStat software, version 3.5 (Chicago, IL, USA); other analyses were performed with the GraphPad InStat software, version 3 (San Diego, CA, USA). All directional P values were 2-tailed, and a value of .05 or less was considered significant for all tests.

3.4 Results

3.4.1 Omentum ASCs characterization

ASCs were derived from mouse omentum adipose tissues by collagenase digestion; these cells were attached culture and appear fibroblast-like shape. Omentum ASCs were characterized by surface marker expression via flow cytometry analysis. The results presented in Fig 3-2A indicate that the omentum ASCs expressed CD29, CD44, CD90, CD105, but these cells did not express the

endothelial marker CD31 or the hematopoietic marker CD34. Differentiation ability was assessed, omentum ASCs was cultured in adipogenic media toward the adipocytes after 14 days induction, lipid vacuole accumulation was demonstrated by Oil Red O staining (Fig. 3-2B1); Following 16 days of hepatogenic induction, glycogen deposition was staining with PAS (Fig. 3-2B2); Undergo 21 days of osteogenic differentiation, positive staining for Alizarin Red S confirmed the differentiation of omentum ASCs into osteocytes (Fig. 3-2B3). Therefore, the cells that were derived from mouse omentum tissue expressed specific surface markers for MSCs and possessed multi-lineage differentiation ability. These results indicate that omentum is an alternative source to obtain ASCs for subsequent studies or therapy.

3.4.2 Effects of omentum ASCs on APAP-induced damage in isolated hepatocytes

To investigate whether the omentum ASCs protect against APAP toxicity in primary mouse hepatocytes, we isolated primary hepatocytes and exposed them to various APAP concentrations to measure their ROS production by CellROX assay. The ROS generation was dose dependent and increased significantly in response to 15 mM and 20 mM of APAP exposure (Fig. 3-3B). The viability of the hepatocytes decreased significantly to 70% of the pretreatment level after treating with 10 mM APAP, and it decreased dramatically to 35% after treating with 15 mM APAP (Fig. 3-3A). We chose to administer 15 mM APAP during the subsequent in vitro co-culture mechanistic studies because no differences in viability were observed in omentum ASCs at this APAP concentration (Fig. 3-3A). The viability of APAP-treated hepatocytes increased significantly after co-culture with omentum ASCs compared with APAP exposure alone at 24 hours (52% compared with 35% at 15 mM APAP, $P<0.001$) (Fig. 3-3C). The LDH release after APAP treatment was higher than that of the control hepatocytes ($P<0.001$), but it was reduced in the omentum ASCs co-culture group ($P<0.05$) (Fig. 3-3D). These results show that omentum ASCs significantly increased the viability and markedly reduced the LDH release in hepatocytes that were treated with

APAP. NAPQI is a toxic metabolite of APAP that is able to cause GSH depletion by covalently binding to hepatic GSH. The GSH content of omentum ASCs co-cultured hepatocytes increased to 5.4 μg/ml (compared with 4.7 μg/ml in normal hepatocytes, $P<0.05$). The GSH content in cultured hepatocytes decreased to 1.67 μg/ml after APAP exposure but then increased to 2.78 μg/ml in APAP-treated hepatocytes that were co-cultured with omentum ASCs ($P<0.01$) (Fig. 3-4A). These results show that omentum ASCs increased hepatocytes hepatic GSH content, which could attenuate toxic NAPQI formation. Furthermore, the activity of antioxidant enzymes in hepatocytes significantly decreased after APAP exposure for 24 hours (catalase activity: 64.9%, Fig. 3-4D and GPx activity: 53.9%, Fig. 3-4B). The activity of antioxidant enzymes in APAP-treated hepatocytes increased significantly after co-culture with omentum ASCs (SOD and catalase activity: 10%, $P<0.05$ and GPx activity: 20%, $P<0.05$). Subsequently, we studied whether MAPK pathways were involved in the protection of omentum ASCs against APAP hepatotoxicity. The levels of JNK and ERK phosphoproteins were significantly increased in hepatocytes at 12 hours and 24 hours after APAP exposure but were suppressed after co-culture with omentum ASCs (Fig. 3-5). Therefore, the activation of the JNK/ERK/P38 pathway by APAP metabolites was diminished by omentum ASCs treatment.

3.4.3 Omentum ASCs improve the survival rate of mice on acute liver failure induced by APAP

To explore the therapeutic effects of omentum ASCs on ALF, we used the ALF mouse model induced by APAP. Eight of 20 mice were died within 24 to 72 hours after 600 mg/kg of APAP injection (60% of survival rate), only 10% of mice were died after omentum ASCs treatment (90% of survival rate vs. control group). The overall differenece in survival rate between groups with and without omentum ASCs was significant ($P \leq 0.01$, Fig. 3-6A). The severity of APAP-induced liver damage was evaluated by measuring the plasma liver enzyme level at 6, 24, and 168 hours after

APAP injection. The plasma GPT level decreased significantly at both time points after treatment with omentum ASCs (5,097 ± 703 IU/L compared with 2,787± 260 IU/L at 6 hours, $P<0.01$, and 11259 ± 1,159 IU/L compared with 8,141 ± 910 IU/L at 24 hours, $P<0.05$) (Fig. 3-6C). The plasma GOT level was decreased but no statistic significant at 24 hours after APAP injection (Fig. 3-6B). In addition, liver histological staining showed extensive necrosis with inflammation and ballooning in the centrolobular region at 6 hours after APAP exposure (Fig. 3-7A, 3-7E) (histological necrosis score: 3.8, Fig. 3-6D) and extremely severe necrosis (score: 4) at 24 hours after APAP administration (Fig. 3-7C, 3-7G). The transplantation of omentum ASCs decreased the area of cell necrosis (Fig. 3-7B, 3-7F, 3-7D, 3-7H) and significantly attenuated the histological necrosis score severity (2.5 at both 6 and 24 hours, $P<0.01$, Fig. 3-6D). These results showed that omentum ASCs have therapeutic effects on APAP-induced liver toxicity.

3.4.4 Omentum ASC transplantation prevents GSH depletion and enhances antioxidant enzyme activity

Whether the hepatoprotective effect of omentum ASCs was associated with antioxidant activity in APAP-induced liver injury? The GSH levels dramatically declined after 6 hours of APAP exposure, indicating that the high oxidative stress was induced after APAP injection. However, the depletion of the liver GSH content significantly improved 6 hours after omentum ASC transplantation, with higher hepatic GSH content than the content after APAP administration ($P<0.01$) (Fig. 3-12A). Moreover, APAP overdose caused oxidative stress that resulted from an imbalance between oxidant generation and antioxidant defense. Transplantation with omentum-derived ASCs significantly increased hepatic antioxidant enzyme activity. SOD activity (Fig. 3-12B) was increased by 47%, GPx activity (Fig. 3-12D) was enhanced by 28%, and catalase activity (Fig. 3-12C) increased by as much as 12% compared with the activity levels in the APAP administered group. Furthermore, Nrf2 is a master regulator of the transcriptional activation of

genes related to the antioxidant defense system, and it controls downstream heme oxygenase-1 (HO-1) expression. We examined Nrf2, HO-1 and NADPH quinone oxidoreductase 1 (NQO1) gene expression by Q-PCR and found that these gene expression significantly increased in the omentum ASC group compared with the APAP-treated group (Fig. 3-13). These results suggested that omentum-derived ASCs protect against APAP toxicity by enhancing antioxidant defense and reducing GSH depletion.

3.4.5 Omentum ASCs affect the metabolism of APAP

We further studied whether the transplantation of omentum ASCs affected APAP metabolism. CYP2E1 is an important cytochrome enzyme that is responsible for the toxic metabolism of APAP to NAPQI, which depletes GSH. Additionally, CYP2E1 binds to vital proteins and causes cell death. Immunohistology revealed that CYP2E1 was strongly expressed 6 hours after APAP treatment (Fig. 3-8A, 3-8E) but weakly expressed in the omentum ASCs group (Fig. 3-8B, 3-8F)). The transplantation of omentum ASCs markedly reduced the expression of CYP2E1 protein 24 hours after APAP treatment (Fig. 3-8C, 3-8G). Beside, other forms of cytochrome P450 expression were revealed that CYP1A2 protein was decreased significantly at 24 hours (Fig. 3-11A) and Cyp2a5 gene level was reduced significantly at 6 hours after omentum ASCs transplantation (Fig. 3-11B). Oxidative stress induces lipid peroxidation to produce 4-HNE, and 4-HNE is considered a biomarker of lipid peroxidation. After 24 hours of APAP exposure, the liver sections showed increased 4-HNE-positive cells that were localized in the centrilobular area (Fig. 3-9A. 3-9E). Immunohistology and western blots showed that the 4-HNE expression in the omentum ASC transplantation group was lower than that of the APAP group (Fig. 3-9, 3-11). Moreover, APAP overdose caused nitrotyrosine protein formation in the centrilobular region. Protein nitration, which is a marker of oxidative stress that is caused by peroxynitrite, occurs through the rapid reaction of superoxide with nitric oxide. Nitrotyrosine protein increased strongly in the centrilobular regions 24

hours after APAP injection (Fig. 3-10A, 3-10C) but was weakly expressed in the omentum ASC treatment group (Fig. 3-10B. 3-10D). Therefore, the transplantation of omentum ASCs suppressed cytochrome P450 activity by decreasing the production of the toxic APAP metabolite NAPQI. This response led to the decreased consumption of GSH and decreased oxidative stress, protecting hepatocytes from APAP-induced cell damage.

3.4.6 Omentum ASCs attenuate MAPK signal activation and the inflammatory response in vivo

Accumulated toxic APAP metabolites can generate oxidative stress and subsequently activate mitogen-activated protein kinases (MAPK) signaling and inflammatory cytokine production to induce further cell damage. The gene expression of the pro-inflammatory cytokines IL-1α (Fig. 3-14A) and IL-1β (Fig. 3-14B) decreased significantly in the omentum ASC group 6 hours after APAP injection. Gene expression of the anti-inflammatory cytokines IL-6 (Fig. 3-14C) and IL-10 (Fig. 3-14D) increased significantly in the omentum ASC group 6 hours after APAP injection. MAPK signaling pathways play critical roles in mediating APAP hepatotoxicity. The phosphorylation of the ERK and JNK proteins (pERK and pJNK) increased 6 hours after APAP injection, but this response was suppressed in the omentum ASC group (Fig. 3-15). These results showed that the protective effect of omentum ASCs against APAP toxicity also suppressed MAPK activation and attenuated the inflammatory response.

3.5 Discussion

With plenty of ASCs, the omentum has not yet been well studied. Omentum ASCs have the potential to be an alternative source for cell therapy. In this dissertation, we tried to identify whether the omentum-derived ASCs therapy can rescue the APAP-induced acute liver failure. Results showed the transplantation of omentum ASCs is able to improve significantly the survivals of mice

with APAP-induced acute liver failure, and these cells can scavenge ROS generation through downregulation of Nrf2 activation and decrease toxic peroxynitrite formation by suppressing CYP2E1 expression. Finally, the omentum ASCs can attenuate the subsequent inflammatory response and MAPK signal activation to protect APAP-induced hepatocyte death (Fig. 16). We deduce that the mechanism of the protective effects of omentum ASCs are immunosuppressing, though downregulation of proinflammatory cytokines (IL-1α, IL-1β) and upregulation of anti-inflammatory (IL-6, IL-10). And paracrine properties of ASC improved the liver function and guided ASCs homing to injury site mediated by their expression of growth factors and cytokines. It is worth noting that protective effects of ASCs are antioxidant. Based on these observations, omentum ASCs are highly resistant to APAP-induced death and scavenge ROS, with increased intracellular GSH levels and antioxidant enzyme activity mediated by Nrf2 expression.

APAP toxicity is mediated by cytochrome P450 metabolism to NAPQI, which causes hepatic GSH depletion, lipid peroxidation and nitrotyrosine protein accumulation, and leads to cell death. It has been suggested that an effective strategy for preventing APAP hepatotoxicity is the inhibition of CYP2E1 activity (McGill MR et al., 2013; Kay HY et al., 2011). Lee also showed that CYP2E1-knockout mice were less susceptible to APAP toxicity (Lee SS et al., 1996; Abdelmegeed MA et al., 2010). Immunohistology results showed that CYP2E1 expression decreased significantly in the omentum ASC group. In addition, CYP1A2 and CYP2A5 have metabolic activity toward APAP. The CYP1A2 and CYP2A5 were inhibited after omentum ASCs transplantation. Therefore, the suppression of cytochrome P450 activity would contribute the hepatoprotective effect of omentum ASCs. APAP-induced hepatotoxicity consists of a metabolic phase and an oxidative phase. During the metabolic phase, the metabolite NAPQI causes GSH depletion and covalent binding to liver proteins, which triggers cell dysfunction and generates ROS that induce lipid peroxidation and interfere with antioxidant defense mechanisms during the

oxidative phase (Reid AB et al., 2005). Nrf2 is a transcription factor that regulates the expression of phase II enzymes and transports protein metabolites to protect cells against oxidative stress (Gum SI et al., 2013). Chan et al. demonstrated that *Nrf2*$^{-/-}$ mice are more sensitive to APAP toxicity and have lower levels of liver GSH (Chan K et al., 2001). MSCs can also act as an antioxidant to regulate the oxidative microenvironment (Song H et al., 2010; Kuo TK et al., 2008; Cho KA et al., 2012). In a recent study (Liu Z et al., 2014; Salomone F et al., 2013) on MSC antioxidant ability, MSC transplantation was reported with reduced oxidative stress by supplying GSH in the liver of animals with APAP overdose. Thus, the protective effects of our data were consistent with their finding. Furthermore, key findings in the current study is that omentum ASCs were essential to upregulating Nrf2, and they inhibited cytochrome P450 expression to protect cells from APAP toxicity. It is possible that MSCs express CD44 markers, for the markers have already been reported with activation of the Nrf2 pathway to protect against APAP toxicity (Reid AB et al., 2005; Kim HJ et al., 2005; Harrill AH et al., 2009). We successfully isolated ASCs from the omentum and demonstrated their MSC properties. The results revealed that the omentum-derived ASCs significantly increased Nrf2 expression to activate antioxidant enzyme activity (SOD, GPx, and catalase) and cellular GSH synthesis. Omentum ASCs were able to scavenge excess ROS by activating the Nrf2 pathway, and lead to increased GSH synthesis and enhanced antioxidant defense. N-acetylcysteine (NAC) protects against APAP hepatotoxicity by increasing the intracellular GSH content that is available to conjugate to NAPQI in animal experiments (Yang R et al., 2009), indicating a role for these cells as a potential therapy for APAP-induced acute liver failure in clinical practice (Heard KJ et al., 2008). However, the NAC is limited with short therapeutic time window, adverse gastrointestinal effect and anaphylactoid reaction (Larsen A et al., 2007). Consequently, the antioxidative effect of omentum ASCs offers another therapeutic approach to protect against APAP hepatotoxicity in clinical practice.

The toxic metabolites of APAP damage hepatocytes with the release of inflammatory mediators, particularly IL-1α and IL-1β (Nakagawa H et al., 2008), which in turn induce further cell damage. MSCs also exhibit immunomodulatory properties (Yagi H et al., 2010; Sart S et al., 2014). Our results showed that omentum ASCs significantly suppressed the release of pro-inflammatory cytokines (IL-1α and IL-1β) and increased the release of anti-inflammatory cytokines (IL-6 and IL-10). The immunomodulation effect of omentum ASCs also contributed the efficiency of protection against APAP-induced hepatotoxicity. These inflammatory mediators are regulated by MAPK signal transduction, which plays a central role in cell survival, proliferation, apoptosis, and inflammation (Nakagawa H et al, 2012). One potential anti-inflammatory therapeutic strategy is to reduce pro-inflammatory cytokine release and to promote anti-inflammatory cytokine production through suppression of the activation of the MAPK (Ayroldi E et al., 2012; Salomone F et al., 2013). Our results showed that omentum ASCs also have an immunomodulatory effect by regulating the MAPK pathway. In this dissertation, we successfully obtained a novel adipose stem cells from omentum adipose tissue, and proved the ability of differentiation and expression of MSC marker. Taken together, omentum ASCs have hepatoprotective effect on APAP-induced ALF mice model through regulate CYP enzyme and activate Nrf2 to increase antioxidant enzyme activate.

Table 3-1. Primer sequence

Primer	Sequence (5′→ 3′)
HO-1, Forward	CACGCATATACCCGCTACCT
HO-1, Reverse	CCAGAGTGTTCATTCGAGCA
Nrf2, Forward	TTGGAAGGGCTAATGTCCAC
Nrf2, Reverse	CTCCAGCCTCTTGGTTTCTG
NQO1, Forward	TTCTGTGGCTTCCAGGTCTT
NQO1, Reverse	AGGCTGCTTGGAGCAAAATA
IL-1α, Forward	ACATCTTTGACGTTTCAGAGGTT
IL-1α, Reverse	ACGAAGACTACAGTTCTGCCATT
IL-1β, Forward	CCACAGCCACAATGAGTGATACT
IL-1β, Reverse	GAACTCAACTGTGAAATGCCACC
IL-6, Forward	ATTGGAAATTGGGGTAGGAAG
IL-6, Reverse	ACAAGAAAGACAAAGCCAGAGTC
IL-10, Forward	TGGGTTGCCAAGCCTTATCGG
IL-10, Reverse	ACCTGCTCCACTGCCTTGCTC
GAPDH, Forward	TGCAGTGGCAAAGTGGAGATT
GAPDH, Reverse	TCGCTCCTGGAAGATGGTGAT

HO-1, heme oxygenase-1; Nrf2, NF-E2-related factor 2; NQO1, NADPH quinone oxidoreductase 1.

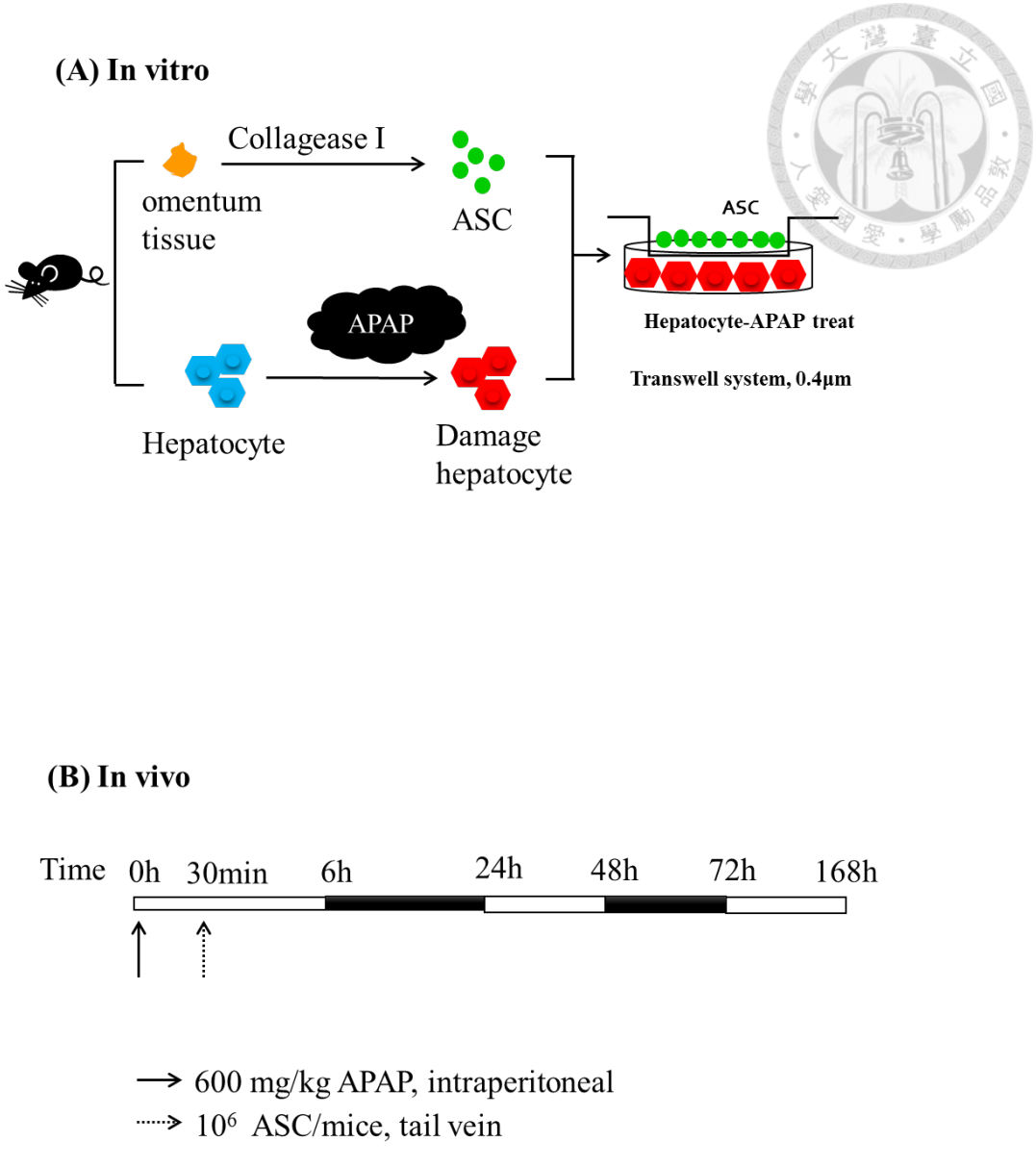

Figure 3-1 Experimental design. (A) The experimental design for in vitro: ASC were derived from mice omentum adipose tissue and using transwell system coculture with hepatocytes with APAP treated for assess protect against toxicity induced cell injury. (B) The experimental design for in vivo: Injectcion with 600 mg/kg of APAP via intraperitoneal for induce acute liver failure. After 30 mintures of APAP chanellege, transplant with omentum-derivedASCs by tail vein infusion to assess the therapeutic potential in acute liver failure. For survival assay, mice were monitored for 168h; for liver function and histology, the serum and tissue were collected at 6h and 24h. ASC, adipose stem cell; APAP, acetaminophen.

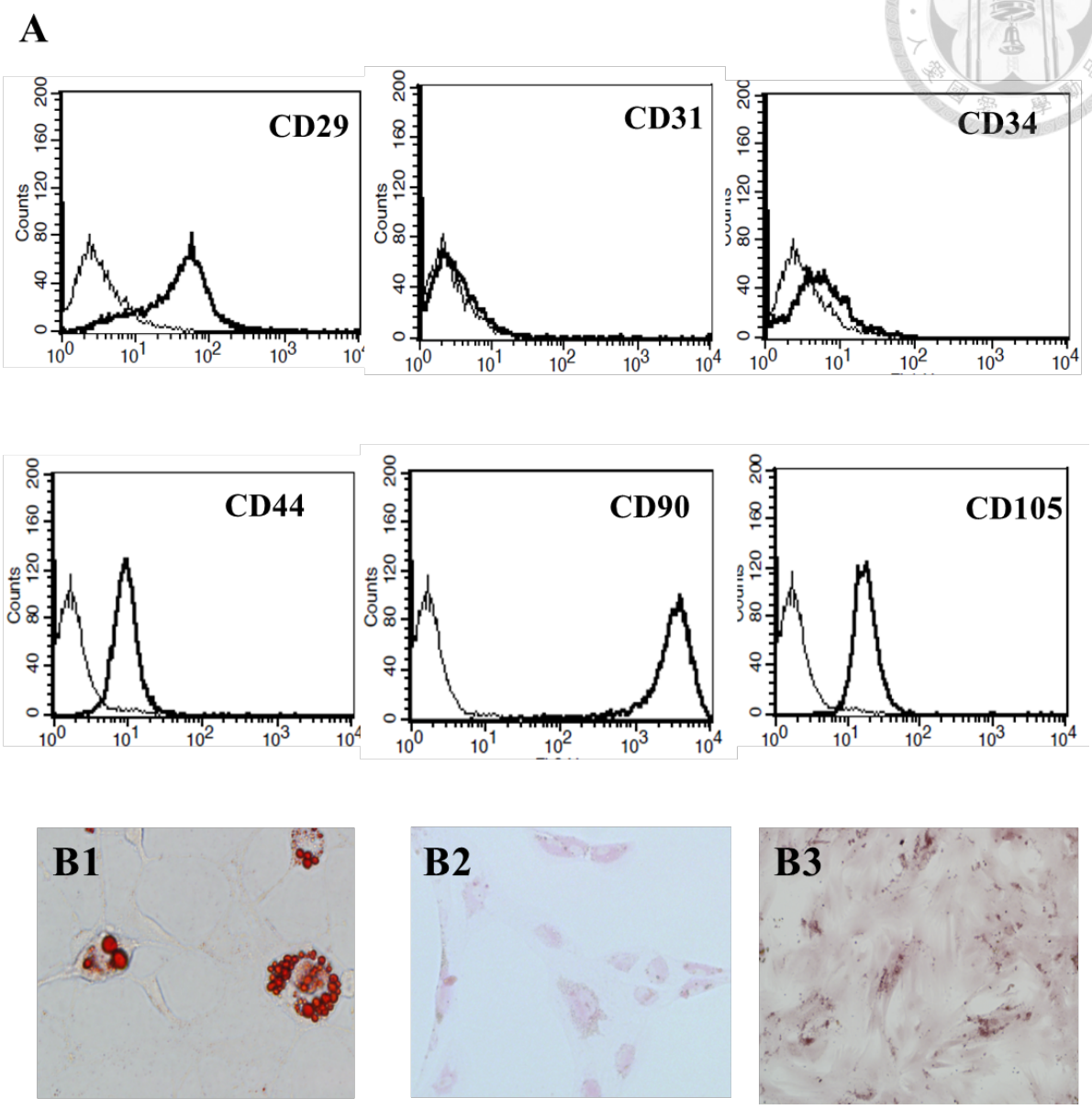

Figure 3-2 Phenotype and differentiation capacity of omentum ASCs. (A) Omentum-derived ASCs were stained with surface marker and analyze by flow cytometry. (B) Differentiation ability were assessed by omentum-derived ASCs culture in differentiation conditions. B1: adipogenic differentiation (Oil-O-red staining); B2: hepatogenic differentiation (periodic acid schiff (PAS) staining); B3: osteogenic differentiation (alizarin red staining), x200.

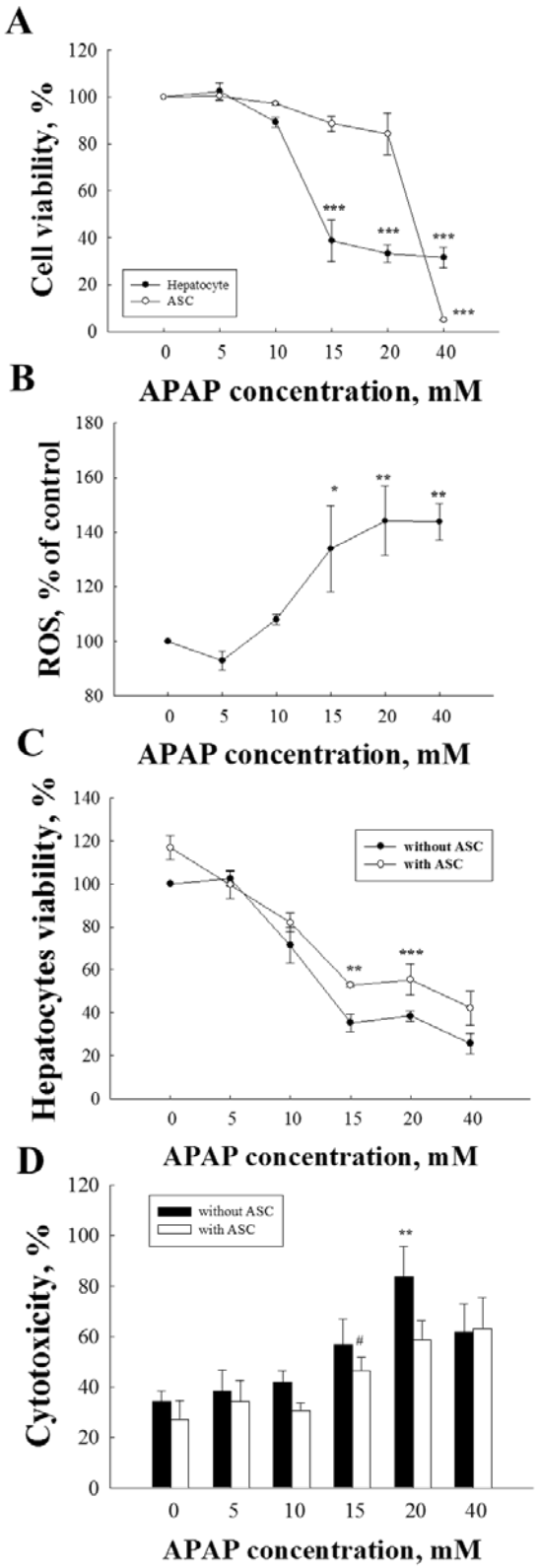
A
Cell viability, %
Hepatocyte
ASC
APAP concentration, mM
B
ROS, % of control
APAP concentration, mM
C
Hepatocytes viability, %
without ASC
with ASC
APAP concentration, mM
D
Cytotoxicity, %
without ASC
with ASC
APAP concentration, mM

Figure 3-3 Protective effect of omentum-derived ASCs on APAP induced hepatotoxicity. (A) Different dose of APAP were exposure to primary hepatocytes and omentum-derived ASCs for 24 hours. Using the MTT assay to measure the cell viability. (B) To measure the intracellular ROS levels by CellROX assay after 24h of APAP exposure to primary hepatocytes. Primary hepatocytes treated with APAP and culture with/without omentum-derived ASCs by transwell coculture system for 24h, hepatocytes viability were assessed by MTT assay (C), the culture media were collected for LDH activity. Data were expressed as the mean ± SEM, $n \geq 5$, *P<0.05, **P<0.01, ***P<0.001.

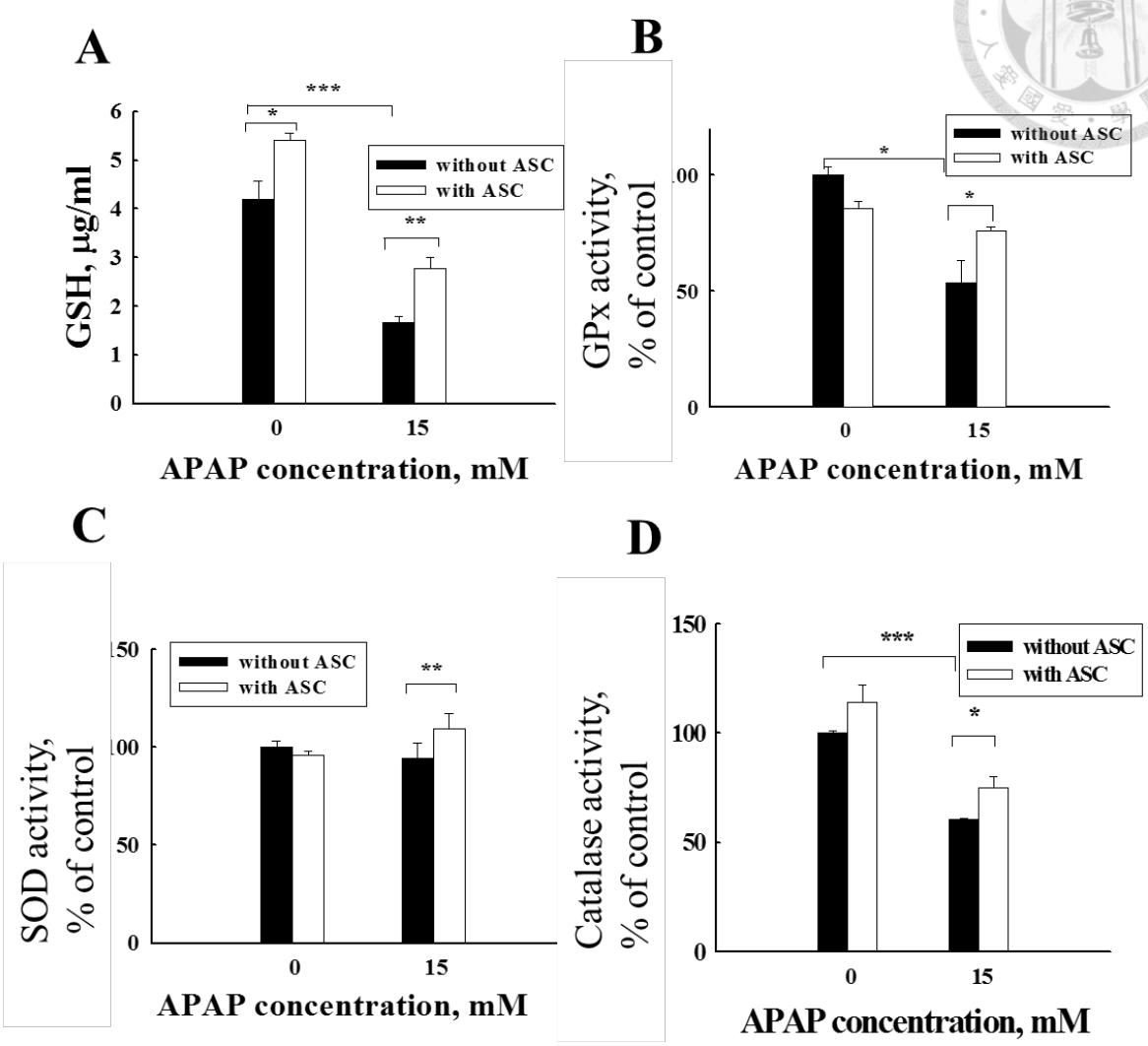

Figure 3-4 Effect of omentum-derived ASCs on antioxidant enzyme activity in hepatocytes after APAP exposure. Primary hepatocytes treated with 15 mM of APAP and culture with/without omentum-derived ASCs by transwell coculture system for 24h. The cell lysae were measured the GSH content (A), antioxidant enzyme activity: GPx (B), SOD (C), catalase (D). Data were expressed as the mean ± SEM, n ≥ 5, *P<0.05, **P<0.01, ***P<0.001.

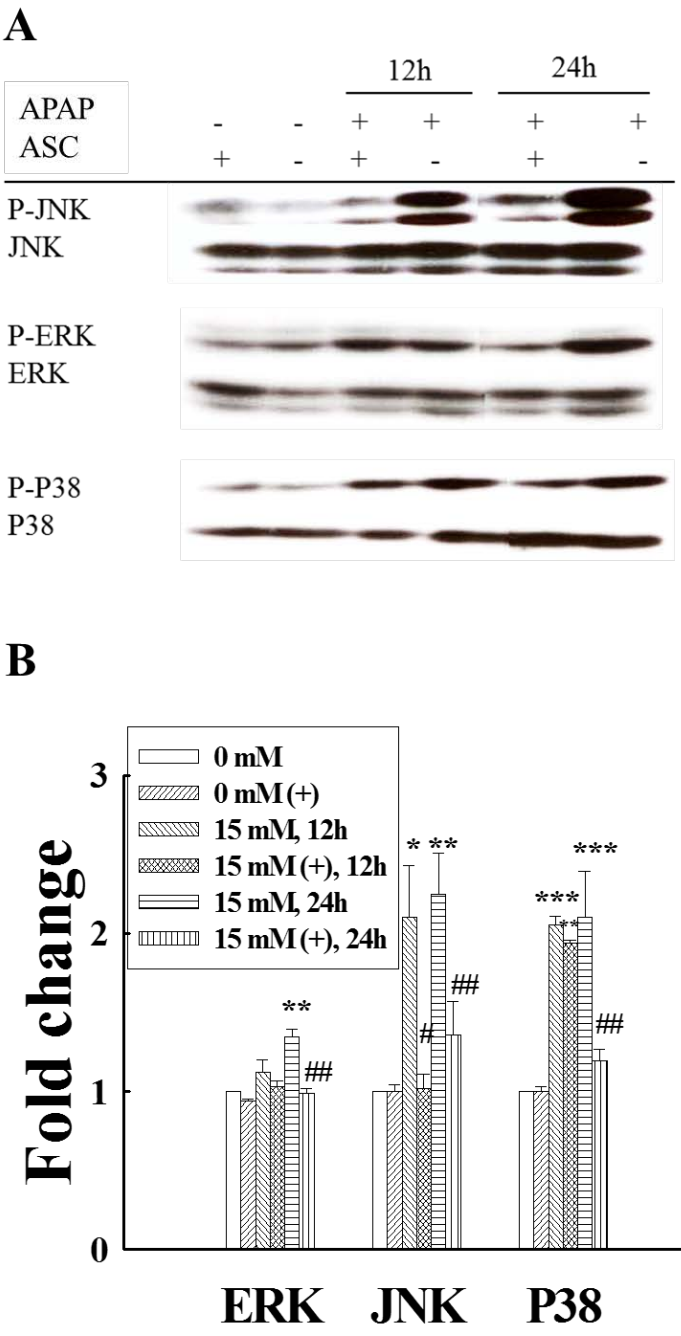

Figure 3-5 Effect of omentum-derived ASCs on MAPK in hepatocytes exposure to APAP. Primary hepatocytes treated with 15 mM of APAP and culture with/without omentum-derived ASCs by transwell coculture system for 12h and 24h. Cells were lysed and detected expression of ERK, JNK, and P38 by westerm blot (A). Quantification of phosphorylation in each lane was normalized by total protein levels. Data were expressed as the mean ± SEM, n ≥ 5, *P<0.05, **P<0.01, ***P<0.001. # indicates significant difference at same time.

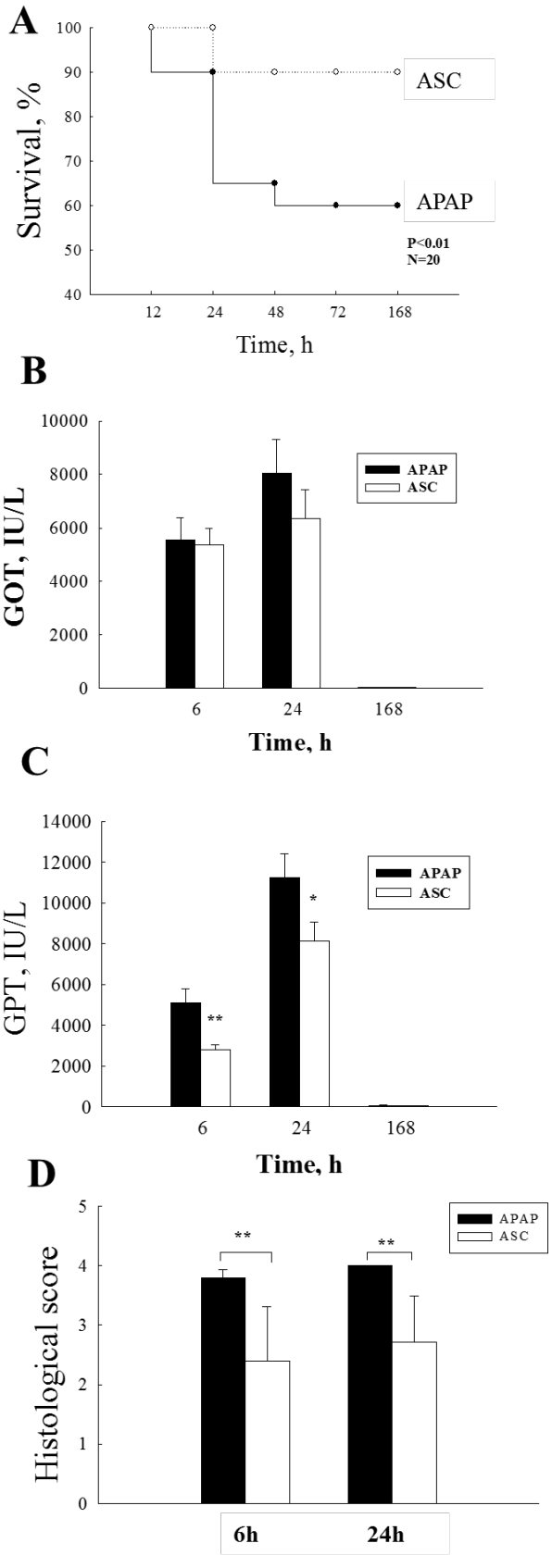
A
Survival, %
100
90
80
70
60
50
40
ASC
APAP
P<0.01
N=20
12
24
48
72
168
Time, h
B
GOT, IU/L
10000
8000
6000
4000
2000
0
APAP
ASC
6
24
168
Time, h
C
GPT, IU/L
14000
12000
10000
8000
6000
4000
2000
0
APAP
ASC
**
*
6
24
168
Time, h
D
Histological score
5
4
3
2
1
0
APAP
ASC
**
**
6h
24h

Figure 3-6 Omentum-derived ASCs improve survival and liver function in APAP-induced acute liver injury. Transplant with omentum-derived ASCs to acute liver failure mice induced by APAP (600mg/kg, i.p.) Survival rate was monitored for 7 days in with/without omentum-derived ASCs treatment on APAP-induced injury mice (n=20) (A). Plasma liver enzyme activity were measured at 6, 24 and 168 hours after omentum-derived ASCs treated on APAP-induced injury mice (B: GOT levels; C: GPT levels). Histological grade were analyzed by H&E section (D). Data were expressed as the mean ± SEM, $n \geq 5$, *P<0.05, **P<0.01.

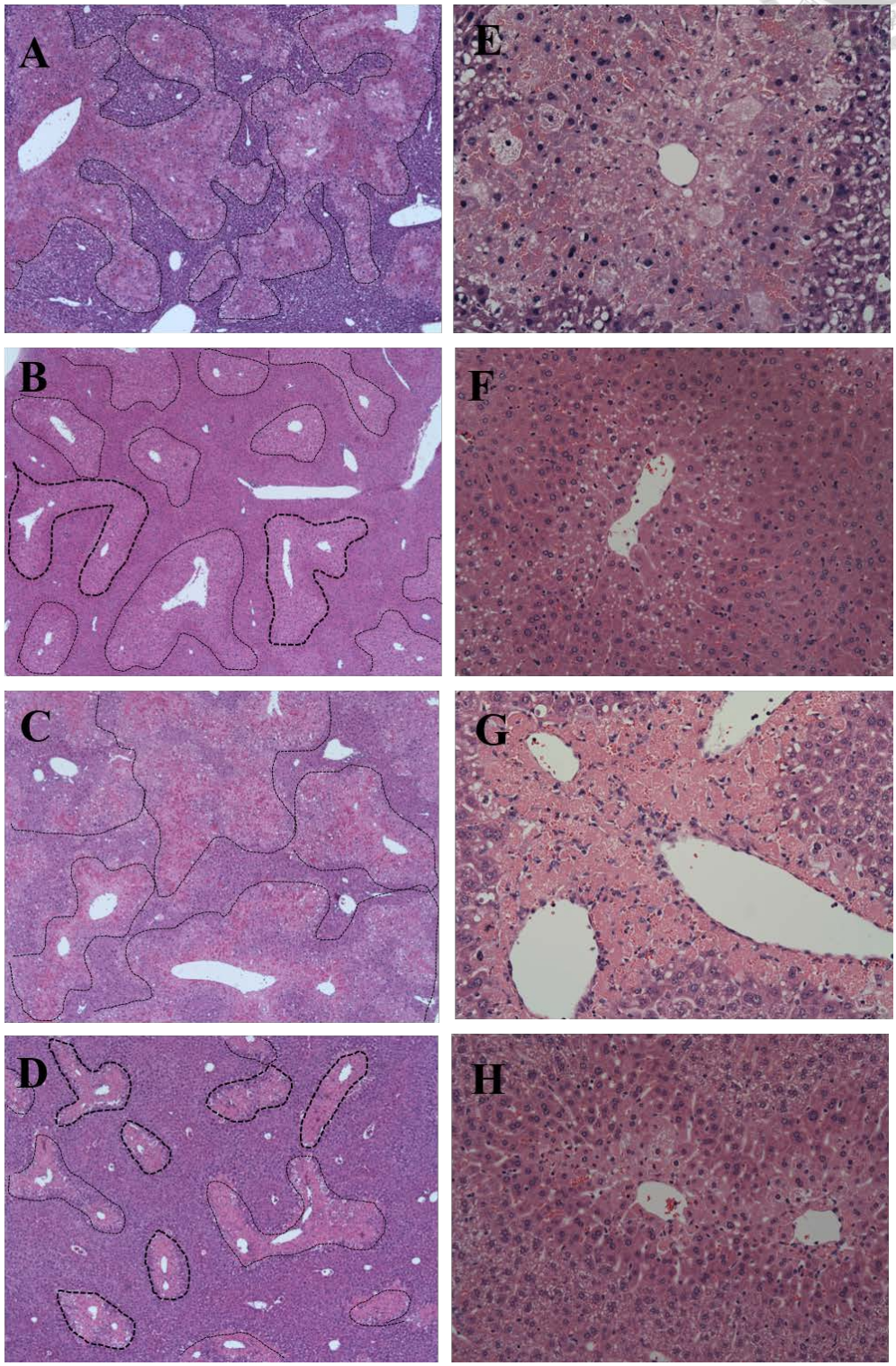
A
E
B
F
C
G
D
H

Figure 3-7 Omentum-derived ASCs reduces liver injury and inflammation in APAP-induced acute liver failure. Transplant with omentum-derived ASCs to acute liver failure model induced by APAP. HE staining showing APAP cause severe centriobular at 6h (A and E) and 24h (C and G), transplant with omentum-derived ASC reduces necrotic area (B and F at 6h; D and H at 24h). Dashed lines exemplify necrotic area. Magnification, 100x (A - D) 200x (E - H).

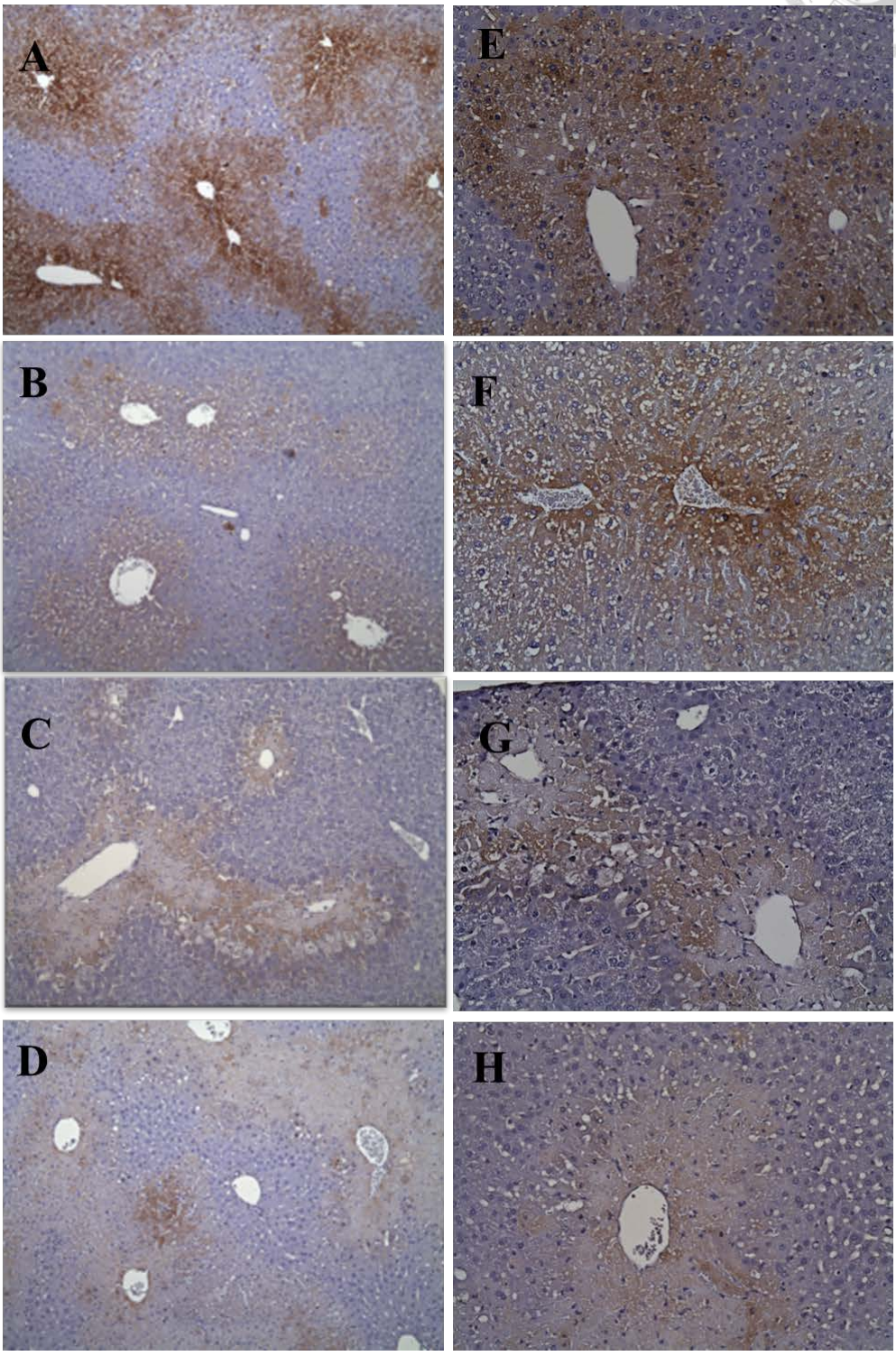
A
E
B
F
C
G
D
H

Figure 3-8 Omentum-derived ASCs reduces cytochrome P450 2E1 in APAP-induced acute liver failure. Transplant with omentum-derived ASCs to acute liver failure model induced by APAP. Immunohistology showing APAP increase cyptochrome P450 2E1 (brown) expression at 6h (A and E) and 24h (C and G), and decrease in omentum-derived ASC group (B and F at 6h; D and H at 24h). Magnification, 100x (A - D) 200x (E - H).

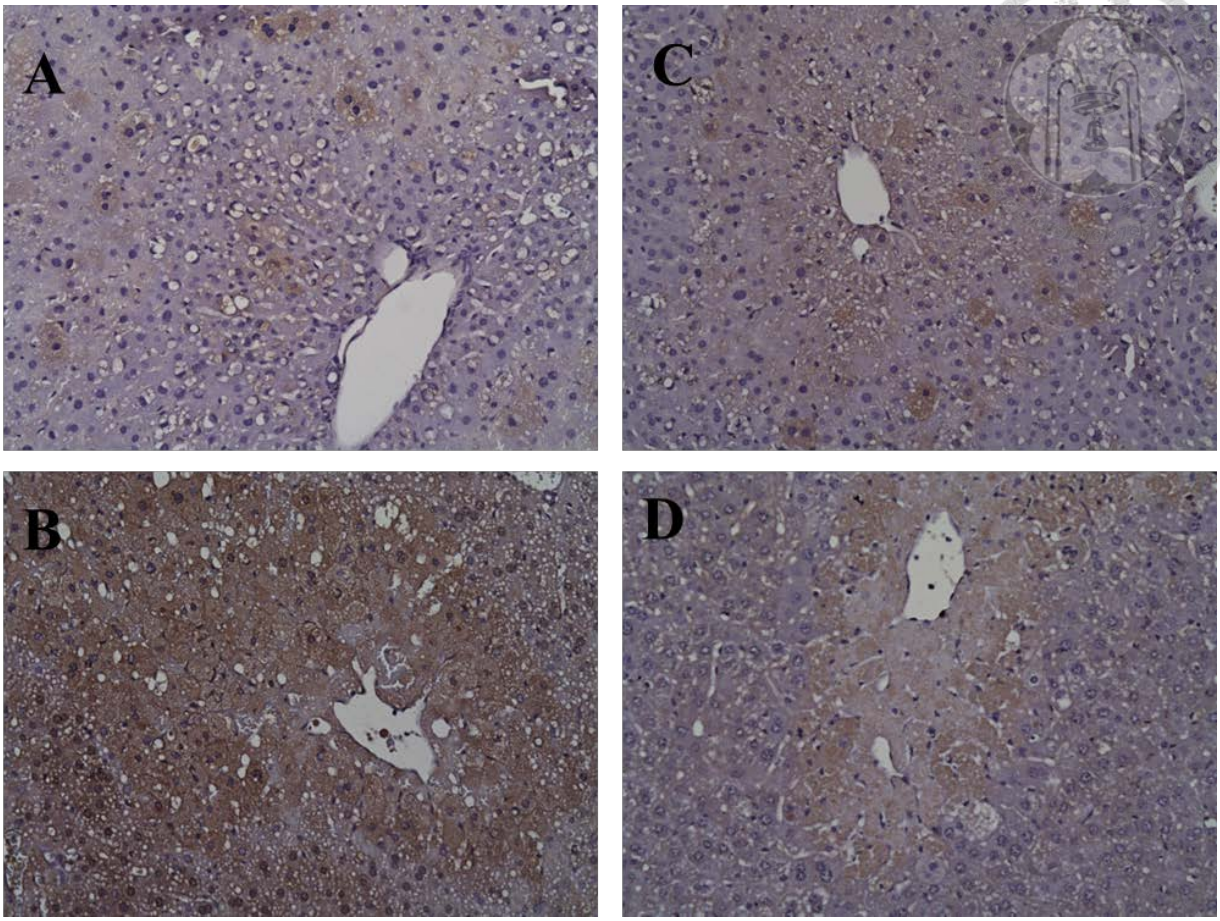

Figure 3-9 Omentum-derived ASCs reduces lipid peroxidation in APAP-induced acute liver failure. Transplant with omentum-derived ASCs to acute liver failure model induced by APAP. Immunohistology showing APAP increase expression of lipid peroxidation marker-4-HNE (brown) at 6h (A) and 24h (B), and reduce 4-HNE expression in omentum-derived ASC group (C at 6h; D at 24h). Magnification, 200x. 4-HNE: 4-hydroxynonenal.

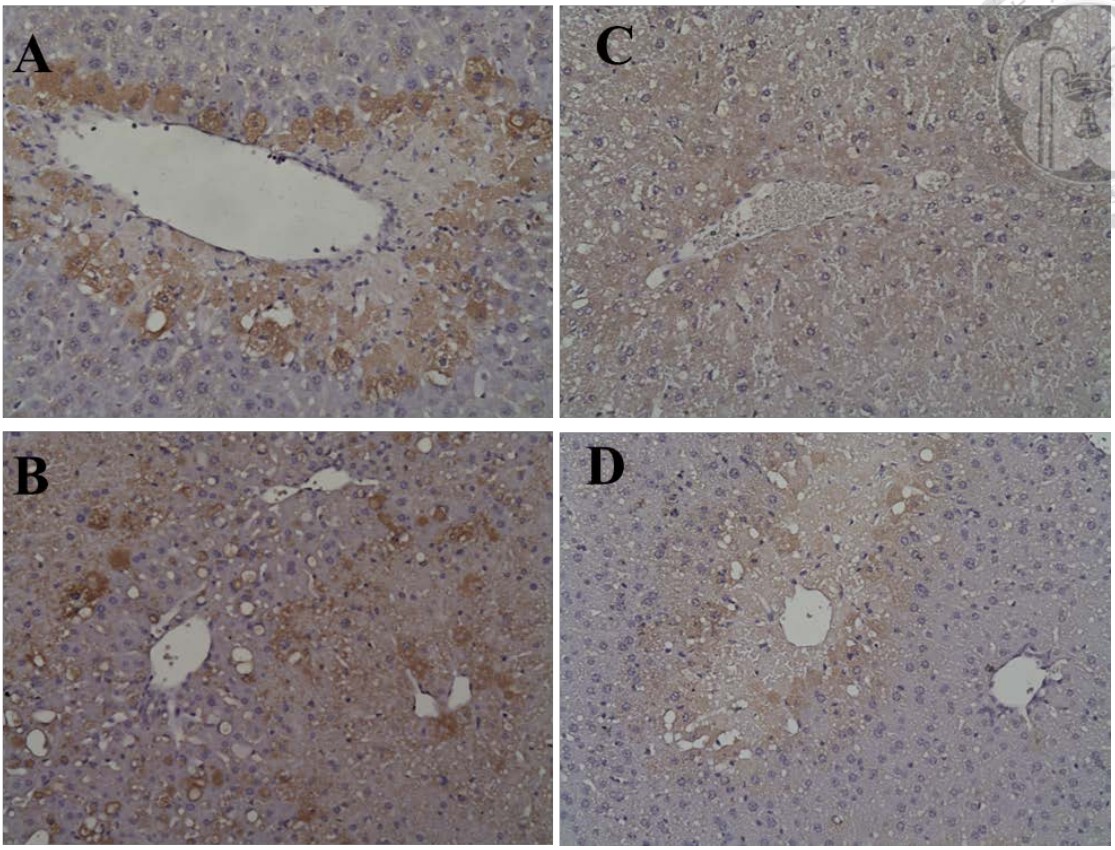

Figure 3-10 Omentum-derived ASCs reduces protein nitration in APAP-induced acute liver failure. Transplant with omentum-derived ASCs to acute liver failure model induced by APAP. Immunohistology showing APAP increase expression of NTR (brown) at 6h (A) and 24h (B), and reduce NTR expression in omentum-derived ASC group (C at 6h; D at 24h). Magnification, 200x. NTR, nitrotyrosine.

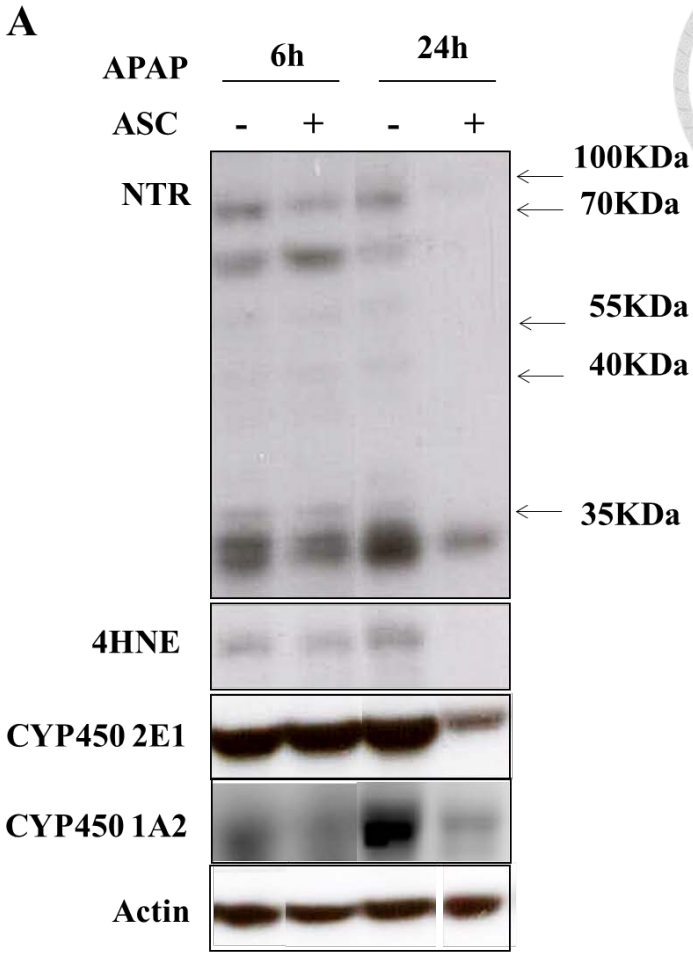
A
APAP
6h
24h
ASC
-
+
-
+
NTR
100KDa
70KDa
55KDa
40KDa
35KDa
4HNE
CYP450 2E1
CYP450 1A2
Actin
B
Cyp 2a5, relative expression
1.2
1.0
0.8
0.6
0.4
0.2
0.0
*
APAP
ASC
6h
24h

Figure 3-11 Omentum-derived ASCs alter metabolism of APAP in acute liver failure. (A) Following omentum-derived ASCs transplantation for 6 and 24 h, cytochrome P450 2E1 and cytochrome P450 1A2, 4HNE, NTR were detected by western blot. (B) Gene expression of cytochrome P450 2A5 were analysis by Q-PCR. Data were expressed as the mean ± SEM, $n \geq 5$, *$P<0.05$. 4-HNE: 4-hydroxynonenal, NTR: nitrotyrosine.

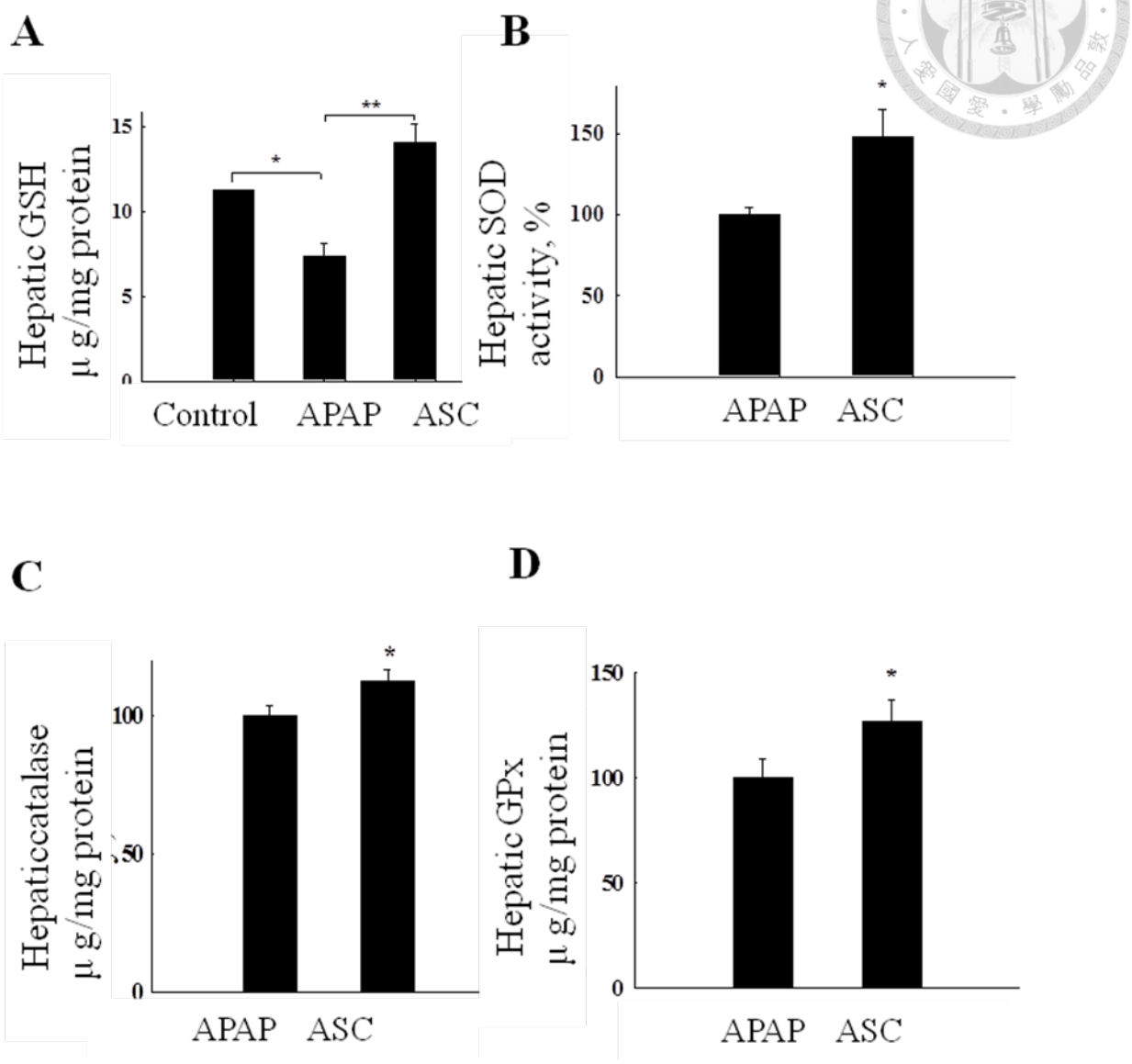

Figure 3-12 Omentum-derived ASCs enhance hepatic GSH contents and antioxidant activity for protect against APAP-induced acute liver failure. Following omentum-derived ASCs transplantation for 6h, the liver tissues were homogenized and measured the GSH levels (A) and antioxidant enzyme activities (B: SOD; C: catalase; D: GPx) in mice with APAP-induced acute liver failure. Data were expressed as the mean ± SEM, n ≥ 5, *P<0.05,**P<0.01. SOD, superoxide dismutase; GPx, glutathione peroxidase.

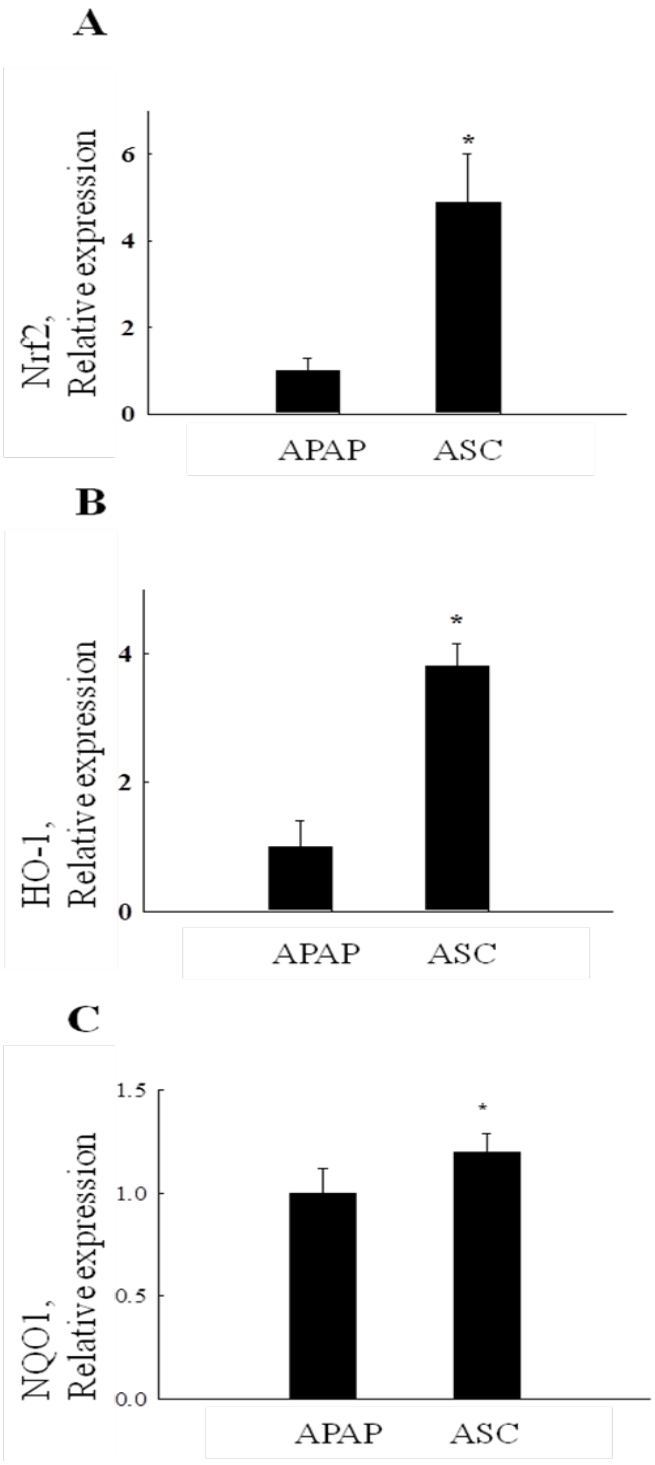
A
Nrf2,
Relative expression
6
4
2
0
*
APAP
ASC
B
HO-1,
Relative expression
4
2
0
*
APAP
ASC
C
NQO1,
Relative expression
1.5
1.0
0.5
0.0
*
APAP
ASC

Figure 3-13 Omentum-derived ASCs enhance Nrf2 expression on APAP-induced acute liver failure. Following omentum-derived ASCs transplantation into APAP-induced acute liver failure for 24h, hepatic Nrf2 (A), HO-1 (B), and NQO1 (C) mRNA expression were measured by QPCR assay. Data were expressed as the mean ± SEM, $n \geq 5$, *$P<0.05$.

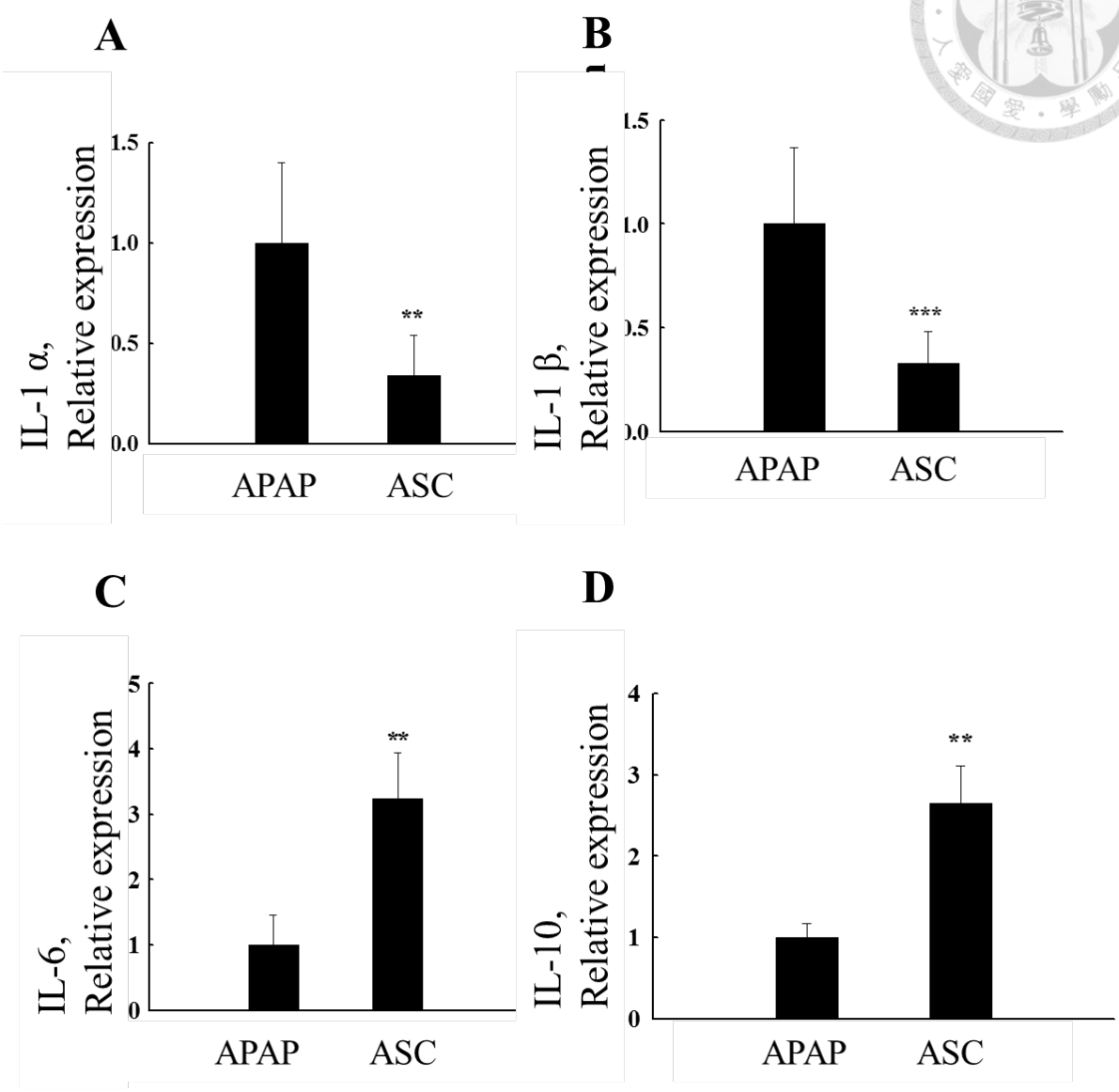

Figure 3-14 Omentum-derived ASCs inhibits inflammation in APAP-induced acute liver failure. Following omentum-derived ASCs transplantation into APAP-induced acute liver failure for 6h, RNA were extracted from liver tissues for measured the hepatic IL-1α (A), IL-1β (B), IL-6 (C), IL-10 (D) mRNA expression by QPCR assay. Data were expressed as the mean ± SEM, n ≥ 5, **P<0.01, ***P<0.001.

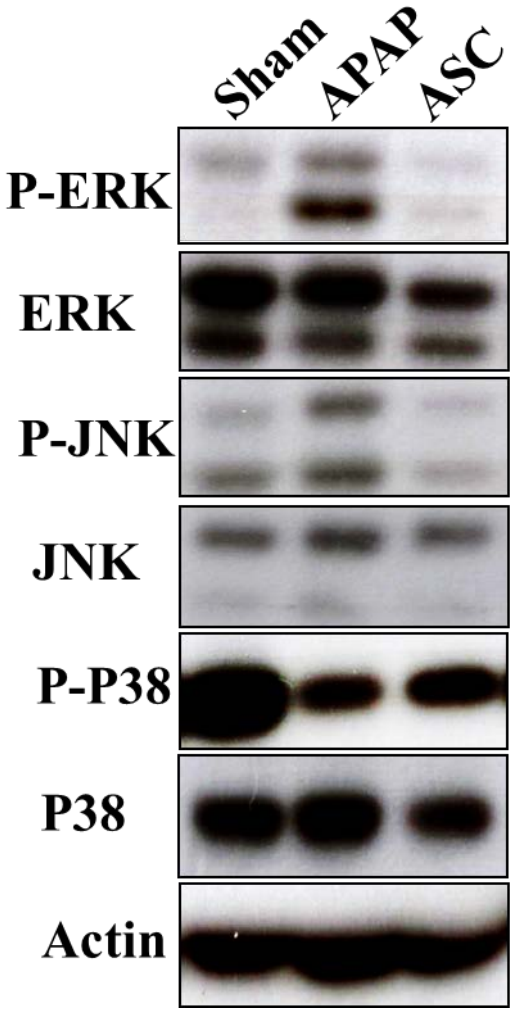

Figure 3-15 Omentum-derived ASCs suppressed MAPK activation in APAP-induced acute liver failure. Western blot shows MAPK signal was activate by APAP, while suppressed phospho-ERK, phospho-JNK expression in omentum-derived ASCs transplantation group at 6h.

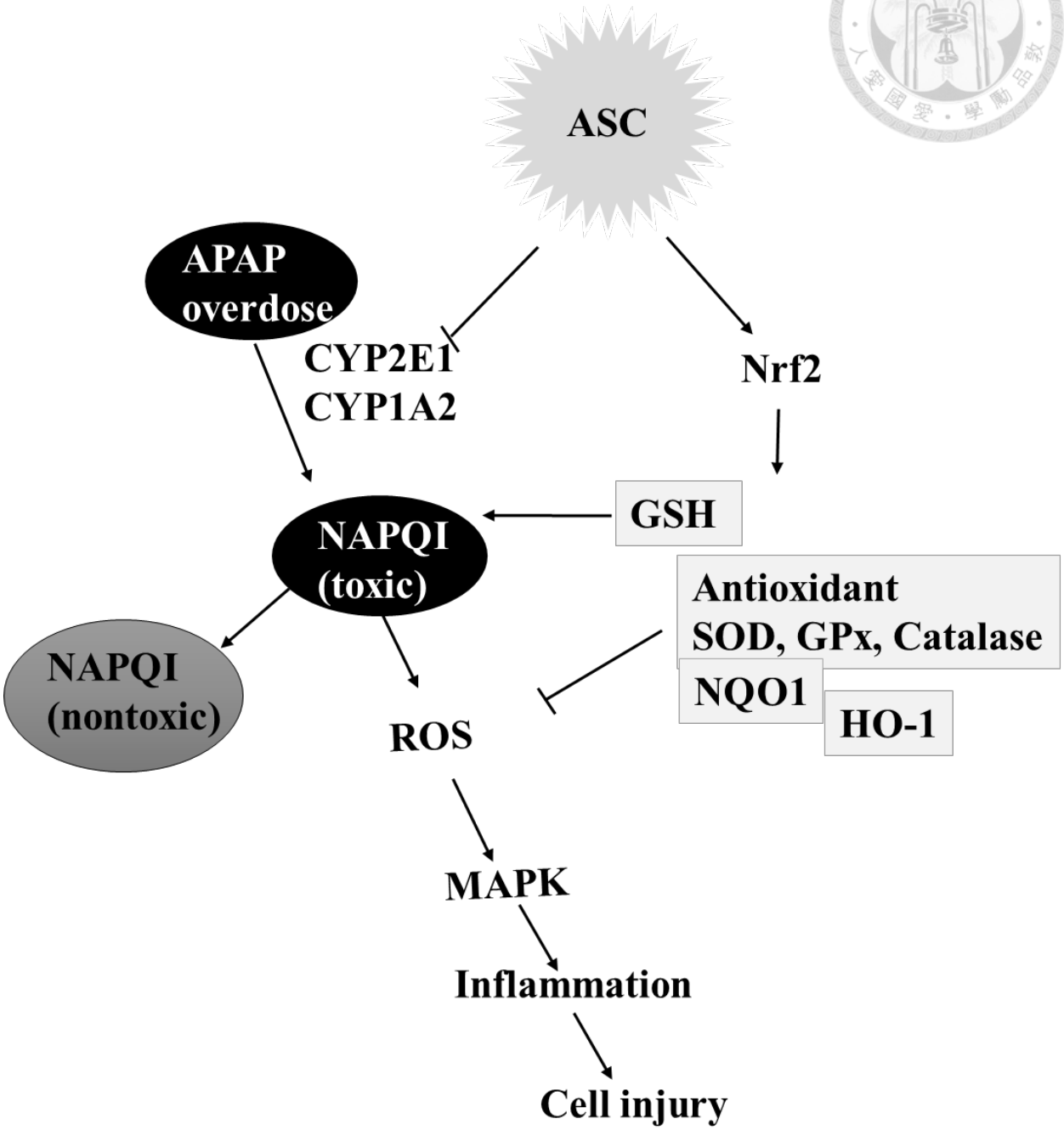
ASC
APAP overdose
CYP2E1
CYP1A2
Nrf2
GSH
NAPQI (toxic)
NAPQI (nontoxic)
Antioxidant
SOD, GPx, Catalase
NQO1
HO-1
ROS
MAPK
Inflammation
Cell injury

Figure 3-16 Schematic illustration of potential targets for omentum-derived ASCs protection against APAP-induced hepatotoxicity. APAP overdose is metabolized by CYP2E1 and CYP1A2 to form the toxic metabolite NAPQI, which rapidly consumes intracellular GSH and causes ROS generation followed by the activation of the MAPK pathway, leading to inflammation and cell death. However, omentum-derived ASCs suppress CYP2E1 and CYP1A2 activity and activate Nrf2 expression to reduce the formation of the toxic metabolite NAPQI and subsequent ROS generation, resulting in attenuated APAP-induced toxicity. APAP: acetaminophen; ASC: adipose tissue-derived stem cells; CYP2E1: cytochrome P450 subfamily 2E1; CYP1A2: cytochrome P450 subfamily 1A2; NAPQI: N-acetyl-p-benzoquinoneimine; GSH: glutathione; ROS: reactive oxygen species; MAPK: mitogen-activated protein kinases; Nrf2: NF-E2-related factor 2; SOD: superoxide dismutase; GPx: glutathione peroxidase; NQO1: NADPH quinone oxidoreductase 1; HO-1: heme oxygenase-1.

Prospective Aspects

The liver transplantation has been accommodated as the treatment of choice for kinds of end stage liver disease. However, although with the increasing rate of living-related liver transplantation, the shortage of donor organ remained a major problem. For the reason, hepatocyte transplantation is expected, and a good cell source is urgently needed for cell therapy. In this dissertation, we tried to differentiate iPSCs into functional hepatocytes in vitro, and then transplant these cells into HB mice to assess their therapeutic potential. The results showed that iPSCs could differentiat into functional hepatocytes in our optimized culture conditions, and the iPSCs-derived hepatocyte transplantation would result in enhanced FIX clotting activity and improved hemostasis. To develop and ensure the varieties of the cell source, another study was conducted to isolate ASC from omentum adipose tissue, and then demonstrate the protective function of ASC against APAP-induced acute liver failure (ALF) through the mediation of Nrf2 and cytochrome P450 expression.

Based on our study and previously reported evidences, iPSCs-derived hepatocyte is a good alternative source for cell therapy to treat HB, though some obstacles are still hanging without resolution for clinical application. It is important to eliminate the undifferentiated cells before transplantation, and a life-long follow-up may be need to monitor the risk of tumorigenesis. In our study for therapeutic potential of ASC for ALF, we demonstrated that the ASCs can be obtained from omentum adipose tissues, and the obtained cell possessed antioxidant and anti-inflammatory properties for providing protection against APAP-induced hepatotoxicity. In brief, omentum ASCs have the potential to be an alternative source for cell therapy, and to be an effective therapeutic strategy for APAP-induced liver failure in clinical practice. Although the study of stem cell therapy is heading for resolving the organ shortage and/or bridging the waiting time for liver transplantation, puzzles for the safety and efficacy remained unsolved before clinical application. Concomitant questions always raise along the development of new technology. How many cells are enough? Where and how do we obtain the standard donor cells? Which routes of delivery is effective for

clinical? Which type of stem cell is most promising? Admittedly, stem cell therapy is a road, strewn with flowers and beset with brambles. We wish, with our work, a simple, minimally invasive and comparatively therapeutic option might be opened for a new perspective in treatment of severe liver diseases.

Reference

- Abdelmegeed MA, Moon KH, Chen C, Gonzalez FJ, Song BJ. Role of cytochrome P450 2E1 in protein nitration and ubiquitin-mediated degradation during acetaminophen toxicity. Biochem Pharmacol. 2010;79:57-66.
- Ayroldi E, Cannarile L, Migliorati G, Nocentini G, Delfino DV, Riccardi C. Mechanisms of the anti-inflammatory effects of glucocorticoids: genomic and nongenomic interference with MAPK signaling pathways. FASEB J. 2012;26:4805-20.
- Banas A, Teratani T, Yamamoto Y, Tokuhara M, Takeshita F, Osaki M, Kawamata M, Kato T, Okochi H, Ochiya T. IFATS collection: in vivo therapeutic potential of human adipose tissue mesenchymal stem cells after transplantation into mice with liver injury. Stem Cells. 2008;26:2705-12.
- Basma H, Soto-Gutiérrez A, Yannam GR, Liu L, Ito R, Yamamoto T, Ellis E, Carson SD, Sato S, Chen Y, Muirhead D, Navarro-Alvarez N, Wong RJ, Roy-Chowdhury J, Platt JL, Mercer DF, Miller JD, Strom SC, Kobayashi N, Fox IJ. Differentiation and transplantation of human embryonic stem cell-derived hepatocytes. Gastroenterology. 2009;136(3):990-999.
- Belema-Bedada F, Uchida S, Martire A, Kostin S, Braun T. Efficient homing of multipotent adult mesenchymal stem cells depends on FROUNT-mediated clustering of CCR2. Cell Stem Cell. 2008;2(6):566-575.
- Bernal W, Wendon J. N Engl J Med. Acute liver failure 2013;369(26):2525-2534.
- Bigger BW, Siapati EK, Mistry A, Waddington SN, Nivsarkar MS, Jacobs L, Perrett R, Holder MV, Ridler C, Kemball-Cook G, Ali RR, Forbes SJ, Coutelle C, Wright N, Alison M, Thrasher AJ, Bonnet D, Themis M.Permanent partial phenotypic correction and tolerance in a mouse model of hemophilia B by stem cell gene delivery of human factor IX. Gene Ther.2006;13(2):117-126..
- Blum B, Bar-Nur O, Golan-Lev T, Benvenisty N. The anti-apoptotic gene surviving contributes to teratome formation by human embryonic stem cells. Nat Biotechnol. 2009;27(3):281-287.
- Bolton-Maggs PH, Pasi KJ. Haemophilias A and B. Lancet 2003;361(9371):180-1809.
- Burlina AB Hepatocyte transplantation for inborn errors of metabolism. J. Inherit. Metab. Dis. 2004;27(3):373-383.

• Calne RY, Rolles K, White DJ, Thiru S, Evans DB, McMaster P, Dunn DC, Craddock GN, Henderson RG, Aziz S, Lewis P. Cyclosporin A initially as the only immunosuppressant in 34 recipients of cadaveric organs: 32 kidneys, 2 pancreases, and 2 livers. Lancet. 1979;2(8151):1033-1036.

• Caplan AI, Bruder SP. Mesenchymal stem cells: building blocks for molecular medicine in the 21st century. Trends Mol Med. 2001;7:259-64.

• Chan K, Han XD, Kan YW. An important function of Nrf2 in combating oxidative stress: detoxification of acetaminophen. PNAS 2001;98:4611-4616.

• Chen YF, Tseng CY, Wang HW, Kuo HC, Yang VW, Lee OK. Rapid generation of mature hepatocyte-like cells from human induced pluripotent stem cells by an efficient three-step protocol. Hepatology.2012;55(4)1193-1203.

• Chen YT, Sun CK, Lin YC, Chang LT, Chen YL, Tsai TH, et al. Adipose-derived mesenchymal stem cell protects kidneys against ischemia-reperfusion injury through suppressing oxidative stress and inflammatory reaction. J Transl Med. 2011;9:51.

• Chen, Y. F.; Tseng, C. Y.; Wang, H. W.; Kuo, H. C.; Yang, V. W.; Lee, O. K. Rapid generation of mature hepatocyte-like cells from human induced pluripotent stem cells by an efficient three-step protocol. Hepatology 2012;55(4):1193-1203.

• Cheng Z, Ou L, Zhou X, Li F, Jia X, Zhang Y, Liu X, Li Y, Ward CA, Melo LG, Kong D, Targeted migration of mesenchymal stem cells modified with CXCR4 gene to infarcted myocardium improves cardiac performance. Mol her. 2008;16(3):571-579.

• Chin MH, Pellegrini M, Plath K, Lowry WE. Molecular analyses of human induced pluripotent stem cells and embryonic stem cells. Cell Stem Cell 2010;7:263-267.

• Cho KA, Woo SY, Seoh JY, Han HS, Ryu KH. Mesenchymal stem cells restore CCl4-induced liver injury by an antioxidative process. Cell Biol Int. 2012;36:1267-1274.

• Choi SM, Kim Y, Liu H, Chaudhari P, Ye Z, Jang YY. Liver engraftment potential of hepatic cells derived patient-specific induced pluripotent stem cells. Cell Cycle. 2011;10(15):2423-2427.

• Condic ML. Totipotency: what it is and what it is not. Stem Cells Dev. 2014 15;23(8):796-812.

• de Lázaro I, Yilmazer A, Kostarelos K Induced pluripotent stem (iPS) cells: a new source for cell-based therapeutics? J Control Release 2014;185:37-44.

- Ding Y, Xu D, Feng G, Bushell A, Muschel RJ, Wood KJ. Mesenchymal stem cells prevent the rejection of fully allogenic islet grafts by the immunosuppressive activity of matrix metalloproteinase-2 and -9. Diabetes. 2009;58(8):1797-1806.
- Fox IJ, Chowdhury JR, Kaufman SS, Goertzen TC, Chowdhury NR, Warkentin PI, Dorko K, Sauter BC, Strom SC. Treatment of the Crigler-Najjar syndrome type I with hepatocyte transplantation. N Engl J Med. 1998;14:338(20)1422-1426.
- Fox IJ, Daley GQ, Goldman SA, Huard J, Kamp TJ, Trucco M. Stem cell therapy. Use of differentiated pluripotent stem cells as replacement therapy for treating disease. Science 2014;345(6199):1247391.
- Groth CG, Arborgh B, Bjorken C, Sundberg B, Lundgren G. Correction of hyperbilirubinemia in the glucuronyltransferase-deficient rat by intraportal hepatocyte transplantation. Transplant Proc. 1977;9(1):313-6.
- Gum SI, Cho MK. Recent updates on acetaminophen hepatotoxicity: the role of nrf2 in hepatoprotection. Toxicol Res. 2013;29:165-72.
- Gupta S, Lee CD, Vemuru RP, Bhargava KK. Therapeutic potential of adult bone marrow stem cells in liver disease and delivery approaches. Hepatology. 1994;19(3):750-7.
- Hanna J, Wernig M, Markoulaki S, Sun CW, Meissner A, Cassady JP, Beard C, Brambrink T, Wu LC, Townes TM, Jaenisch R. Treatment of sickle cell anemia mouse model with iPS cells generated from autologous skin. Science 2007;318:1920-1923.
- Harrill AH, Watkins PB, Su S, Ross PK, Harbourt DE, Stylianou IM, et al. Mouse population-guided resequencing reveals that variants in CD44 contribute to acetaminophen-induced liver injury in humans. Genome Res. 2009;19:1507-1515.
- Heard KJ. Acetylcysteine for acetaminophen poisoning. N Engl J Med. 2008;359:285-292.
- Hughes RD, Mitry RR, Dhawan A, Current status of hepatocyte transplantation. Transplantation 2012;93(4):342-347.
- Inoue H, Nagata N, Kurokawa H, Yamanaka S. iPS cells: a game changer for future medicine. Embo j 2014;33(5):409-417.
- James LP, Mayeux PR, Hinson JA. Acetaminophen-induced hepatotoxicity. Drug Metab Dispos. 2003;31:1499-506.

- Jin SZ, Meng XW, Sun X, Han MZ, Liu BR, Wang XH, Pei FH. Hepatocyte growth factor promotes liver regeneration induced by transfusion of bone marrow mononuclear cells in a murine acute liver failure model Hepatobiliary Pancreat Sci. 2011;18(3):397-405.
- Jorge LP, Gonsebatt ME. The role of antioxidants and antioxidant-related enzymes in protective responses to environmentally induced oxidative stress. Mutat Res. 2009;674:137-147.
- Jorns C, Ellis EC, Nowak G, Fischler B, Nemeth A, Strom SC, Ericzon BG. Hepatocyte transplantation for inherited metabolic diseases of the liver. J Intern Med. 2012;272(3):201-223.
- Kaji, E. H.; Leiden, J. M. Gene and stem cell therapies. JAMA 2001;285(5):545-550.
- Kay HY, Kim YW, Ryu H, Sung SH, Hwang SJ, Kim SG. Nrf2-mediated liver protection by sauchinone, an antioxidant lignan, from acetaminophen toxicity through the PKCδ-GSK3β pathway. Br J Pharmacol. 2011;163:1653-1665.
- Kim HJ, Nel AE. The role of phase II antioxidant enzymes in protecting memory T cells from spontaneous apoptosis in young and old mice. J Immunol. 2005;175:2948-2959.
- Kuo TK, Hung SP, Chuang CH. Stem cell therapy for liver disease: parameters governing the success of using bone marrow mesenchymal stem cells. Gastroenterology. 2008;134:2111-2121.
- Kurtz A. Mesenchymal stem cell delivery routes and fate. Int J Stem Cells.2008;1(1):1-7.
- Larsen A. Acetominophen hepatoxicity. Clin Liver Dis. 2007;11:525-548.
- Lee OK, Kuo TK, Chen WM, Lee KD, Hsieh SL, Chen TH. Isolation of multipotent mesenchymal stem cells from umbilical cord blood. Blood. 2004;103(5)1669-1675.
- Lee SS, Buters JT, Pineau T, Fernandez-Salguero P, Gonzalez FJ. Role of CYP2E1 in the hepatotoxicity of acetaminophen. J Biol Chem. 1996;271:12063-7.
- Li HY, Chien Y, Chen YJ, Chen SF, Chang YL, Chiang CH, Jeng SY, Chang CM, Wang ML, Chen LK, Hung SI, Huo TI, Lee SD, Chiou SH. Reprogramming induced pluripotent stem cells in the absence of c-Myc for differentiation into hepatocyte-like cells Biomaterials. 2011;32(26):5994-6005.
- Li T, Zhu J, Ma K, Liu N, Feng K, Li X, Wang S, Bie P. Autologous bone marrow-derived mesenchymal stem cell transplantation promotes liver regeneration after portal vein embolization in cirrhotic rats. J Surg Res 2013;184:1161–1173
- Liu Z, Meng F, Li C, Zhou X, He Y, Mrsny RJ, et al. Human umbilical cord mesenchymal stromal cells rescue mice from acetaminophen-induced acute liver failure. Cytotherapy. 2014;16:1207-1219.

- Lowry WE, Richter L, Yachechko R, Pyle AD, Tchieu J, Sridharan R, Clark AT, Plath K. Generation of human induced pluripotent stem cells from dermal fibroblasts. Proc Natl Acad Sci USA 2008;105:2883-2888.
- Malliaras K, Marbán E. Cardiac cell therapy: where we've been, where we are, and where we should be headed. Br Med Bull.2011;98:161-185.
- Matas AJ. Hepatocellular transplantation for metabolic deficiencies: decrease of plasma bilirubin in Gunn rats. Science. 1976;192:892-894.
- McGill MR, Jaeschke H. Metabolism and disposition of acetaminophen: recent advances in relation to hepatotoxicity and diagnosis. Pharm Res. 2013;30:2174-87.
- Meier RP, Müller YD, Morel P, Gonelle-Gispert C, Bühler LH.Transplantation of mesenchymal stem cells for the treatment of liver diseases, is there enough evidence? Stem Cell Res. 2013;11(3):1348-1364.
- Meirelles Júnior RF, Salvalaggio P, Rezende MB, Evangelista AS, Guardia BD, Matielo CE, Neves DB, Pandullo FL, Felga GE, Alves JA, Curvelo LA, Diaz LG, Rusi MB, Viveiros Mde M, Almeida MD, Pedroso PT, Rocco RA, Meira Filho SP. Liver transplantation: history, outcomes and perspectives. Einstein (Sao Paulo). 2015;13(1):149-152.
- Nakagawa H, Maeda S, Hikiba Y. Deletion of apoptosis signal-regulating kinase 1 attenuates acetaminophen-induced liver injury by inhibiting c-Jun N-terminal kinase activation. Gastroenterology. 2008;135:1311-1321.
- Nakagawa H, Maeda S. Molecular mechanisms of liver injury and hepatocarcinogenesis: focusing on the role of stress-activated MAPK. Patholog Res Int. 2012;2012:172894.
- Pareja E, Cortes M, Bonora A, Fuset P, Orbis F, Lopez R, Mir J.New alternatives to the treatment of acute liver failure. ransplant Proc. 2010;42(8):2959-2961.
- Parekkadan B, van Poll D, Suganuma K, Carter EA, Berthiaume F, Tilles AW, Yarmush ML. Mesenchymal stem cell-derived molecules reverse fulminant hepatic failure. PLoS One. 2007 Sep 26;2(9):e941.
- Peyvandi F, Jayandharan G, Chandy M, Srivastava A, Nakaya SM, Johnson MJ, THompon AR, Goodeve A, Garagiola I, Lavoretano S, Menegatti M, Palla R, Spreafico M, Tagliabue L, Asselta R, Duga S, Mannucci PM. Genetic diagnosis of haemophilia and other inherited bleeding disorders. Haemophilia 2006;12 Suppl 3:82-89.

• Rashid ST, Corbineau S, Hannan N, Marciniak SJ, Miranda E, Alexander G, Huang-Doran I, Griffin J, Ahrlund-Richter L, Skepper J, Semple R, Weber A, Lomas DA, Vallier L. Modeling inherited metabolic disorders of the liver using human induced pluripotent stem cells. Clin Invest. 2010;120(9):3127-3136.

• Reid AB, Kurten RC, McCullough SS, Brock RW, Hinson JA. Mechanisms of acetaminophen-induced hepatotoxicity: role of oxidative stress and mitochondrial permeability transition in freshly isolated mouse hepatocytes. J Pharmacol Exp Ther. 2005;312:509-516.

• Ren G, Zhao X, Zhang L, Zhang J, L'Huillier A, Ling W, Roberts AI, Le AD, Shi S, Shao C, Shi Y. Inflammatory cytokine-induced intercellular adhesion molecule-1 and vascular cell adhesion molecule-1 in mesenchymal stem cells are critical for immunosuppression. J Immunol. 2010;184(5):2321-2328.

• Ries C, Egea V, Karow M, Kolb H, Jochum M, Neth P. MMP-2, MT1-MMP, and TIMP-2 are essential for the invasive capacity of human mesenchymal stem cells: differential regulation by inflammatory cytokines. Blood. 2007;109(9):4055-4063.

• Robinton DA, Daley GQ. The promise of induced pluripotent stem cells in research and therapy. Nature 2012;481(7381):295-305.

• Rosenthal RJ, Chen SC, Hewitt W, Wang CC, Eguchi S, Geller S, Phillips EH, Demetriou AA, Rozga J. Acute impairment of hepatic microcirculation and recruitment of nonparenchymal cells by intrasplenic hepatocyte transplantation. Surg Endosc. 1996;10(11):1075-9

• Rugsta HE, Robinson SH, Yannoni C, Tashjian AH, Jr. Transfer of bilirubin uridine diphosphate-glucuronyltransferase to enzyme-deficient rats. Science. 1970;30:170(3957):553-555.

• Salomone F, Barbagallo I, Puzzo L, Piazza C, Li Volti G. Efficacy of adipose tissue-mesenchymal stem cell transplantation in rats with acetaminophen liver injury. Stem Cell Res. 2013;11:1037-44.

• Sancho-Bru, P.; Najimi, M.; Caruso, M.; Pauwelyn, K.; Cantz, T.; Forbes, S.; Roskams, T.; Ott, M.; Gehling, U.; Sokal, E.; Verfaillie, C. M.; Muraca, M. Stem and progenitor cells for liver repopulation: can we standardise the process from bench to bedside? Gut 2009;58(4):594-603.

• Sart S, Ma T, Li Y. Preconditioning stem cells for in vivo delivery. Biores Open Access. 2014;3:137-49.

• Sebastiano, V.; Maeder, M. L.; Angstman, J. F.; Haddad, B.; Khayter, C.; Yeo, D. T.; Goodwin, M.

J.; Hawkins, J. S.; Ramirez, C. L.; Batista, L. F.; Artandi, S. E.; Wernig, M.; Joung, J. K. In situ genetic correction of the sickle cell anemia mutation in human induced pluripotent stem cells using engineered zinc finger nucleases. Stem Cells 2011;29(11):1717-1726.

- Shi M, Li J, Liao L, Chen B, Li B, Chen L, Jia H, Zhao RC. Regulation of CXCR4 expression in human mesenchymal stem cells by cytokine treatment: role in homing efficiency in NOD/SCID mice. Haematologica. 2007;92(7):897-904.
- Si-Tayeb K, Noto FK, Nagaoka M, Li J, Battle MA, Duris C, North PE, Dalton S, Duncan SA. Highly efficient generation of human hepatocyte-like cells from induced pluripotent stem cells.Hepatology. 2010;51(1):297-305.
- Song H, Cha MJ, Song BW. Reactive oxygen species inhibit adhesion of mesenchymal stem cells implanted into ischemic myocardium via interference of focal adhesion complex. Stem Cells. 2010;28:555-563.
- Song, Z.; Cai, J.; Liu, Y.; Zhao, D.; Yong, J.; Duo, S.; Song, X.; Guo, Y.; Zhao, Y.; Qin, H.; Yin, X.; Wu, C.; Che, J.; Lu, S.; Ding, M.; Deng, H. Efficient generation of hepatocyte-like cells from human induced pluripotent stem cells. Cell Res 2009;19(11):1233-1242.
- Starzl TE, Groth CG, Brettschneider L, Penn I, Fulginiti VA, Moon JB, Blanchard H, Martin AJ Jr, Porter KA. Orthotopic homotransplantation of the human liver. Ann Surg. 1968;168(3):392-415.
- Starzl TE, Marchioro TL, Vonkaulla KN, Hermann G, Brittain RS, Waddell Wr. Homotransplantation of the liver in humans. Surg Gynecol Obstet 193;117:659-676.
- Strong RW, Lynch SV, Ong TH, Matsunami H, Koido Y, Balderson GA. Successful liver transplantation from a living donor to her son. N Engl J Med. 1990;322(21):1505-1507.
- Takahashi, K; Yamanaka, S. Induction of pluripotent stem cells from mouse embryonic and adult fibroblast cultures by defined factor. Cell 2016;126 (4): 663–676.
- Takami T, Terai S, Sakaida I. Stem cell therapy in chronic liver disease, Techniques for intrasplenic hepatocyte transplantation in the large animal model.Curr Opin Gastroenterol 2012;28:203-208.
- Wernig M, Zhao JP, Pruszak J, Hedlund E, Fu D, Soldner F, Broccoli V, Constantine-Paton M, Isacson O, Jaenisch R. Neurons derived from reprogrammed fibroblasts functionally

integrate into the fetal brain and improve symptoms of rats with Parkinson's disease. Proc Natl Acad Sci U S A 2008;105:5856-5861.

- Wilhelm A, Leister I, Sabandal P, Krause P, Becker H, Markus PM. 111Indium labeling of hepatocytes for analysis of short-term biodistribution of transplanted cells. J Pediatr Surg. 2004;39(8):1214-1219.
- Wu SM, Hochedlinger K, Harnessing the potential of induced pluripotent stem cells for regenerative medicine. Nat Cell Biol. 2011;13(5):497-505.
- Wu YM, Joseph B, Berishvili E, Kumaran V, Gupta S. Hepatocyte transplantation and drug-induced perturbations in liver cell compartments. Hepatology. 2008;47(1):279-287.
- Wynn RF, Hart CA, Corradi-Perini C, O'Neill L, Evans CA, Wraith JE, Fairbairn LJ, Bellantuono I. A small proportion of mesenchymal stem cells strongly expresses functionally active CXCR4 receptor capable of promoting migration to bone marrow. Blood. 2004;104(9):2643-2645.
- XU D, AlipioZ, Fink LM, Adcock DM, Yang J, Ward DC, Ma Y. Phenotypic correction of murine hemophilia A using an iPS cell-based therapy. Proc Natl Acad Sci USA. 2009;106(3):803-813.
- Xu YQ, Liu ZC. Therapeutic potential of adult bone marrow stem cells in liver disease and delivery approaches. Stem Cell Rev. 2008;4(2):101-112.
- Yagi H, Soto-Gutierrez A, Parekkadan B, Kitagawa Y, Tompkins RG, Kobayashi N, et al. Mesenchymal stem cells: mechanisms of immunomodulation and homing. Cell Transplant. 2010;19:667-679.
- Yagi T, Hardin JA, Valenzuela YM, Miyoshi H, Gores GJ, Nyberg SL.Caspase inhibition reduces apoptotic death of cryopreserved porcine hepatocytes. Hepatology 2001;33(6):1432-1440.
- Yang R, Miki K, He X, Killeen ME, Fink MP. Prolonged treatment with N-acetylcystine delays liver recovery from acetaminophen hepatotoxicity. Crit Care. 2009;13:R55.
- Yu Y, Fisher JE, Lillegard JB, Rodysill B, Amiot B, Nyberg SL.Cell therapies for liver diseases. Liver Transpl. 2012;18(1):9-21.
- Zhu X, He B, Zhou X, Ren J. Effects of transplanted bone-marrow-derived mesenchymal stem cells in animal models of acute hepatitis. Cell Tissue Res 2013;351:477–486.

• Zuk PA, Zhu M, Ashjian P, De Ugarte DA, Huang JI, Mizuno H, Alfonso ZC, Fraser JK, Benhaim P, Hedrick MH. Human adipose tissue is a source of multipotent stem cells. Mol Biol Cell. 2002;13(12):4279-4295.

List of Publications

Wu YM , Huang YJ , Chen P , Hsu YC , Lin SW , Lai H , Lee HS. Hepatocyte-like cells derived from mouse induced pluripotent stem cells produce functional coagulation factor IX in a hemophilia B mouse model. Cell Transplantation 2015.

Huang YJ, Chen P, Lee CY, Yang SY, Lin MT, Lee HS, Wu YM. Protection against acetaminophen-induced acute liver failure by omentum adipose tissue derived stem cells through the mediation of Nrf2 and cytochrome P450 expression. Journal of Biomedical Science (2016) 23:5.

DOI: 10.3727/096368915X689541

CT-1450 Provisionally Accepted 09/18/2015 for publication in

"Cell Transplantation"

Hepatocyte-like cells derived from mouse induced pluripotent stem cells produce functional coagulation factor IX in a hemophilia B mouse model

*Yao-Ming Wu,[1] *Yu-Jen Huang,[1,2] Poda Chen,[3] Yu-Chen Hsu,[4] Shu-Wha Lin,[4] Hong-Shiee Lai,[1] Hsuan-Shu Lee[2,5]

[1] Department of Surgery, National Taiwan University Hospital and National Taiwan University College of Medicine, Taipei, Taiwan

[2] Institute of Biotechnology, National Taiwan University, Taipei, Taiwan.

[3] Department of Surgery, National Taiwan University Hospital Yun-Lin Branch, Yunlin, Taiwan.

[4] Department of Clinical Laboratory Sciences and Medical Biotechnology, National Taiwan University College of Medicine, Taipei, Taiwan

[5] Department of Internal Medicine, National Taiwan University Hospital and National Taiwan University College of Medicine, Taipei, Taiwan.

*Equal contribution

Running head:

iPS derived hepatocytes transplantation for HB

Correspondence to:

[1] Prof. Hsuan-Shu Lee

Department of Internal Medicine, National Taiwan University Hospital and National Taiwan University College of Medicine & Institute of Biotechnology, National Taiwan University, Taipei, Taiwan.

Email: benlee@ntu.edu.tw

[2] Prof. Hong-Shiee Lai

Department of Surgery, National Taiwan University Hospital and National Taiwan University College of Medicine, Taipei, Taiwan

Email: hslai@ntu.edu.tw

Address: Department of Surgery, National Taiwan University Hospital No. 7, Chung-Shan South Road, Taipei, Taiwan

Phone: +886-2-23123456#65118

Fax: +886-2-33223476

CT-1450 Cell Transplantation early e-pub; provisional acceptance 09/18/2015

Abstract

Hemophilia B (HB) is an inherited deficiency in coagulation factor IX (FIX) that leads to prolonged bleeding after injury. Although hepatocyte transplantation has been demonstrated to be an effective therapeutic strategy for HB, the quality and sources of hepatocytes still limit their application. Recently, stem cells were proposed as an alternative source of donor cells for cell-based therapy. Much research has been devoted to the properties of stem cells that can be differentiated into functional hepatocytes, thereby providing a new cell source for cell-based therapy. Induced pluripotent stem (iPS) cells represent a renewable source of hepatocytes for cell-based therapy; these cells exhibit pluripotency and differentiation ability and can be derived from somatic cells. These iPS cells are highly similar to embryonic stem (ES) cells. We hypothesized that hepatocyte-like cells derived from iPS cells would have therapeutic efficiency in a mouse model of HB. To test this hypothesis, we differentiated iPS cells toward hepatocytes by stepwise protocol and then transplanted these cells into HB mice. We found that these cells shared many characteristics with hepatocytes, such as albumin synthesis, metabolic capacity, glycogen storage, and ureagenesis. Moreover, iPS-derived hepatocyte transplantation led to increased coagulation factor IX activity, improved thrombus generation, and better hemostasis parameters, and the transferred cells were localized in the liver in recipient HB mice. In conclusion, our results clearly demonstrate that hepatocyte-like cells derived from iPS cells represent a potential cell source for cell-based therapy in the treatment of HB.

Key words: Hemophilia B, factor IX, induced pluripotent stem cells, transplantation

CT-1450 Cell Transplantation early e-pub; provisional acceptance 09/18/2015

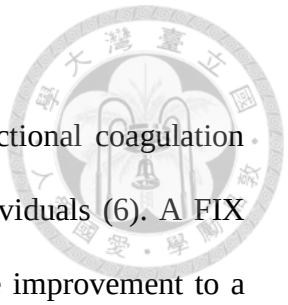

Introduction

Hemophilia B (HB) is a bleeding disorder caused by lack of functional coagulation factor IX (FIX). This disorder is X-linked and affects 1 in 30,000 individuals (6). A FIX activity level of 1% results in severe disease and possibly death, while improvement to a level of approximately 5% is sufficient to prevent spontaneous and life-threatening bleeding events (1). Current therapies include FIX replacement and gene therapy. However, FIX replacement is not completely efficient, and some issues remain unresolved, such as its high cost, high risk of anaphylaxis and life-threatening hemorrhagic complications. Gene therapy is also limited by host immune tolerance and the long-term expression of therapeutic gene products (4,16). Hepatocyte transplantation offers promise for the treatment of many metabolic liver diseases.First confirmed that efficacy of hepatocyte transplantation on hemophilia B by Tatsumi K et al. (21), consistent with our previously published study, we showed that bioengineering FIX to treat HB was successful 24); however, the next issue to be considered is cell sourcing. Although natural hepatocytes are an excellent cell resource for cell based-therapy for liver failure, obstacles remain in sourcing and maintaining viable hepatocytes. Over the past few years, a considerable number of studies have investigated the production of hepatocyte-like cells from stem cells, and these cells provide exciting new opportunities for cell-based therapy 10,22). For instance, one recent study demonstrated that endothelial cells derived from iPS cells showed therapeutic potential in a hemophilia A mouse disease model (25). Thus, we hypothesized that iPS-derived hepatocytes could also be used to treat HB.

A growing body of literature has demonstrated that somatic cells can be reprogrammed into pluripotent stem cells through the introduction of several transcription

factors (Oct4, Sox2, c-Myc and Klf4) (20). These induced pluripotent stem (iPS) cells are highly similar to embryonic stem (ES) cells with respect to their morphology, gene expression, differentiation potential and teratoma formation (3,13), thus bypassing the ethical and immunological concerns regarding ES cells. Modern research has shed significant light on cell-based therapy, disease modeling, personalized medicine, and drug toxicity screening (9,17). In particular, there is considerable evidence supporting the therapeutic potential of iPS cells in regenerative medicine, and numerous publications have been devoted to the study of iPS technology. Because of their wide differentiation potential, iPS cells have been used to generate somatic cells to treat several diseases (11,12), such as Parkinson's disease, Alzheimer's disease, sickle cell anemia and heart disease. In hepatology, numerous studies have investigated iPS cell differentiation into hepatocytes; however, little is known about the therapeutic potential of iPS-derived hepatocytes in genetic disease.

In this report, we assessed the therapeutic potential of iPS-derived hepatocytes in an HB mouse model. Our results demonstrated that iPS cells could be differentiated into hepatocytes that expressed FIX both in vivo and in vitro. Moreover, these iPS-derived hepatocytes were successfully engrafted within the hepatic parenchyma, where they produced FIX. These findings indicate that iPS-derived hepatocytes represent another potential cell source for the clinical treatment of hemophilia and other genetic disorders.

Materials and Methods

Animal model

All mouse experiments were approved by the institutional animal care and use committee at National Taiwan University. The HB mice (male, 6 to 8 weeks old) used in this study were obtained from Professor Lin SW. HB mice deficient in FIX were used as recipient mice in this study. C57BL/6 mice were used to isolate normal hepatocytes as the control group and purchased from National Laboratory Animal Center, Taipei, Taiwan. A preconditioned animal model was generated according to previous experiments (23). Rifampicin (Sigma-Aldrich, St Louis, MO) was dissolved in 20 M sodium hydroxide (NaOH; Sigma-Aldrich, St Louis, MO), and monocrotaline (MCT; Sigma-Aldrich, St Louis, MO) was dissolved in normal saline at a pH of 7.4. HB mice received 75 mg/kg rifampicin intraperitoneally daily for 2 days. MCT was administered intraperitoneally as a single 200 mg/kg dose on the third day. Cells were transplanted on the fourth day. Each mouse was injected intrasplenically with 5×10^5 iPS-derived hepatocytes. Thirty minutes before surgery, HB mice were infused intravenously with 100 IU/kg recombinant FIX protein (Bene FIX®; Wyeth Pharmaceuticals, PA, USA) (Fig. 1). In the cell tracing experiment, the differentiated cells or primary hepatocytes were stained with PKH26 fluorescent dye (Sigma-Aldrich, St Louis, MO) according to the manufacturer's instructions. After fluorescent staining, the cells were transplanted into HB mice. At 1 and 4 weeks after transplantation, the recipient mice were sacrificed, and the liver tissue was embedded in TissueTek OCT (Sakura Fintek, Torrance, CA) for immunocytochemistry. For quantitation

assay, number of PKH positive cells was examined under x 200 magnification and counted by 20 continuous field per liver lobule for three individual mice.

Cell culture and hepatocyte differentiation

Mouse iPS cells were obtained from Yamanaka S. The iPS cells were cultured and expanded from mouse embryonic fibroblasts with mytomycin C (Sigma-Aldrich, St Louis, MO) treatment in Dulbecco's modified Eagle's Medium (DMEM; Gibco, Grand Island, NY) supplemented with 10% fetal bovine serum (FBS, Hyclone Laboratories, Logan, UT), 0.3% leukemia inhibitory factor (LIF; Millipore, Bedford, MA), 1 mM L-glutamine, 1% nonessential amino acid and 0.1 mM β-mercaptoethanol (all were purchased from Gibco, Grand Island, NY).

Derivation of hepatocytes from iPS cells was performed according to the protocols described and modified by Song Z et al. (20). The iPS cells were cultured on low-attachment dishes (Corning Life Science, NY) to form embryonic bodies, which were cultured in Iscove's modified Dulbecco's Medium (IMDM; Gibco, Grand Island, NY) supplemented with 1% FBS and 100 ng/ml activin A (ProSpec, Israel) for 1 day. On the following days, 0.1% insulin–transferrin–selenium (ITS; Sigma-Aldrich, St Louis, MO) was added to this medium, and 1% ITS was added 1 day later. After endoderm induction, the cells were cultured in IMDM supplemented with 10% FBS, 30 ng/ml FGF4 and 20 ng/ml BMP2 for 5 days (all were purchased from ProSpec, Israel). Next, the cells were incubated in IMDM supplemented with 10% FBS, 10 ng/ml HGF(ProSpec, Israel), 10 ng/ml oncostatin M (ProSpec, Israel) and 0.1 μM dexamethasone (Sigma-Aldrich, St Louis, MO) for 5 days (Fig. 1A).

Reverse transcription-polymerase chain reaction (RT-PCR)

Total RNA was extracted using RNeasy mini kits (Qiagen Ltd, Crawley, UK), and RT-PCR was performed using a Fast-Run™ Hotstart RT-PCR kit (Protech Technology, Taiwan) according to the manufacturer's instructions. The PCR program consisted of 35 cycles of 94°C for 30 s, 72°C for 1 min and extension at 72°C for 5 min. All PCR primers are shown in Table 1.

Functional assay for iPS-derived hepatocytes

Periodic acid–Schiff (PAS) staining was performed to identify glycogen storage. Cells were fixed in 4% paraformaldehyde (Sigma-Aldrich, St Louis, MO) for 20 min and then stained with PAS (Sigma-Aldrich, St Louis, MO). Cellular uptake and indocyanine green (ICG; Sigma-Aldrich, St Louis, MO) release were measured. ICG (1 mg/ml) was added to the culture medium for 30 min at 37°C, and ICG release was measured after 6 h. During cell differentiation, albumin and uric acid were secreted into the culture medium. The albumin concentration was quantified using a mouse albumin enzyme linked immunosorbent assay (ELISA) kit (Bethyl Laboratories, Montgomery, TX). The total protein content was determined using a BCA protein assay kit (Pierce, Rockford, IL). The albumin content was normalized to the total cellular protein level. The uric acid levels were measured using a uric acid assay kit (BioVision, CA, USA) according to the manufacturer's protocol.

Immunofluorescence

Cells were fixed in 4% paraformaldehyde for 20 min, permeabilized in 0.1% Triton X-100 (Sigma-Aldrich, St Louis, MO) for 20 min and blocked in 3% bovine serum albumin (BSA; Sigma-Aldrich, St Louis, MO) for 1 h. The cells were then incubated with the primary antibody at 4°C overnight. The mouse anti-α-fetoprotein (Cell Signaling

Technology, Beverly, MA), rabbit anti-albumin (Abcam, Cambridge, UK), rabbit anti-cytokeratin 7 (Abcam, Cambridge, UK), anti-cytokeratin 18(Abcam, Cambridge, UK) and sheep anti-FIX (Molecular innovations, Michigan, USA) primary antibodies were used at a dilution of 1:100, and the rabbit anti-cytokeratin 19 (Abcam, Cambridge, UK) primary antibody was used at a dilution of 1:1,000. After washing with PBS-0.02% Tween-20 (Sigma-Aldrich, St Louis, MO), cells were incubated with FITC- or PE-conjugated secondary antibody (Invitrogen, Carlsbad, CA) diluted to 1:200 for 2 h and then stained with DAPI (Biogenex, San Ramon, CA) to stain the cell nuclei.

FIX clotting activity assay

FIX clotting activity was determined using the APTT reagent (Actin® FSL; Dade Behring, Newark, DE) as the activator in a semi-automated blood coagulation analyzer according to the manufacturer's instructions (CA-50; Sysmex, Kobe, Japan). Pooled mouse plasma was obtained from inbred C57BL/6 male mice (n = 18) to generate standard curves for the quantification of test samples. FIX clotting activity in the standard was assumed to be 100%. The test samples were diluted 1:5 in imidazole buffer prior to analysis. A one-stage clotting assay was performed by incubating 50 µl of the test sample with 50 µl of human FIX-deficient plasma (American Diagnostica, Stamford, CT, USA) for 1 min at 37°C, after which 50 µl of activator was added for 3 min at 37°C. Next, 50 µl of 25 mM calcium chloride ($CaCl_2$; Sigma-Aldrich, St Louis, MO) was added, and the time required for clotting was measured. Each value was reported after subtracting the mean baseline level in HB mice.

Hemostatic function assay

Whole blood mixed with a one-tenth volume of 3.2% sodium citrate (Sigma-Aldrich, St Louis, MO) was assayed by thromboelastography (TEG® analyzer; Haemoscope, Braintree, MA, USA) using the citrated-kaolin mode. Analyses for the variables were conducted according to the manufacturer's instructions.

Statistical analysis

Data are shown as the mean ± standard error of the mean (SEM) and were compared using two-tailed unpaired Student's *t*-tests or one-way analysis of variance (ANOVA) and post hoc test followed by Turkey's multiple comparisons. Statistical significance was set at $p < 0.05$.

Results

Generation and characterization of hepatocytes from mouse iPS cells

We previously demonstrated that hepatocyte transplantation improved liver function in an HB mouse model (24). In this study, we examined the therapeutic potential of hepatocyte-like cells derived from iPS cells to treat genetic liver diseases (Fig 1). We utilized HB mice as a proof-of-principle preclinical model to test the therapeutic potential of iPS-derived hepatocytes, and we used a previously developed preconditioned animal model to investigate graft cell engraftment (23).

Following hepatic differentiation protocol, iPS cells (Fig. 2A) were through the endoderm induction by Activin A induced, differentiation to hepatoblast stage by BMP2 and FGF4 (at day 7, Fig. 2B), and finally differentiation to hepatocyte-like cell by HGF/OSM/Dex (at day 20, Fig.2C). During the differentiation, the cell morphology change from colonical to polygonal. We checked the mRNA expression at day 18 in hepatocyte

expression. RT-PCR result demonstrated these expression hepatocyte markers, including AFP, ALB, HNF4, G6P, TAT, CK18, further, to detect protein expression by immunofluoresencent staining. AFP was expressed in immature hepatocyte and detected at day 10, ALB and CK7 were expressed at day 15, and more differentiated cells expression CK18 and CK19 at day 20 (Fig. 3). Importantly, the RT-PCR and immunofluorescence results confirmed that the iPS-derived hepatocytes expressed FIX mRNA (Fig. 2D) and protein (first detected at day 10, Fig. 3). Taken together, these data show that hepatocytes can be derived from iPS cells using our differentiation procedure.

We further examined the functionality of the iPS-derived hepatocytes. PAS staining demonstrated the ability of the derived cells to store glycogen (Fig. 2D), and ICG analysis indicated their capacity to accumulate and excrete compounds (Fig. 2E). Protein synthesis is another characteristic of functional hepatocytes, which can be monitored by the secretion of proteins into the culture medium. Thus, we monitored the concentration of albumin during the period of differentiation. Albumin production was first detected after 13 days of differentiation, and reaching the maximum level on 21 days of differentiation (1.51 ± 0.65 ng/mg protein/day) (Fig. 2F). Moreover, after 18 days of differentiation, the uric acid production level was 4.45 ± 0.48 nmole/ml/day (Fig. 2G). These results revealed that the generated iPS-derived hepatocytes exhibited hepatic functionality.

Transplantation of iPS-derived hepatocytes

Next, we assessed the therapeutic efficacy of iPS-derived hepatocytes in the HB mouse model. The HB mice were divided into two groups, one that received normal hepatocyte transplantation and the other iPS-derived hepatocyte transplantation, and the circulating FIX activity was monitored after 4 weeks of transplantation. Our data showed

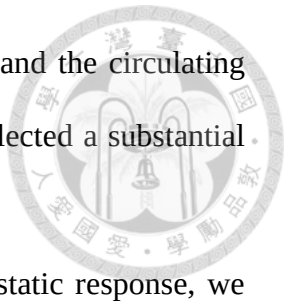

that iPS-derived hepatocytes enhanced FIX clotting activity by 2–3%, and the circulating FIX activity were stable for up to 1 month (Fig. 4A). These results reflected a substantial improvement in disease in HB mice.

Because the clotting test could not fully reflect the in vivo hemostatic response, we utilized the TEG assay to further examine the in vivo hemostatic state. Moreover, we used transplantation to improve the therapeutic efficacy. For this purpose, HB mice underwent a second intrasplenic transplantation (separated by 1 week) of iPS-derived hepatocytes or normal hepatocytes, and we assessed hemostasis in whole blood 7 days after the second transplantation. The peak level of thrombin generation progressively decreased, and the time of thrombus generation was 43 min in HB mice. However, repeated normal hepatocyte transplantation improved the peak thrombin level and reduced the time of thrombus generation to 14 min. In addition, the effects of repeated iPS-derived hepatocyte transplantation were similar to the effects of repeated normal hepatocyte transplantation (Fig. 4B). Moreover, repeated iPS-derived hepatocyte transplantation improved both the reaction time and strength of thrombus generation and the coagulation index (CI) value, which is another hemostatic parameter that reflects the overall coagulability of blood. The CI value of mice after repeated iPS-derived hepatocyte transplantation improved to -6.4 (the value before transplantation was -32.3; Table 2). Taken together, these results indicate that iPS-derived hepatocyte transplantation markedly improved hemostasis, suggesting that iPS-derived hepatocytes could be used to treat HB.

Engraftment of iPS-derived hepatocytes

Finally, to investigate whether the iPS-derived hepatocytes were retained in the liver parenchyma, we utilized immunofluorescence to trace the grafted cells in recipient mice.

Before transplantation, the differentiated cells were stained with PKH26 fluorescent dye, and liver sections were examined at 1 week after transplantation. The immunofluorescence staining showed that PKH26-positive cells were localized in the livers of recipient mice, thus indicating that the transplanted cells were engrafted (Fig. 4C and 4D). To improve the engraftment efficiency, we adopted a preconditioned model that included immunosuppression (MCT and rifampicin). For iPS-derived hepatocyte engraftment in the livers of preconditioned animals 1 week after transplantation, the number of engrafted cells was similar to the value observed in non-preconditioned mice (Fig. 4F), whereas more PKH26-positive cells were detected at 4 weeks after transplantation (Fig. 4E). These results indicated that the transplantation of iPS-derived hepatocytes into the livers of preconditioned mice could enhance the efficiency of engraftment. Additionally, we assessed hemostasis in the preconditioned animal model with iPS-derived hepatocyte transplantation. The TEG assay revealed that the time of thrombin generation for iPS-derived hepatocyte transplantation was similar to the result for normal hepatocyte transplantation, with a shorter time of thrombus generation. Meanwhile, iPS-derived hepatocyte transplantation resulted in improved CI values and hemostasis parameters in the preconditioned model, compared with the normal hepatocyte transplantation group. Therefore, iPS-derived hepatocytes possess therapeutic potential in HB mice.

Discussion

Our previous study demonstrated the therapeutic efficacy of hepatocyte transplantation in the HB mouse model, although the shortage of hepatocyte sources limits their therapeutic application. Therefore, another hepatocyte source is urgently needed for cell-based therapy.

The use of iPS cells has revolutionized the field of regenerative medicine, as these cells have been shown to represent a novel source of hepatocytes for drug development and cell-based therapy (8). In this study, we utilized the ability of iPS cells to differentiate into functional hepatocytes in vitro and then transplanted these cells into HB mice to assess their therapeutic potential. Our results showed that iPS cells differentiated into functional hepatocytes in our optimized culture conditions and that iPS-derived hepatocyte transplantation resulted in enhanced FIX clotting activity and improved hemostasis.

Recently, numerous reports have indicated that iPS cell-based therapy could improve liver function in disease models. Specifically, Xu et al. reported that the transplantation of iPS-derived endothelial cells to a hemophilia A mouse model resulted in factor VIII expression, providing a proof-of-principle for genetic disorder treatment (25). Moreover, iPS-derived hepatocytes transplanted into mice with lethal acute hepatic failure induced by thioacetamide, a hepatotoxin that causes the production of reactive oxygen species, alleviated acute hepatitis. These results indicate that iPS-derived hepatocytes can improve liver function and prevent oxidative stress-induced damage (15). In another liver failure model, iPS-derived hepatocyte transplantation improved survival and protected against liver injury induced by CCL4 (7). Here, we demonstrated that iPS-derived hepatocyte transplantation in HB mice resulted in FIX clotting activity and improved hemostasis. Similar effects of transplantation have been reported for other diseases. Furthermore, the combination of iPS cell-based therapy and gene therapy has been reported for therapeutic applications in sickle cell anemia (19). It is precisely on such grounds that we believe that gene therapy combined with iPS cell-based therapy holds promise for treating HB in the future (14).

The repopulation capacity of grafted cells may limit the efficiency of cell-based therapy; however, 2–5% replacement has been shown to sufficiently improve liver function (18). To examine this aspect, we adopted a preconditioned model (23) and repeated transplantation to improve the engraftment efficiency. Our data reveal that repeated transplantation can improve hemostasis in HB mice with results similar to normal hepatocyte transplantation. Further experiments showed that the engraftment efficiency of iPS-derived hepatocyte transplantation was further improved in the preconditioned model, and the transplanted cells were engrafted in the liver parenchyma. Although the time of thrombus generation was shortened, the strength of thrombus was insufficient, partly because the differentiated cells did not fully acquire hepatic function. This problem will hinder clinical application, as undifferentiated cells can induce tumorigenicity. Currently, none of the strategies for fully separating differentiated cells from heterogeneous cell populations eliminates the risk of teratoma formation. It is need to providing a promising strategy for separating cell populations.

In this study, we acquired functional hepatocyte from iPS cells by stepwise differentiation protocol and compared iPS-derived hepatocyte and fresh isolated hepatocyte to assess therapeutic efficacy in HB mice. Although iPS-derived hepatocyte can as an alternative source of cell therapy to treat HB, still require overcome some obstacles for clinical application. It is important to eliminate the undifferentiation cells before transplantation and long-term follow up throughout their lifetimes for to assess risk of tumorigenesis.

Acknowledgements

This study was supported by a grant from the National Science Council NSC 101-2314-B-002-016 and NSC 2314-B-002-038.

Conflicts of Interest

The authors have no conflicts of interest to declare.

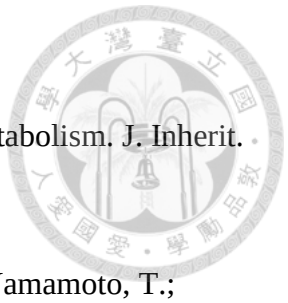

References

1. Burlina, A. B. Hepatocyte transplantation for inborn errors of metabolism. J. Inherit. Metab. Dis. 27(3):373-383; 2004.
2. Basma, H.; Soto-Gutierrez, A.; Yannam, G. R.; Liu, L.; Ito, R.; Yamamoto, T.; Ellis, E.; Carson, S. D.; Sato, S.; Chen, Y.; Muirhead, D.; Navarro-Alvarez, N.; Wong, R. J.; Roy-Chowdhury, J.; Platt, J. L.; Mercer, D. F.; Miller, J. D.; Strom, S. C.; Kobayashi, N.; Fox, I. J. Differentiation and transplantation of human embryonic stem cell-derived hepatocytes. Gastroenterology 136(3):990-999; 2009.
3. Ben-David, U.; Benvenisty, N. The tumorigenicity of human embryonic and induced pluripotent stem cells. Nat. Rev. Cancer 11(4):268-277; 2011.
4. Bigger, B. W.; Siapati, E. K.; Mistry, A.; Waddington, S. N.; Nivsarkar, M. S.; Jacobs, L.; Perrett, R.; Holder, M. V.; Ridler, C.; Kemball-Cook, G.; Ali, R. R.; Forbes, S. J.; Coutelle, C.; Wright, N.; Alison, M.; Thrasher, A. J.; Bonnet, D.; Themis, M. Permanent partial phenotypic correction and tolerance in a mouse model of hemophilia B by stem cell gene delivery of human factor IX. Gene Ther. 13(2):117-126; 2006.
5. Blum, B.; Bar-Nur, O.; Golan-Lev, T.; Benvenisty, N. The anti-apoptotic gene survivin contributes to teratoma formation by human embryonic stem cells. Nat. Biotechnol. 27(3):281-287; 2009.
6. Bolton-Maggs, P. H.; Pasi, K. J. Haemophilias A and B. Lancet 361(9371):1801-1809; 2003.

7. Chen, Y. F.; Tseng, C. Y.; Wang, H. W.; Kuo, H. C.; Yang, V. W.; Lee, O. K. Rapid generation of mature hepatocyte-like cells from human induced pluripotent stem cells by an efficient three-step protocol. Hepatology 55(4):1193-1203; 2012.

8. Choi, S. M.; Kim, Y.; Liu, H.; Chaudhari, P.; Ye, Z.; Jang, Y. Y. Liver engraftment potential of hepatic cells derived from patient-specific induced pluripotent stem cells. Cell Cycle 10(15):2423-2427; 2011.

9. de Lazaro, I.; Yilmazer, A.; Kostarelos, K. Induced pluripotent stem (iPS) cells: a new source for cell-based therapeutics? J Control Release 185:37-44; 2014.

10. Dianat, N.; Steichen, C.; Vallier, L.; Weber, A.; Dubart-Kupperschmitt, A. Human pluripotent stem cells for modelling human liver diseases and cell therapy. Curr Gene Ther 13(2):120-132; 2013.

11. Fox, I. J.; Daley, G. Q.; Goldman, S. A.; Huard, J.; Kamp, T. J.; Trucco, M. Stem cell therapy. Use of differentiated pluripotent stem cells as replacement therapy for treating disease. Science 345(6199):1247391; 2014.

12. Inoue, H.; Nagata, N.; Kurokawa, H.; Yamanaka, S. iPS cells: a game changer for future medicine. Embo j 33(5):409-417; 2014.

13. Jung, Y.; Bauer, G.; Nolta, J. A. Concise review: Induced pluripotent stem cell-derived mesenchymal stem cells: progress toward safe clinical products. Stem Cells 30(1):42-47; 2012.

14. Kaji, E. H.; Leiden, J. M. Gene and stem cell therapies. JAMA 285(5):545-550; 2001.

15. Li, H. Y.; Chien, Y.; Chen, Y. J.; Chen, S. F.; Chang, Y. L.; Chiang, C. H.; Jeng, S. Y.; Chang, C. M.; Wang, M. L.; Chen, L. K.; Hung, S. I.; Huo, T. I.; Lee, S. D.;

Chiou, S. H. Reprogramming induced pluripotent stem cells in the absence of c-Myc for differentiation into hepatocyte-like cells. Biomaterials 32(26):5994-6005; 2011.

16. Peyvandi, F.; Jayandharan, G.; Chandy, M.; Srivastava, A.; Nakaya, S. M.; Johnson, M. J.; Thompson, A. R.; Goodeve, A.; Garagiola, I.; Lavoretano, S.; Menegatti, M.; Palla, R.; Spreafico, M.; Tagliabue, L.; Asselta, R.; Duga, S.; Mannucci, P. M. Genetic diagnosis of haemophilia and other inherited bleeding disorders. Haemophilia 12 Suppl 3:82-89; 2006.

17. Robinton, D. A.; Daley, G. Q. The promise of induced pluripotent stem cells in research and therapy. Nature 481(7381):295-305; 2012.

18. Sancho-Bru, P.; Najimi, M.; Caruso, M.; Pauwelyn, K.; Cantz, T.; Forbes, S.; Roskams, T.; Ott, M.; Gehling, U.; Sokal, E.; Verfaillie, C. M.; Muraca, M. Stem and progenitor cells for liver repopulation: can we standardise the process from bench to bedside? Gut 58(4):594-603; 2009.

19. Sebastiano, V.; Maeder, M. L.; Angstman, J. F.; Haddad, B.; Khayter, C.; Yeo, D. T.; Goodwin, M. J.; Hawkins, J. S.; Ramirez, C. L.; Batista, L. F.; Artandi, S. E.; Wernig, M.; Joung, J. K. In situ genetic correction of the sickle cell anemia mutation in human induced pluripotent stem cells using engineered zinc finger nucleases. Stem Cells 29(11):1717-1726; 2011.

20. Song, Z.; Cai, J.; Liu, Y.; Zhao, D.; Yong, J.; Duo, S.; Song, X.; Guo, Y.; Zhao, Y.; Qin, H.; Yin, X.; Wu, C.; Che, J.; Lu, S.; Ding, M.; Deng, H. Efficient generation of hepatocyte-like cells from human induced pluripotent stem cells. Cell Res 19(11):1233-1242; 2009.

21. Tatsumi, K.; Ohashi, K.; Shima, M.; Nakajima, Y.; Okano, T.; Yoshioka, A. Therapeutic effects of hepatocyte transplantation on hemophilia B. Transplantation 86(1):167-170; 2008.

22. Teoh, H. K.; Cheong, S. K. Induced pluripotent stem cells in research and therapy. Malays J Pathol 34(1):1-13; 2012.

23. Wu, Y. M.; Joseph, B.; Berishvili, E.; Kumaran, V.; Gupta, S. Hepatocyte transplantation and drug-induced perturbations in liver cell compartments. Hepatology 47(1):279-287; 2008.

24. Wu, Y. M.; Kao, C. Y.; Huang, Y. J.; Yu, I. S.; Lee, H. S.; Lai, H. S.; Lee, P. H.; Lin, C. N.; Lin, S. W. Genetic modification of donor hepatocytes improves therapeutic efficacy for hemophilia B in mice. Cell Transplant. 19(9):1169-1180; 2010.

25. Xu, D.; Alipio, Z.; Fink, L. M.; Adcock, D. M.; Yang, J.; Ward, D. C.; Ma, Y. Phenotypic correction of murine hemophilia A using an iPS cell-based therapy. PNAS 106(3):808-813; 2009.

Tables

Table 1. Primer sequences

Primer	Sequence (5′→ 3′)
CK 18, Forward	CCATGGACTCCGCAAGGT
CK18, Reverse	CTTCCTTGAGTGCCTCGATTTCT
ALB, Forward	GACAAGGAAAGCTGCCTGAC
ALB, Reverse	TTCTGCAAAGTCAGCATTGG
G6P, Forward	GCCTCCGGAAGTATTGTCTCATC
G6P, Reverse	CACCCCTAGCCCTTTTAGTAGCA
TAT, Forward	CGAGCCATTGTGGACAACAT
TAT, Reverse	GGTCCCCAATTGACAGAGAGAT
AFP, Forward	CACTGCTGCAACTCTTCGTA
AFP, Reverse	CTTTGGACCCTCTTCTGTGA
Tdo2, Forward	TCCAGGGAGCACTGATGATATATTT
Tdo2, Reverse	AGCGTGTCAATGTCCATAAGTGA
HNF4, Forward	GAGGCTCCCCTGAGAATAGACA

HNF4, Reverse	TGTTTGGTGTGAAGGTCATGATTAG
Factor IX, Forward	GGAAGCAGTATGTTGATGG
Factor IX, Reverse	ACCAGAAGTCCTGTGAACCA
β-actin, Forward	ACGGCCAGGTCATCACTATTG
β-actin, Reverse	CAAGAAGGAAGGCTGGAAAAGA

Abbreviations: CK18, cytokeratin 18; ALB, albumin; G6P, glucose-6-phosphate; TAT, tyrosine aminotransferase; AFP, α-fetoprotein; Tdo2, tryptophan 2,3-dioxygenase; HNF4, hepatic nuclear factor 4α.

Table 2. Effects of transplantation on whole blood hemostasis in HB recipient mice

	B6	HB	B6 repeated	iPS repeated	Precondition
R (min)	**4.10 ± 0.84**	**43.88 ± 4.39**	**14.43 ± 4.98****	**15.45 ± 7.73****	**2.20 ± 0.67***
K (min)	**1.20 ± 0.18**	**14.13 ± 2.17**	**2.80 ± 0.52****	**4.65 ± 2.31****	**7.13 ± 1.13***
Angle (deg)	**73.83 ± 2.28**	**18.73 ± 2.95**	**58.20 ± 5.57****	**54.1 ± 10.66****	**35.80 ± 3.40*****
MA (mm)	**67.65 ± 0.63**	**65.53 ± 7.57**	**71.27 ± 5.24**	**74.38 ± 2.92**	**55.30 ± 9.10**
CI	**2.95 ± 0.67**	**−32.30 ± 4.28**	**−5.1 ± 3.46****	**−6.40 ± 6.50****	**−2.43 ± 1.31***
MRTG	**19.20 ± 2.87**	**2.08 ± 0.39**	**9.24 ± 1.99**	**10.10 ± 3.07**	**3.34 ± 0.28***
TMRTG	**5.27 ± 0.75**	**52.81 ± 4.70**	**17.42 ± 5.59****	**19.48 ± 8.63****	**4.17 ± 1.86***

B6, inbred C57BL/6 mice; HB, hemophilia B mice; R (reaction time), the time to initial fibrin formation; K, the speed to reach a specific level of clot strength; Angle, the rapidity of fibrin build-up and cross-linking; MA (maximum amplitude), the reflection of clot strength contributed by platelets and fibrin; CI (coagulation index), overall assessment of coagulability; MRTG, maximum rate of thrombus generation; TTG, total thrombus generation. Data are expressed as the mean ± SEM, $n \geq 3$. Compared with the HB group, $^{**}p < 0.01$.

Figure Legends

Figure 1. (A) Strategy for differentiating iPS cells into hepatocyte-like cells and subsequent transplantation. (B) Strategy for preconditioning. EB, embryonic body; Dex, dexamethasone.

Figure 2. Generation of hepatocytes from mouse iPS cells

Mouse iPS cells (A) were differentiated into hepatocyte-like cells for 7 (B) and 20 days (C). At day 18, the differentiated cells were expressed hepatocyte-related gene by RT-PCR (D). These cells showed functional characteristics of hepatocytes, including glycogen storage, as determined by PAS staining (E); ICG uptake (F), ALB secretion (G) and uric acid production (H) as measured by ELISA; Data are expressed as the mean ± SEM. Magnification, ×100. Scar bar 100 μm.

Figure 3. Immunostaining analysis

Expression of AFP and FIX in day 10 induced differentiated cells. ALB and CK7 were expressed in day 15 induced differentiated cells, and CK218 and CK19 were expressed in day 20 induced differentiated cells. Magnification, ×100, scar bar 100 μm (AFP, CK7 and CK18) or ×200, scar bar 50 μm (ALB, CK19 and FIX).

Figure 4. Hepatocyte transplantation in the HB mouse model

(A) FIX clotting activity was monitored sequentially at 1, 2, 3 and 4 weeks after transplantation with iPS-derived hepatocytes (iPS-Hep) or normal hepatocytes (WT-Hep). Data are expressed as the mean ± SEM. (B) The iPS-Hep cells induced greater thrombus generation. Cell localization 1 week after WT-Hep (C) and iPS-Hep (D) transplantation. (E) Preconditioning model. The arrows in (C)–(E) denote transplanted cells. (F) Quantification

of iPS-Hep engraftment in the HB mice. Red, PKH 26; blue, DAPI. Magnification, ×200, scar bar 50Mm.

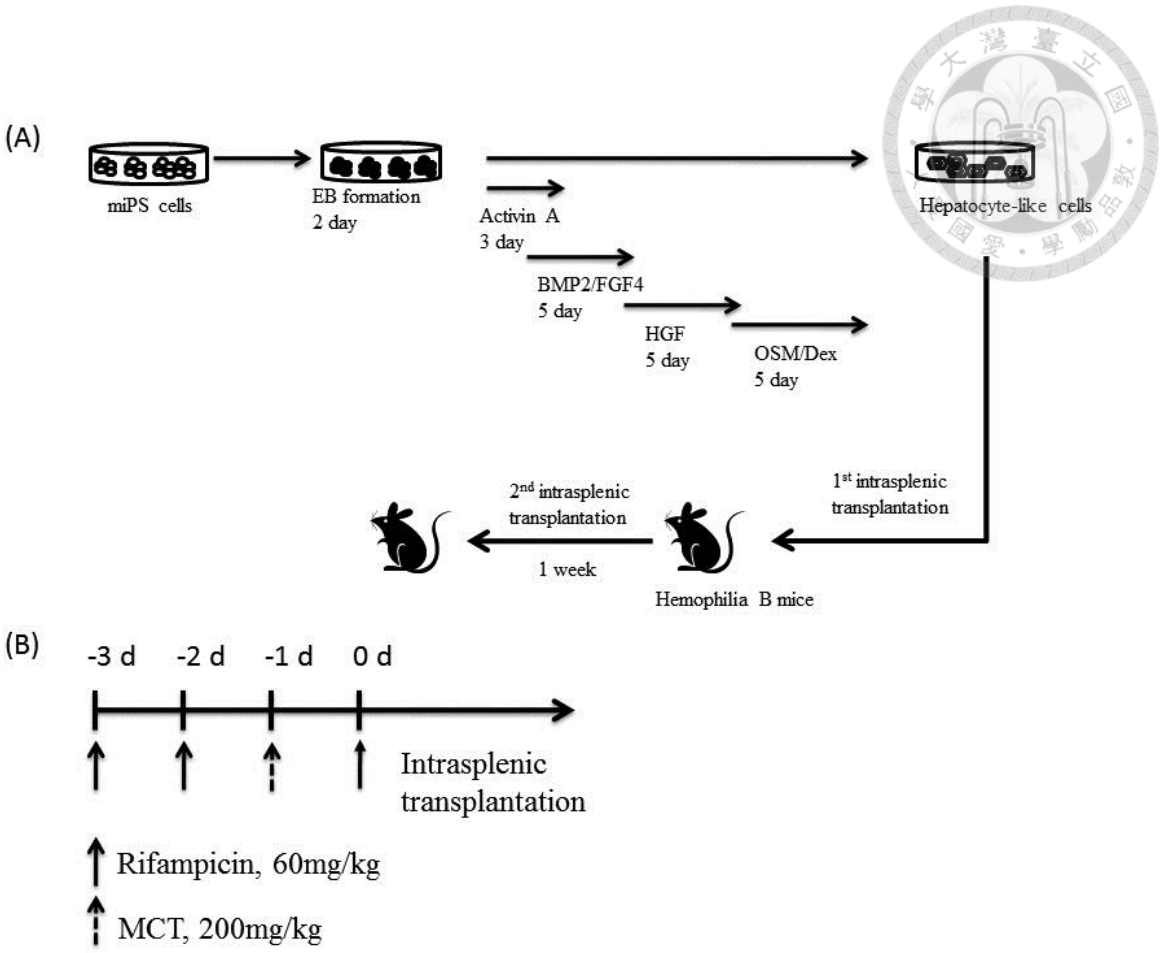
(A)
miPS cells
EB formation
2 day
Activin A
3 day
BMP2/FGF4
5 day
HGF
5 day
OSM/Dex
5 day
Hepatocyte-like cells
1st intrasplenic transplantation
2nd intrasplenic transplantation
1 week
Hemophilia B mice
(B)
-3 d
-2 d
-1 d
0 d
Intrasplenic transplantation
Rifampicin, 60mg/kg
MCT, 200mg/kg

Figure 1

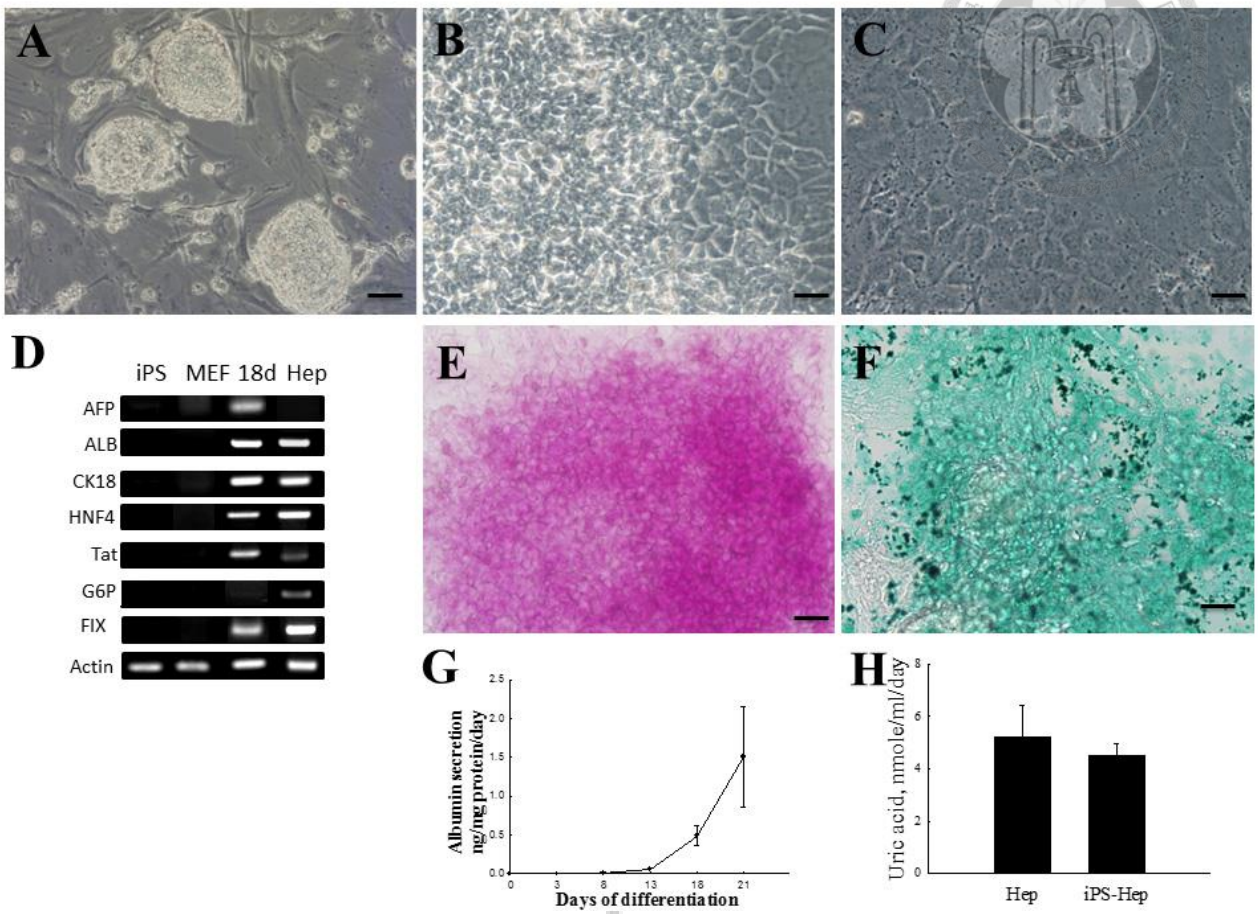
A
B
C
D
iPS MEF 18d Hep
AFP
ALB
CK18
HNF4
Tat
G6P
FIX
Actin
E
F
G
Albumin secretion ng/mg protein/day
Days of differentiation
H
Uric acid, nmole/ml/day
Hep
iPS-Hep

Figure 2

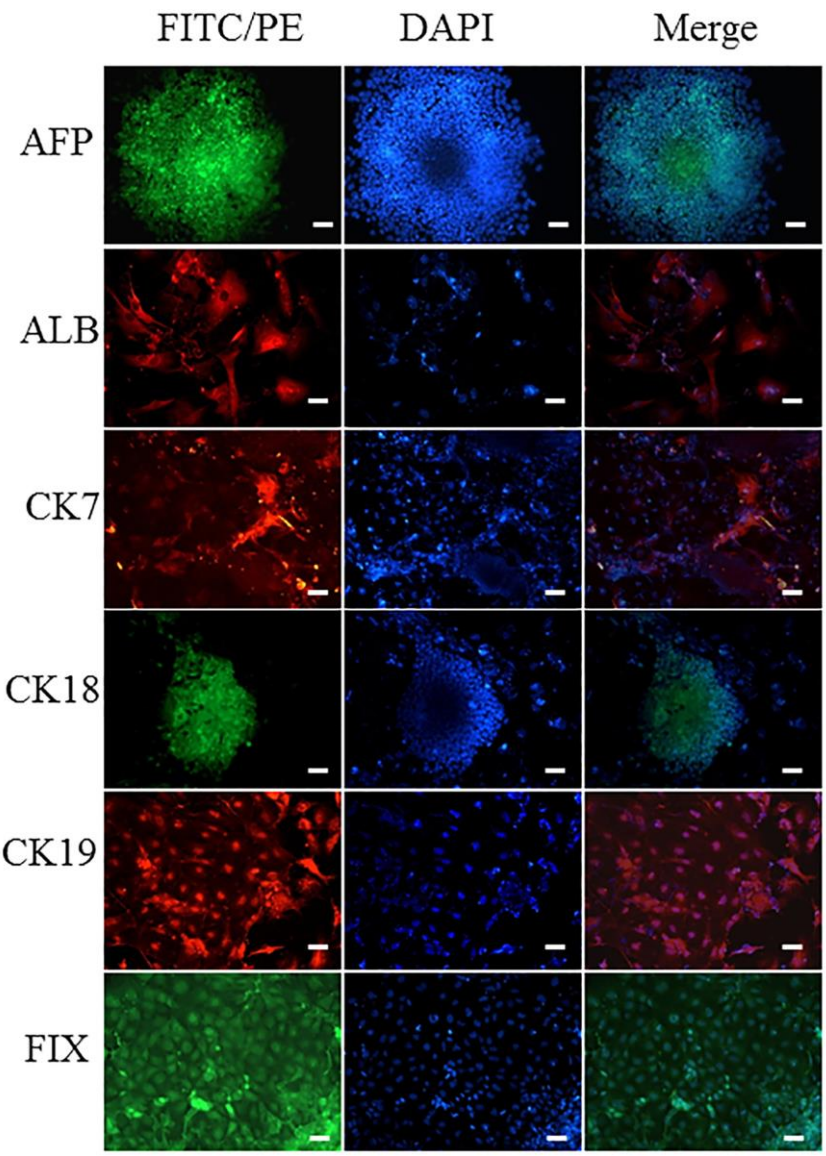

Figure 3

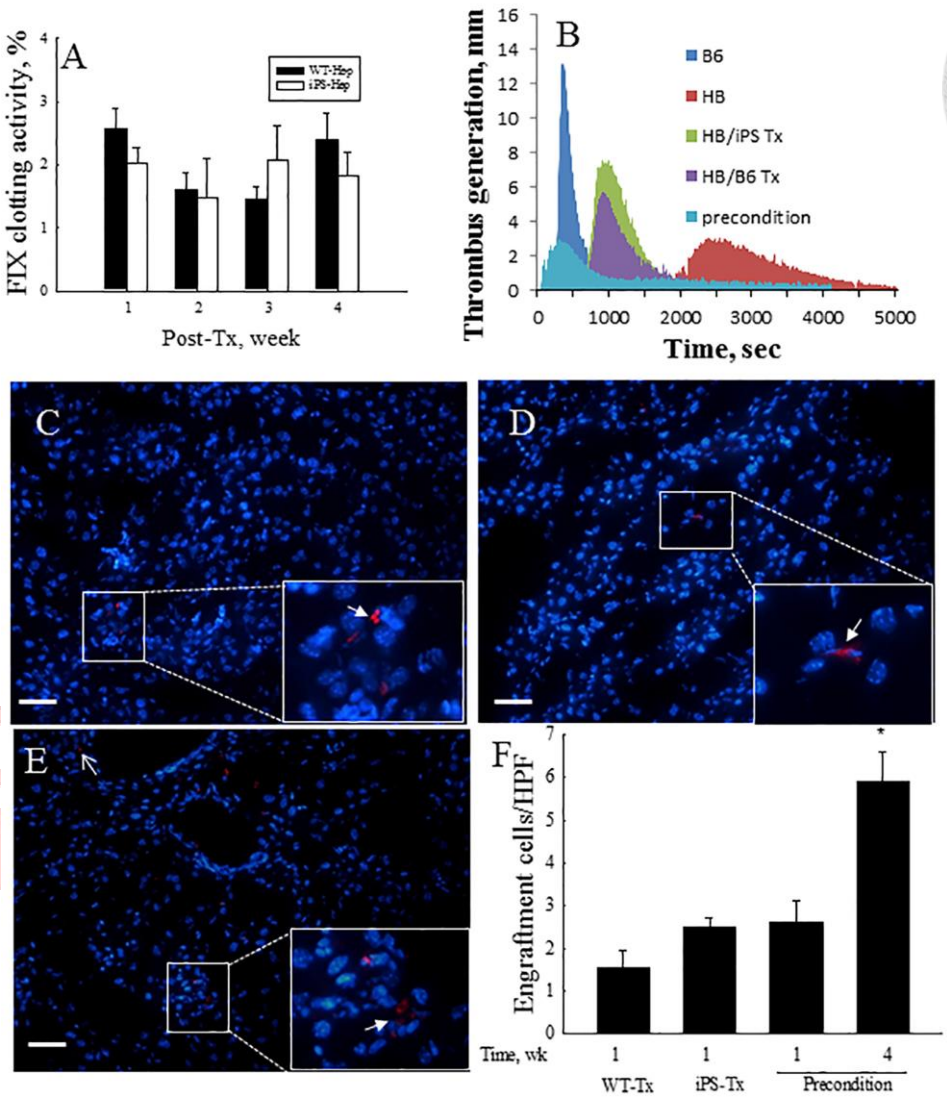
A
FIX clotting activity, %
WT-Hep
iPS-Hep
Post-Tx, week
B
Thrombus generation, nm
B6
HB
HB/iPS Tx
HB/B6 Tx
precondition
Time, sec
C
D
E
F
Engraftment cells/HPF
Time, wk
1
1
1
4
WT-Tx
iPS-Tx
Precondition

Figure 4

Huang et al. Journal of Biomedical Science (2016) 23:5
DOI 10.1186/s12929-016-0231-x

Journal of Biomedical Science

RESEARCH Open Access

Protection against acetaminophen-induced acute liver failure by omentum adipose tissue derived stem cells through the mediation of Nrf2 and cytochrome P450 expression

Yu-Jen Huang[1,2], Poda Chen[3], Chih-Yuan Lee[2], Sin-Yu Yang[2], Ming-Tsan Lin[2,4], Hsuan-Shu Lee[1,5*] and Yao-Ming Wu[2,6*]

Abstract

Background: Acetaminophen (APAP) overdose causes acute liver failure (ALF) in animals and humans via the rapid depletion of intracellular glutathione (GSH) and the generation of excess reactive oxygen species (ROS) that damage hepatocytes. Stem cell therapy is a potential treatment strategy for ALF.

Methods: We isolated mesenchymal stem cells (MSCs) from mice omentum adipose tissue-derived stem cells (ASCs) and transplanted them into a mouse model of APAP-induced ALF to explore their therapeutic potential. In addition, we performed in vitro co-culture studies with omentum-derived ASCs and primary isolated hepatocytes to demonstrate the hepatoprotective effect of omentum-derived ASCs on hepatocytes that were subjected to APAP-induced damage.

Result: ASC transplantation significantly improved the survival rate of mice with ALF and attenuated the severity of APAP-induced liver damage by suppressing cytochrome P450 activity to reduce the accumulation of toxic nitrotyrosine and the upregulation of NF-E2-related factor 2 (Nrf2) expression, resulting in an increase in the subsequent antioxidant activity. These effects protected the hepatocytes from APAP-induced damage through the suppression of downstream MAPK signal activation and inflammatory cytokine production.

Conclusions: our results demonstrate that omentum-derived ASCs are an alternative source of ASCs that regulate the antioxidant response and may represent a beneficial therapeutic strategy for ALF.

Keywords: Acetaminophen, Acute liver failure, Omentum adipose tissue-derived stem cells, Hepatoprotection

Background

Acetaminophen (APAP) is an effective analgesic and antipyretic drug, but it can cause severe liver damage. APAP overdose can result in liver failure, and it is a common cause of acute liver failure (ALF) in Western countries [1]. APAP toxicity is controlled by cytochrome P450, particularly cytochrome P450 subfamily 2E1 (CYP2E1), through the formation of N-acetyl-p-benzoquinoneimine (NAPQI), a highly reactive intermediary and toxic metabolite. This compound subsequently induces oxidative stress and covalently binds to liver proteins, causing cell death and dysfunction. At therapeutic doses, NAPQI conjugates with intracellular glutathione (GSH) and is excreted from the kidney. However, APAP overdose leads to increased NAPQI production, the rapid depletion of GSH and peroxynitrite formation [2]. Excessive NAPQI formation can trigger cell damage via an imbalance in oxidative stress involving high levels of reactive oxygen species (ROS), such as superoxide (O_2^-), hydroxyl radicals (OH·), and peroxynitrite, and it leads to low levels of antioxidant enzymes, such as superoxide dismutase

* Correspondence: benlee@ntu.edu.tw; wyaoming@gmail.com
[1]Institute of Biotechnology, College of Bioresources and Agriculture, National Taiwan University, Taipei, Taiwan
[2]Department of Surgery, National Taiwan University Hospital, Taipei, Taiwan
Full list of author information is available at the end of the article

(SOD), glutathione peroxidase (GPx), and catalase. Antioxidant defenses can scavenge the excess ROS. For example, SOD can convert O_2^- into H_2O_2 and then further convert H_2O_2 into H_2O and O_2 by GPx and catalase [3]. Consequently, GSH can prevent the covalent binding of toxic metabolites and suppress oxidative stress, which is a potential approach to attenuate APAP toxicity and promote tissue repair/regeneration.

Growing evidence shows that mesenchymal stem cell (MSC) therapy offers advantages for tissue repair and regeneration in animal and clinical studies, based on its immunomodulatory, anti-inflammatory and anti-fibrosis effects and its effects on homing [4]. Adipose tissues have recently been considered as a potential ideal source of MSCs for clinical application because of the minimally invasive procedures needed for collection, the ability to harvest large quantities and their higher potential immunomodulation and anti-inflammatory functions compared with those of other sources [5]. In addition, adipose tissue-derived stem cells (ASCs) exert protective effects and antioxidant properties, enhancing tissue repair and regeneration in animal models of kidney [6] and liver failure [7]. However, the subsequent mechanisms underlying the antioxidant effects and the potential survival benefits are not fully understood. The omentum is the primary and largest intraperitoneal reservoir of adipose tissue. This tissue can be harvested easily during abdominal surgery, and it is even available through a minimally invasive surgery approach. The omentum is therefore a potential source of ASCs; however, the therapeutic potential of omentum-derived ASCs has not yet been evaluated in a disease model. The purpose of this study is to characterize omentum-derived ASCs and to determine whether the transplantation of omentum-derived ASCs exerts therapeutic effects on mice with APAP-induced acute liver failure.

Methods

Animals

C57BL/6 mice (male, ~6–8 weeks old) were used as cell donors (hepatocytes and ASCs) and to establish an ALF mouse model for transplantation. All animals were purchased from the National Laboratory Animal Center in Taipei, Taiwan. The mice were housed and handled in accordance with the ethical guidelines for laboratory animal care of the National Taiwan University College of Medicine, and the procedures were approved by the Institutional Animal Care and Use Committee.

Cells

Mouse hepatocytes were isolated using a 2-step collagenase perfusion method as previously described [8]. ASCs were isolated from mouse omentum adipose tissue, which was cut into small pieces and digested in 0.5 units/ml of collagenase type I (Life Technologies, Paisley, UK) for one hour at 37 °C. After centrifugation at 1500 rpm for 5 min, the pellet was resuspended with PBS (Corning, NY, USA) and seeded into minimum essential medium eagle-alpha modification (α-MEM) supplemented with 1 × antibiotic (Invitrogen, NY, USA) and 10 % fetal bovine serum (FBS, SBI Biological Industries, Belt Haemak, Israel). After 24 h of incubation, the cells were washed with phosphate-buffered saline (PBS), and then the medium was replaced with fresh medium. For all experiments, the cells were used after 3–7 passages and the medium was changed every 3 days. For ASC characterization, the cells were stained with CD31-PE-CY7, CD34-FITC, CD44-PE, CD90-PE (BD Pharmingen, San Diego, CA, USA), CD105-PE (eBioscience, San Diego, CA, USA), and CD29-FITC (BioLegend, San Diego, CA, USA) and then analyzed by flow cytometry (all antibodies were diluted 1:100 with PBS containing 2 % FBS). To evaluate the cell differentiation ability, adipogenic and osteogenic assays were modified according to Sotiropoulon et al. [9]. To evaluate hepatogenic differentiation, the cells were cultured in α-MEM containing 20 ng/ml epidermal growth factor (EGF) and 10 ng/ml fibroblast growth factor (FGF; PeproTech, Rocky Hill, NJ, USA) for 2 days; the medium was then replaced with α-MEM containing 20 ng/ml hepatocyte growth factore (HGF; PeproTech) and 4.9 mM nicotinamine (Sigma-Aldrich, St Louis, MO, USA) for 1 week, followed by treatment with 20 ng/ml oncostatin M (PeproTech), 1 μmol/L dexamethasone (Sigma-Aldrich), and 50 mg/mL insulin-transferrin-selenium (ITS; Gibco, Paisley, UK) that was prepared in α-MEM for 1 week. Glycogen storage was measured by periodic acid-Schiff (PAS) staining (Sigma-Aldrich) [10].

Acute liver failure model and omentum-derived ASC treatment

Acute liver failure was induced in 8-week-old male C57BL/6 mice. APAP (Sigma-Aldrich) was prepared in saline at 70 °C and maintained in a water bath at 37 °C. Mice were fasted overnight and treated with APAP (600 mg/ kg, intraperitoneally) then randomly divided into two groups: one group was infused with PBS (100 μl/mouse), and the other group was infused with omentum-derived ASCs (10^6/100 μl/mouse) via tail vein injection at 30 min after APAP treated. For survival, the mice were monitored by 168 h (20 mice/group); At 6 and 24 h after omentum-derived ASCs with/without infusion (10 mice/group) , liver tissue and serum were collected and stored at −80 °C. The liver enzyme (glutamate-oxaloacetate transaminase, GOT; glutamic-pyruvic transaminase, GPT) were evaluated by the Laboratory Animal Center of National Taiwan University Medicine.

Immunohistology

Liver tissue was fixed in 10 % formaldehyde (Sigma-Aldrich), dehydrated, embedded in paraffin blocks, and sectioned into 5 μm slices. The sections were stained with hematoxylin and eosin (H&E; Sigma-Aldrich) for histology, and the necrosis grade was evaluated in 20 random 100 × images per animal, as described by Liu et al. [11] as follows: "0" indicated normal; "1" indicated necrotic cells in the first cell layer adjacent to the central vein; "2" indicated necrotic cells extending two to three cell layers from the central vein; "3" indicated necrotic cells extending three to six layers from the central vein; "4" indicated necrotic cells extending three to six layers and from one central vein to another; and "5" indicated necrotic cells throughout the section. The sections were deparaffinized and dehydrated for immunohistology, and the endogenous peroxide was inactivated with 3 % hydrogen peroxidase (Sigma-Aldrich). The sections were then blocked with 3 % normal goat serum (DAKO, Glostrup, Denmark) for 1 h, stained with primary antibodies against cytochrome P450 subfamily 2E1 (1:200), 4-hydroxynonenal (1:200, Abcam, Cambridge, MA, USA), or nitrotyrosine (1:50, clone 2A8.2, Millipore, Bedford, MA, USA) for 1 h at 37 °C and then incubated with an horseradish peroxidase (HRP)-detection kit (REAL^{TM} EnVision, DAKO) according to the manufacturer's protocol.

Antioxidant enzyme activity assay and GSH content measurement

The activity of the antioxidant enzymes (SOD, GPx, and catalase) and the GSH content were measured according to the manufacturer's protocol (BioVision, Palo Alto, CA, USA). In brief, the liver tissues from the APAP treatment and the omentum-derived ASC transplantation groups were lysed in PBS by sonication, and the supernatants were collected by centrifugation. For the in vitro experiments, hepatocytes (10^5) that had been treated with 15 mM APAP were grown in the lower chambers of a six-transwell plate (0.4 μm pore size; BD, Bioscience, San Jose, CA, USA), and omentum-derived ASCs (10^5) were added to the upper chambers. Twenty-four hours later, the hepatocytes were washed and lysed, and the lysate was collected by centrifugation.

Western blot

Total proteins were extracted in lysis buffer (300 mM NaCl, 50 mM HEPES pH 7.6, 1.5 mM $MgCl_2$, 10 % glycerol, 1 % Triton X-100, 10 mM $NaPyrPO_4$, 20 mM NaF, 1 mM EGTA, 0.1 mM EDTA, 1 mM DTT, 1 mM PMSF, and 1 mM Na_4VO_3) containing phosphatase inhibitors (all were purchased from Sigma-Aldrich), quantified by protein assay (Bio-Rad, Hercules, CA, USA), separated by 10 % SDS-PAGE (Bio-Rad) and transferred to PVDF membranes (Millipore). After being blocked with 5 % bovine serum albumin (Sigma-Aldrich) in TBS buffer (50 mM Tris–HCl, 150 mM NaCl pH 7.2) with 0.1 % Tween (Sigma-Aldrich) overnight, the membrane was incubated with primary antibody overnight at 4 °C (JNK, phospho-JNK, ERK, phospho-ERK, p38, and phospho-p38 were purchased from Cell Signaling Technology, Danvers, MA, USA 1:2000; cytochrome P450 subfamily 2E1 and 4-hydroxynonenal were purchased from Abcam, 1:1000; and nitrotyrosine and actin were purchased from Millipore at 1:500 and 1:3000, respectively), followed by HRP-conjugated secondary antibody (1:10000, Jackson ImmunoResearch Laboratories, West Grove, PA, USA) for 1 h at room temperature. The protein intensity was detected with electrochemiluminescence (ECL) reagent (Millipore) according to the manufacturer's protocol. The western blot band intensity was quantified with the ImageJ software according to the manufacturer's instructions.

Real-time quantitative PCR

Total RNA was extracted from liver tissue with a Direct-Xol^{TM} RNA MiniPrep kit (Zymo Research, CA, USA). Reverse transcription was performed with an iScript^{TM} cDNA Synthesis kit (Bio-Rad). Q-PCR was performed by using an iCycler real-time detection system and SYBR Green Supermix system (Bio-Rad) according to the manufacturer's protocol. The primer sequences are provided in Table 1. The relative mRNA levels were determined by Q-PCR and normalized to GAPDH.

ROS, viability and LDH assays

For the ROS assays, the primary hepatocytes were seeded in a 96-well plate (Corning) and treated with various concentrations of APAP (0, 5, 10, 15, 20, and 40 mM) for 24 h. CellROX Deep Red reagent (Life Technologies) was added 30 min before the end point and then washed out with PBS. The ROS intensities were determined by using an ELISA reader (Ex/Em: 644/655 nm, BioTek, Instruments, Inc., Winooski, VT). Cell viability was assessed by the MTT assay (Sigma-Aldrich). Cytotoxicity was determined using the LDH activity assay (BioVision) according to the manufacturer's instructions.

Statistical analysis

Values are presented as means ± SEM. Student's paired t-test or one-way ANOVA followed by Tukey's test was used for between-group comparisons of the means. The survival analysis was assessed with the SigmaStat software, version 3.5 (Chicago, IL, USA); other analyses were performed with the GraphPad InStat software, version 3 (San Diego, CA, USA). All directional P values were 2-tailed, and a value of .05 or less was considered significant for all tests.

Table 1 Primer sequences

Primer	Sequence (5′ → 3′)
HO-1, Forward	CACGCATATACCCGCTACCT
HO-1, Reverse	CCAGAGTGTTCATTCGAGCA
Nrf2, Forward	TTGGAAGGGCTAATGTCCAC
Nrf2, Reverse	CTCCAGCCTCTTGGTTTCTG
NQO1, Forward	TTCTGTGGCTTCCAGGTCTT
NQO1, Reverse	AGGCTGCTTGGAGCAAAATA
IL-1α, Forward	ACATCTTTGACGTTTCAGAGGTT
IL-1α, Reverse	ACGAAGACTACAGTTCTGCCATT
IL-1β, Forward	CCACAGCCACAATGAGTGATACT
IL-1β, Reverse	GAACTCAACTGTGAAATGCCACC
IL-6, Forward	ATTGGAAATTGGGGTAGGAAG
IL-6, Reverse	ACAAGAAAGACAAAGCCAGAGTC
IL-10, Forward	TGGGTTGCCAAGCCTTATCGG
IL-10, Reverse	ACCTGCTCCACTGCCTTGCTC
Cyp2a5, Forward	GGACAAAGAGTTCCTGTCACTGCTTC
Cyp2a5, Reverse	GTGTTCCACTTTCTTGGTTATGAAGTCC
GAPDH, Forward	TGCAGTGGCAAAGTGGAGATT
GAPDH, Reverse	TCGCTCCTGGAAGATGGTGAT

Primers used in quantitative PCR

Result

Characterization of omentum adipose tissue-derived stem cells (omentum-derived ASCs)

We acquired ASCs from mouse omentum tissue by collagenase digestion. These cells presented fibroblast-like cell morphology and expressed various stem cell markers, including CD29, CD90, CD105, and CD44. The ASCs were negative for CD31 and CD34 (Fig. 1A). We subsequently applied lineage-specific induction factors to assess the differentiation ability of mouse omentum-derived ASCs. The mouse omentum-derived ASCs differentiated into adipocytes, as demonstrated by Oil Red O staining (Fig. 1B1), and osteoblasts, as demonstrated by alizarin staining (Fig. 1B3) after two weeks of induction. Moreover, these cells also differentiated into hepatocytes, as shown by PAS staining, after induction with hepatogenic medium for 16 days (Fig. 1B2). Therefore, the cells that were derived from mouse omentum tissue expressed specific surface markers for MSCs and possessed multi-lineage differentiation ability. These results indicate that omentum is an alternative source to obtain ASCs for subsequent studies or therapy.

Omentum-derived ASCs protect against APAP-induced liver injury and improve the survival rate of mice with acute liver failure

To explore the therapeutic effects of omentum-derived ASCs on ALF, we used the ALF mouse model induced by APAP. Eight of 20 mice were died within 24–72 h after 600 mg/kg of APAP injection (60 % of survival rate), only 10 % of mice were died after omentum-derived ASC treatment (90 % of survival rate vs. control group). The overall differenece in survival rate between groups with and without omentum-derived ASC was significant ($P \leq 0.01$, Fig. 2A). The severity of APAP-induced liver damage was evaluated by measuring the plasma liver enzyme level and histological necrosis score at 6 and 24 h after APAP injection. The plasma GPT level decreased significantly at both time points after treatment with omentum-derived ASCs (5097 ± 703 IU/L compared with 2787 ± 260 IU/L at 6 h, $P < 0.01$, and 11259 ± 1159 IU/L compared with 8141 ± 910 IU/L at 24 h, $P < 0.05$) (Fig. 2B). In addition, liver histological staining showed extensive necrosis with inflammation and ballooning in the centrolobular region at 6 h after APAP exposure (Fig. 2D2) (histological necrosis score: 3.8) and extremely severe necrosis (score: 4) at 24 h after APAP administration (Fig. 2D4). The transplantation of omentum-derived ASCs decreased the area of cell necrosis (Fig. 2D3, D5) and significantly attenuated the histological necrosis score severity (2.5 at both 6 and 24 h, $P < 0.01$, Fig. 2C). These results showed that omentum-derived ASCs have therapeutic effects on APAP-induced liver toxicity.

Omentum ASC transplantation prevents GSH depletion and enhances antioxidant enzyme activity

Next, we studied whether the hepatoprotective effect of omentum-derived ASCs was associated with antioxidant activity in APAP-induced liver injury. The GSH levels dramatically declined after 6 h of APAP exposure, indicating that the high oxidative stress was induced after APAP injection. However, the depletion of the liver GSH content significantly improved 6 h after omentum-derived ASC transplantation, with higher hepatic GSH content than the content after APAP administration ($P < 0.01$) (Fig. 3a). Moreover, APAP overdose caused oxidative stress that resulted from an imbalance between oxidant generation and antioxidant defense. Transplantation with omentum-derived ASCs significantly increased hepatic antioxidant enzyme activity. SOD activity was increased by 47 %, GPx activity was enhanced by 28 %, and catalase activity increased by as much as 12 % compared with the activity levels in the APAP administered group (Fig. 3b–d). Furthermore, Nrf2 is a master regulator of the transcriptional activation of genes related to the antioxidant defense system, and it controls downstream heme oxygenase-1 (HO-1) expression. We examined Nrf2, HO-1 and NADPH quinone oxidoreductase 1 (NQO1) gene expression by Q-PCR and found that these gene expression significantly increased in the omentum-derived ASC group compared with the APAP-treated group (Fig. 3e–g). These results suggested that omentum-derived ASCs protect against

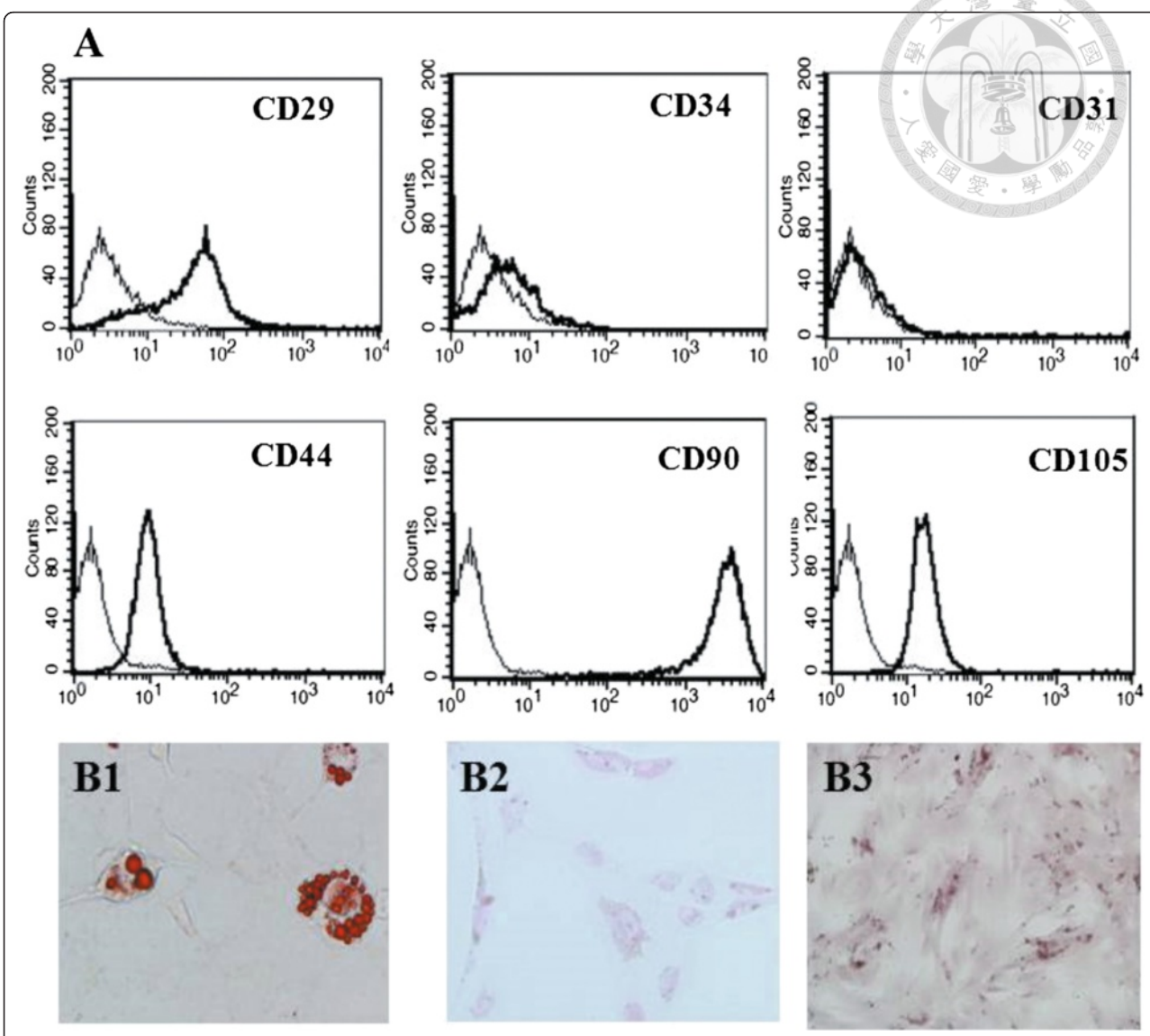

Fig. 1 Phenotype and differentiation capacity of omentum-derived ASCs. (**a**) Omentum-derived ASCs were stained with surface markers and analyzed by flow cytometry. (**b**) The cell differentiation ability was assessed in omentum-derived ASCs that were cultured under various differentiation conditions. B1: adipogenic differentiation (Oil Red O staining); B2: hepatogenic differentiation (periodic acid-Schiff staining); and B3: osteogenic differentiation (alizarin staining), 200x

APAP toxicity by enhancing antioxidant defense and reducing GSH depletion.

Omentum-derived ASCs affect the metabolism of APAP

We further studied whether the transplantation of omentum-derived ASCs affected APAP metabolism. CYP2E1 is an important cytochrome enzyme that is responsible for the toxic metabolism of APAP to NAPQI, which depletes GSH. Additionally, CYP2E1 binds to vital proteins and causes cell death. Immunohistology revealed that CYP2E1 was strongly expressed 6 h after APAP treatment but only weakly expressed in the omentum-derived-ASC-treated group (Fig. 2E). The transplantation of omentum-derived ASCs markedly reduced the expression of CYP2E1 protein 24 h after APAP treatment (Fig. 4f). Beside, other forms of cytochrome P450 expression were revealed that CYP1A2 protein was decreased significantly at 24 h (Fig. 4f) and Cyp2a5 gene level was reduced significantly at 6 h after omentum-derived ASCs transplantation (Fig. 4g). Oxidative stress induces lipid peroxidation to produce 4-HNE, and 4-HNE is considered a biomarker of lipid peroxidation. After 24 h of APAP exposure, the liver sections showed increased 4-HNE-positive cells that were localized in the centrilobular area (Fig. 2F4). Immunohistology and western blots showed that the 4-HNE expression in the omentum-derived ASC transplantation

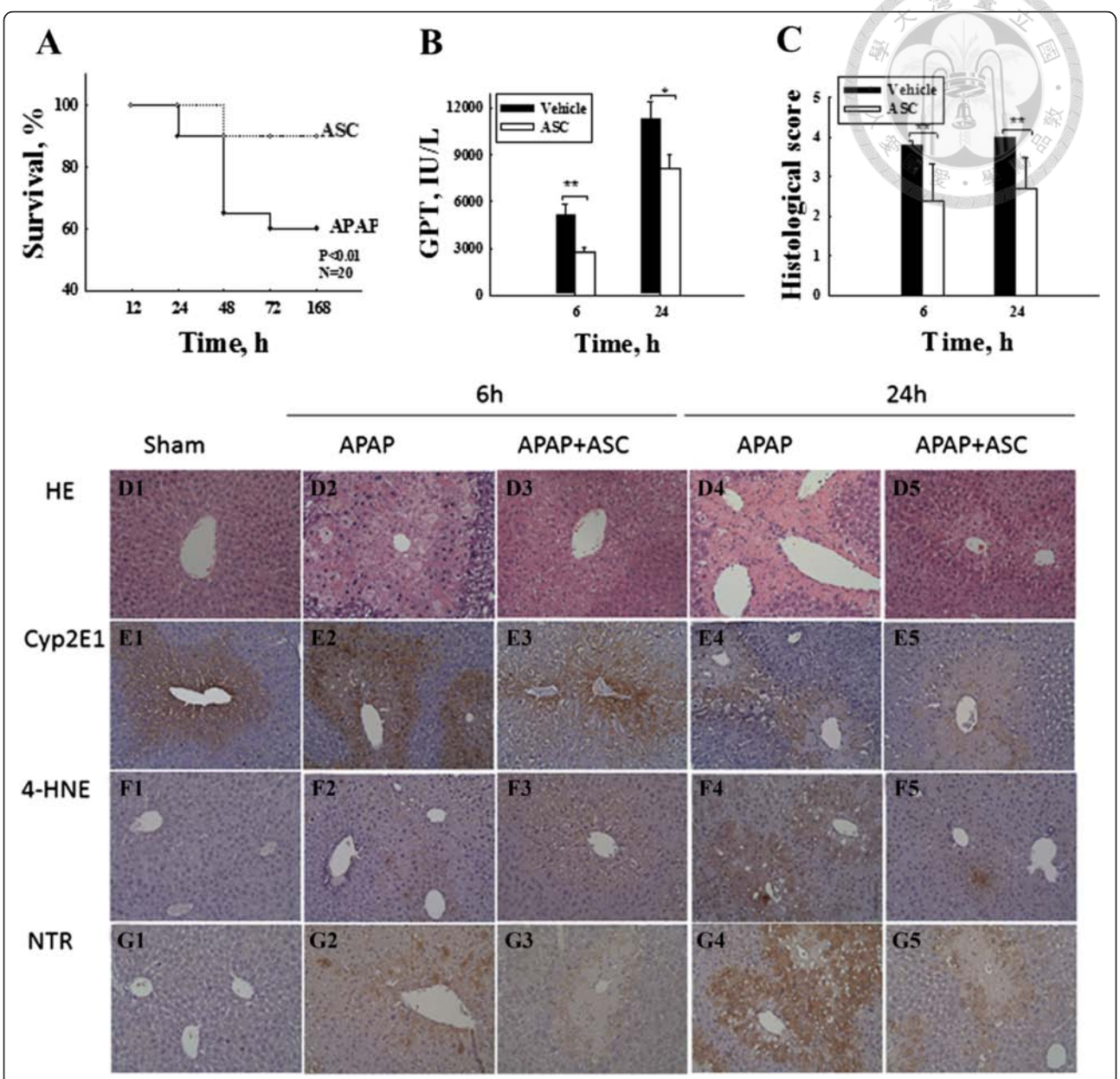

Fig. 2 Omentum-derived ASCs prevent APAP-induced hepatotoxicity. Omentum-derived ASCs were transplanted into mice with acute liver failure that had been induced by APAP (600 mg/kg, i.p.). Mouse omentum-derived ASC transplantation significantly improved the survival rate for mice with acute liver failure ($n = 20$ in each group) (**a**) and significantly decreased the liver damage caused by APAP according to both the serum liver enzyme (GPT) levels (**b**) and the tissue histological grade (**c**). The data are expressed as the means ± SEM, n ≥ 5, $^{*}P < 0.05$, $^{**}P < 0.01$. (D) H&E staining shows that APAP caused severe centrilobular necrosis (D2: 6 h after APAP; D4: 24 h after APAP). Omentum-derived ASC transplantation decreased the severity of liver damage caused by APAP (D3: 6 h after APAP + omentum-derived ASC treatment; D5: 24 h after APAP + omentum-derived ASC treatment). Immunohistological staining shows that APAP treatment induced the expression of CYP2E1 (E2-E5), 4-HNE (F2-F5), and NTR (G2-G5), which were suppressed after omentum-derived ASC transplantation. CYP2E1: cytochrome P450 2E1; 4-HNE: 4-hydroxynonenal; and NTR: nitrotyrosine. Magnification, 200x

group was lower than that of the APAP group (Figs. 2F4 and 4f). Moreover, APAP overdose caused nitrotyrosine protein formation in the centrilobular region. Protein nitration, which is a marker of oxidative stress that is caused by peroxynitrite, occurs through the rapid reaction of superoxide with nitric oxide. Nitrotyrosine protein increased strongly in the centrilobular regions 24 h after APAP injection but was only weakly expressed in the omentum-derived ASC treatment group (Figs. 2G and 4f). Therefore, the transplantation of omentum-derived ASCs suppressed cytochrome P450 activity by decreasing the production of the toxic APAP metabolite NAPQI. This response led to

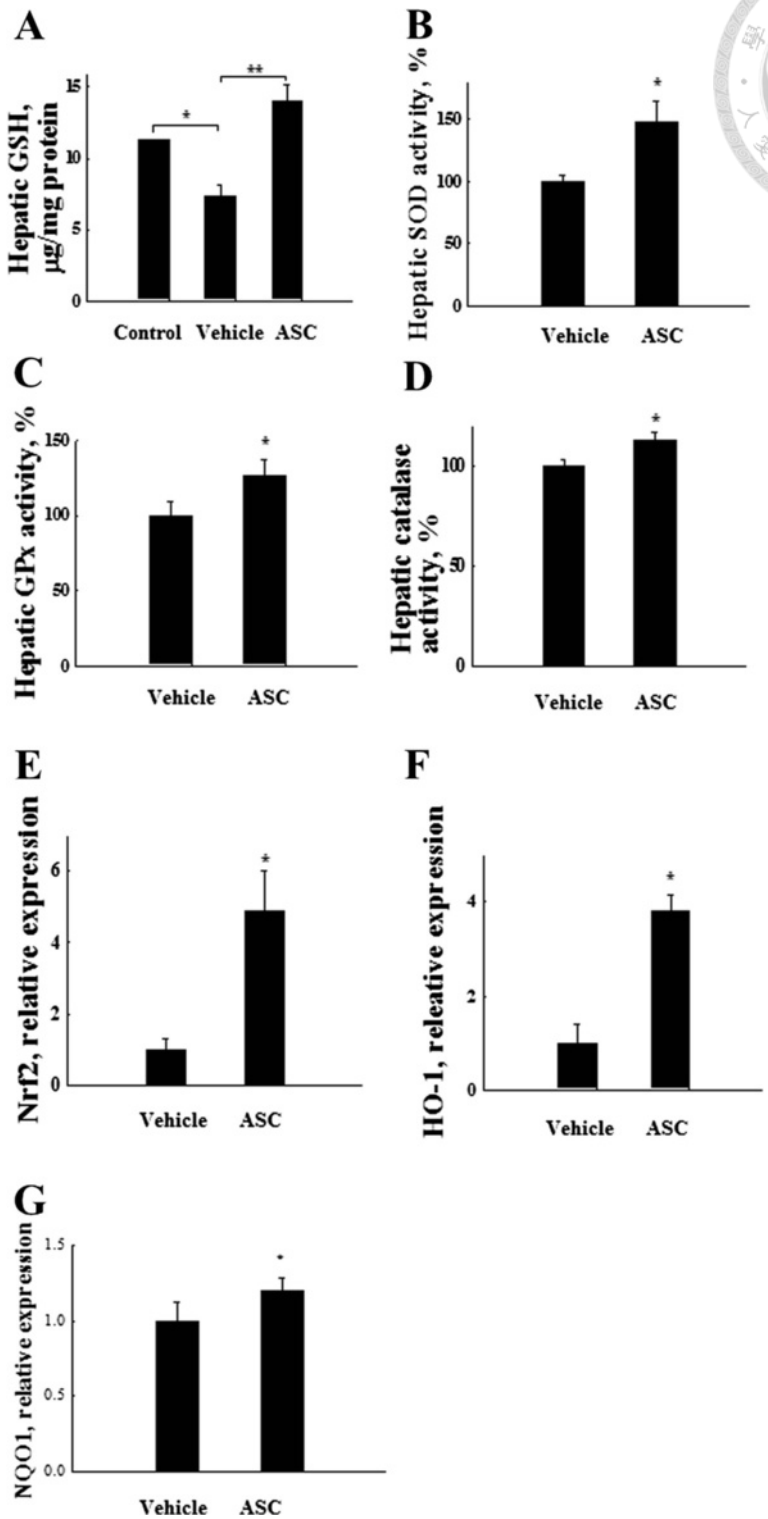

Fig. 3 Omentum-derived ASCs protect the liver against APAP-induced injury via the increased activity of antioxidant enzymes. Liver tissue samples were collected 6 h after omentum-derived ASC transplantation. The lysate was assessed for GSH content and antioxidant enzyme activity. The (**a**) GSH content and antioxidant enzyme activities of (**b**) SOD, (**c**) GPx, and (**d**) catalase increased significantly after omentum-derived ASC transplantation. The expression of (**e**) HO-1, (**f**) Nrf2 and (**g**) NQO1 are increased significantly 24 h after omentum-derived ASC transplantation. The data are expressed as the means ± SEM, n ≥ 5, $^{*}P < 0.05$, $^{**}P < 0.01$

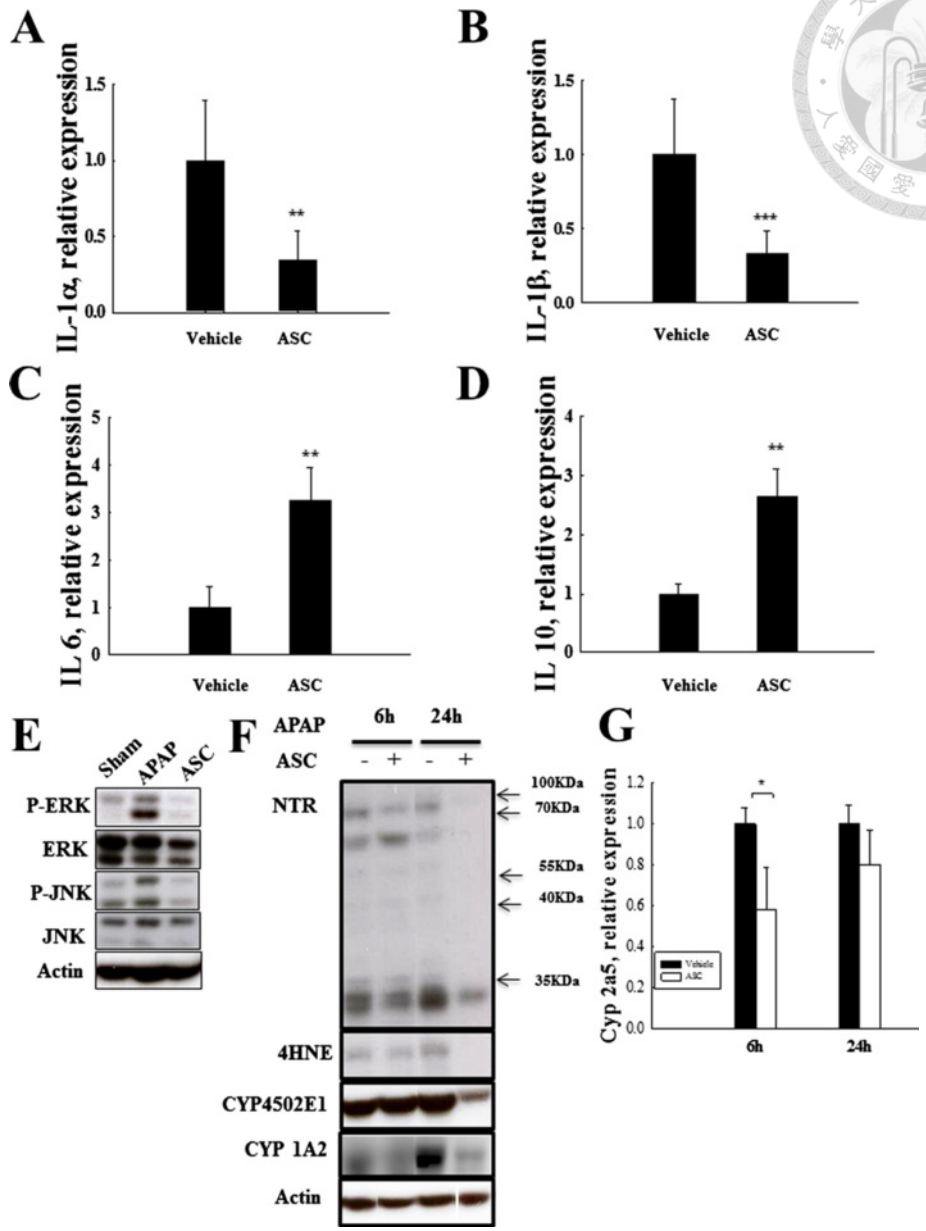

Fig. 4 Omentum-derived ASC transplantation attenuated APAP-induced inflammation, and MAPK signaling activation. Omentum-derived ASC transplantation decreased the expression of the pro-inflammatory cytokines (**a**) IL-1α and (**b**) IL-1β and increased the expression of anti-inflammatory cytokines (**c**) IL-6 and (**d**) IL-10 to a significant degree. Omentum-derived ASC transplantation suppressed the MAPK signaling pathway activation induced by APAP treatment. **e** Liver tissue was collected 6 h after omentum-derived ASC transplantation into APAP-treated mice and used for RT-PCR (**a**, **b**, **c** and **d**) and western blot (**e**) analysis. (**f**) CYP 450 2E1, CYP 450 1A2, NTR, and 4-HNE protein expression by western blot analysis. (**g**) CYP2A5 gene expression by RT-PCR. The data are expressed as the means ± SEM, n ≥ 5, $^{**}P < 0.01$, $^{***}P < 0.001$

the decreased consumption of GSH and decreased oxidative stress, protecting hepatocytes from APAP-induced cell damage.

Omentum ASCs attenuate MAPK signal activation and the inflammatory response in vivo

Accumulated toxic APAP metabolites can generate oxidative stress and subsequently activate mitogen-activated protein kinases (MAPK) signaling and inflammatory cytokine production to induce further cell damage. The gene expression of the pro-inflammatory cytokines IL-1α (Fig. 4a) and IL-1β (Fig. 4b) decreased significantly in the omentum-derived ASC group 6 h after APAP injection. The gene expression of the anti-inflammatory cytokines IL-6 (Fig. 4c) and IL-10 (Fig. 4d) increased significantly in the omentum-derived ASC group 6 h after APAP injection.

MAPK signaling pathways play critical roles in mediating APAP hepatotoxicity. The phosphorylation of the ERK and JNK proteins (pERK and pJNK) increased 6 h after APAP injection, but this response was suppressed in the omentum-derived ASC group (Fig. 4e). These results showed that the protective effect of omentum-derived ASCs against APAP toxicity also suppressed MAPK activation and attenuated the inflammatory response.

Hepatoprotective effect of omentum ASCs on APAP-induced damage in isolated hepatocytes

To clarify whether the omentum-derived ASCs directly protect against APAP toxicity in primary mouse hepatocytes, we isolated primary hepatocytes and exposed them to various APAP concentrations to measure their ROS production by CellROX assay. The ROS generation was dose dependent and increased significantly in response to 15 and 20 mM of APAP exposure (Fig. 5a). The viability of the hepatocytes decreased significantly to 70 % of the pretreatment level after treating with 10 mM APAP, and it decreased dramatically to 35 % after treating with 15 mM APAP (Fig. 5b). We chose to administer 15 mM APAP during the subsequent in vitro co-culture mechanistic studies because no differences in viability were observed in omentum-derived ASCs at this APAP concentration (data not shown). The viability of APAP-treated hepatocytes increased significantly after co-culture with omentum-derived ASCs compared with APAP exposure alone at 24 h (52 % compared with 35 % at 15 mM APAP, $P < 0.001$). The LDH release after APAP treatment was higher than that of the control hepatocytes ($P < 0.001$), but it was reduced in the omentum-derived ASC co-culture group ($P < 0.05$) (Fig. 5c). These results show that omentum-derived ASCs significantly increased the viability and markedly reduced the LDH release in hepatocytes that were treated with APAP. NAPQI is a toxic metabolite of APAP that is able to cause GSH depletion by covalently binding to hepatic GSH. The GSH content of omentum-derived ASCs co-cultured hepatocytes increased to 5.4 μg/ml (compared with 4.7 μg/ml in normal hepatocytes, $P < 0.05$). The GSH content in cultured hepatocytes decreased to 1.67 μg/ml after APAP exposure but then increased to 2.78 μg/ml in APAP-treated hepatocytes that were co-cultured with omentum-derived ASCs ($P < 0.01$) (Fig. 5d). These results show that omentum-derived ASCs increased the hepatic GSH content, which could attenuate toxic NAPQI formation. Furthermore, the activity of antioxidant enzymes in hepatocytes significantly decreased after APAP exposure for 24 h (catalase activity: 64.9 %, Fig. 5f and GPx activity: 53.9 %, Fig. 5g). The activity of antioxidant enzymes in APAP-treated hepatocytes increased significantly after co-culture with omentum-derived ASCs (SOD and catalase activity: 10 %, $P < 0.05$ and GPx activity: 20 %, $P < 0.05$). Finally, we studied whether MAPK pathways were involved in the protection of omentum-derived ASCs against APAP hepatotoxicity. The levels of JNK and ERK phosphoproteins were significantly increased in hepatocytes at 12 h and 24 h after APAP exposure but were suppressed after co-culture with omentum-derived ASCs (Fig. 5h, i). Therefore, the activation of the JNK/ERK pathway by APAP metabolites was diminished by omentum-derived ASC treatment.

Discussion

In this study, we investigated whether omentum-derived ASC therapy could rescue APAP-induced acute liver failure. We found that the transplantation of omentum-derived ASCs significantly improved the survival of mice with APAP-induced acute liver failure. Additionally, we showed that omentum-derived ASCs scavenged ROS through the upregulation of Nrf2 activation, and they decreased toxic peroxynitrite formation by suppressing cytochrome P450 expression. Finally, omentum-derived ASCs attenuated the subsequent inflammatory response and the activation of MAPK signaling to protect against APAP-induced hepatocyte death (Fig. 6). We deduce that mechanism that mediate the protectives effect of omentum-derived ASCs are immunosuppressing, which downregulation of proinflammatory cytokines (IL-1α, IL-1β) and upregulation of anti-inflammatory (IL-6, IL-10). And, paracrine properties of MSC to improve liver function and guide MSCs homes to injury site mediated by their expression of growth factors and cytokines. It is worth nothing that protective effects of MSCs are antioxidant. Based on our observation, omentum-derived ASCs are highly resistant to APAP-induced death and scavenge ROS, increase intracellular GSH levels and antioxidant enzyme activity mediated by Nrf2 expression.

APAP toxicity is mediated by cytochrome P450 metabolism to NAPQI, which causes hepatic GSH depletion, lipid peroxidation, and nitrotyrosine protein accumulation leading to cell death. It has been suggested that an effective strategy for preventing APAP hepatotoxicity is to inhibit CYP2E1 activity [12, 13]. Lee also showed that CYP2E1-knockout mice were less susceptible to APAP toxicity [14, 15]. Our immunohistology results showed that CYP2E1 expression decreased significantly in the omentum-derived-ASC-treated group. In addition, CYP1A2 and CYP2A5 have metabolic activity toward APAP. We also found both CYP1A2 and CYP2A5 were inhibited after omentum-derived ASCs transplantation. Therefore, suppression of cytochrome P450 activity contributed to the hepatoprotective effect of omentum-derived ASCs. APAP-induced hepatotoxicity consists of a metabolic phase and an oxidative phase. During the metabolic phase, the metabolite NAPQI causes GSH depletion and covalent binding to liver proteins, which triggers cell dysfunction and generates ROS

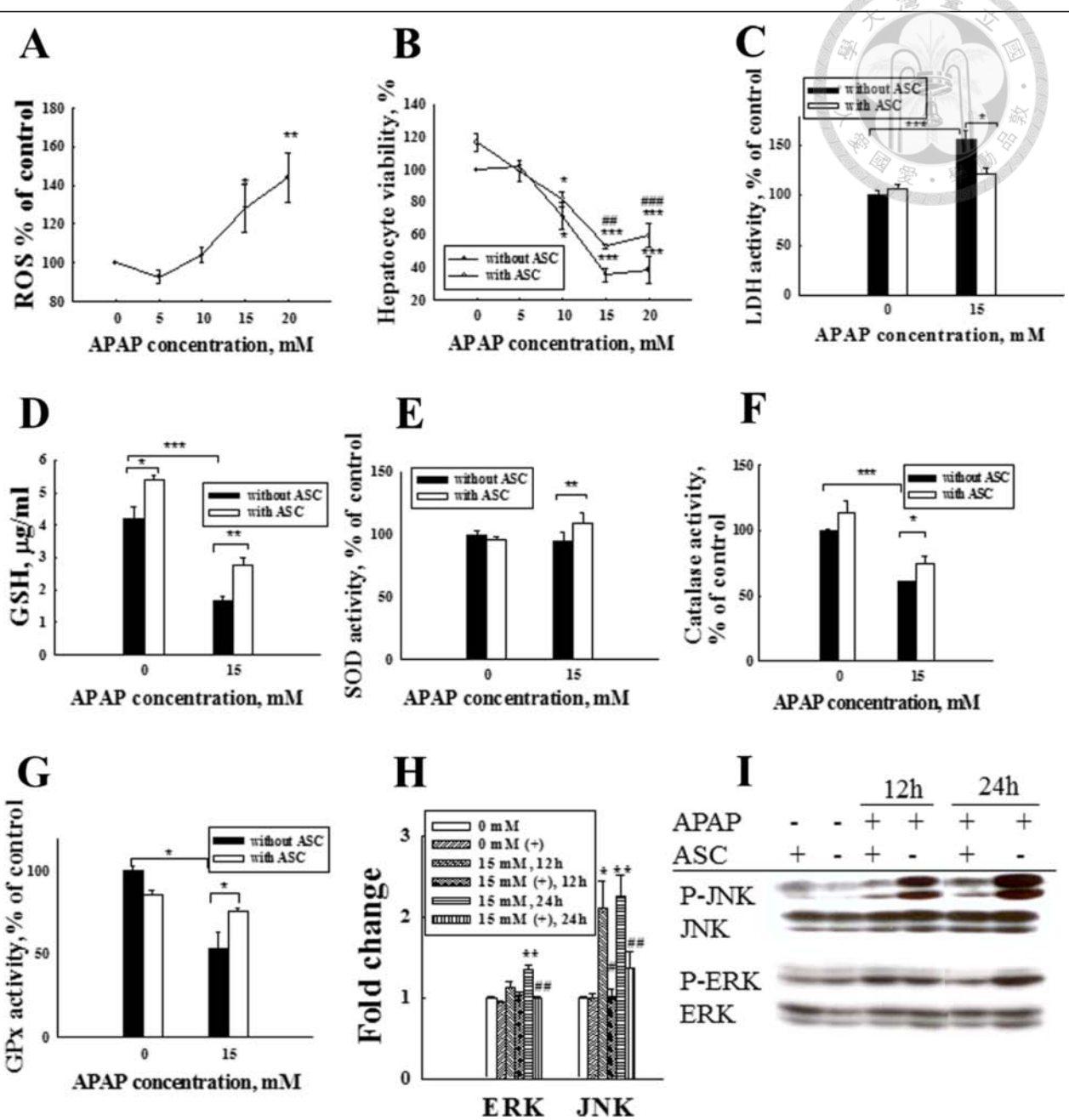

Fig. 5 Omentum-derived ASCs protect primary isolated hepatocytes from APAP-induced toxicity. **a** Primary isolated hepatocytes were exposed to various concentrations of APAP for 24 h, and the intracellular ROS levels were measured by Cell ROX assay. The intracellular ROS levels increased significantly after APAP treatments at concentrations that exceeded 15 mM (**a**). Hepatocyte viability decreased significantly after treatment with the same APAP concentration (**b**). We chose 15 mM APAP for the subsequent in vitro studies. Hepatocytes were treated with APAP and co-cultured with/without omentum-derived ASCs in a transwell co-culture system. The viability of the APAP-treated hepatocytes improved significantly after 24 h of co-culture with omentum-derived ASCs, as shown by the MTT assay (**b**). LDH that was released into the culture medium decreased significantly after co-culture with omentum-derived ASCs (**c**). The GSH content of APAP-treated hepatocytes increased significantly after 24 h of co-culture with omentum-derived ASCs (**d**). The antioxidant enzyme (SOD, catalase, and GPx) activity also increased significantly after co-culture with omentum-derived ASCs (**e**, **f**, **g**). The expression of phosphorylated MAPK signaling pathway proteins (ERK/JNK) in APAP-treated hepatocytes decreased significantly after 24 h of co-culture with omentum-derived ASCs (**h**, **i**). The quantification of the phosphorylated proteins in each lane was normalized to the total protein levels. The data are expressed as the means ± SEM, n ≥ 5, $^{*}P < 0.05$, $^{**}P < 0.01$, and $^{***}P < 0.001$

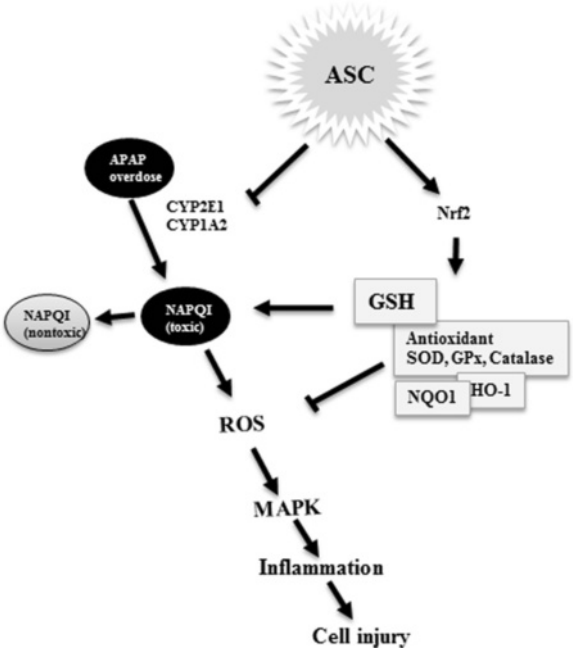

Fig. 6 Schematic of potential targets for omentum-derived ASC protection against APAP-induced hepatotoxicity. APAP overdose is metabolized by CYP2E1 and CYP1A2 to form the toxic metabolite NAPQI, which rapidly consumes intracellular GSH and causes ROS generation followed by the activation of the MAPK pathway, leading to inflammation and cell death. However, omentum-derived ASCs suppress CYP2E1 and CYP1A2 activity and activate Nrf2 expression to reduce the formation of the toxic metabolite NAPQI and subsequent ROS generation, resulting in attenuated APAP-induced toxicity. APAP: acetaminophen; ASC: adipose tissue-derived stem cells; CYP2E1: cytochrome P450 subfamily 2E1; CYP1A2: cytochrome P450 subfamily 1A2; NAPQI: N-acetyl-p-benzoquinoneimine; GSH: glutathione; ROS: reactive oxygen species; MAPK: mitogen-activated protein kinases; Nrf2: NF-E2-related factor 2; SOD: superoxide dismutase; GPx: glutathione peroxidase; NQO1: NADPH quinone oxidoreductase 1; HO-1: heme oxygenase-1

that induce lipid peroxidation and interfere with antioxidant defense mechanisms during the oxidative phase [16]. Nrf2 is a transcription factor that regulates the expression of phase II enzymes and transports protein metabolites to protect cells against oxidative stress [17]. Chan et al. [18] demonstrated that *Nrf2*$^{-/-}$ mice are more sensitive to APAP toxicity and have lower levels of liver GSH. MSCs can also act as an antioxidant to regulate the oxidative microenvironment [19–21]. In a recent study [7, 22] on MSC antioxidant ability, MSC transplantation reportedly reduced oxidative stress by supplying GSH in the liver of animals with APAP overdose. Thus, our results showing protective effects were consistent with their finding. Furthermore, key findings in the current study include that omentum-derived ASCs were essential to upregulating Nrf2 and that they inhibited cytochrome P450 expression to protect cells against APAP toxicity. It is possible that MSCs express CD44 markers, which reportedly activate the Nrf2 pathway to protect against APAP toxicity [16, 23, 24]. We successfully isolated ASCs from the omentum and demonstrated their MSC properties, and the results revealed that the omentum-derived ASCs significantly increased Nrf2 expression to activate antioxidant enzyme activity (SOD, GPx, and catalase) and cellular GSH synthesis. Omentum-derived ASCs were able to scavenge excess ROS by activating the Nrf2 pathway, leading to increased GSH synthesis and enhanced antioxidant defense. N-acetylcysteine (NAC) protects against APAP hepatotoxicity by increasing the intracellular GSH content that is available to conjugate to NAPQI in animal experiments [25], indicating a role for these cells as a potential therapy for APAP-induced acute liver failure in clinical practice [26]. However, the limitations of NAC therapy include a short therapeutic time window, adverse gastrointestinal effects and an anaphylactoid reaction [1]. Consequently, the antioxidative effect of omentum-derived ASCs offers another therapeutic approach to protect against APAP hepatotoxicity in clinical practice.

The toxic metabolites of APAP damage hepatocytes and cause the release of inflammatory mediators, particularly IL-1α and IL-1β [27], which induce further cell damage. MSCs also exhibit immunomodulatory properties [28, 29]. Our results show that omentum-derived ASCs significantly suppressed the release of pro-inflammatory cytokines (IL-1α and IL-1β) and increased the release of anti-inflammatory cytokines (IL-6 and IL-10). The immunomodulation effect of omentum-derived ASCs also contributed to the efficiency of protection against APAP-induced hepatotoxicity. These inflammatory mediators are regulated by MAPK signal transduction, which plays a central role in cell survival, proliferation, apoptosis, and inflammation [30]. One potential anti-inflammatory therapeutic strategy is to suppress the activation of the MAPK to reduce pro-inflammatory cytokine release and promote anti-inflammatory cytokine production [7, 31]. Our results showed that omentum-derived ASCs also have an immunomodulatory effect by regulating the MAPK pathway.

Conclusions

In conclusion, our results show that ASCs can be obtained from omentum adipose tissue, and they possess antioxidant and anti-inflammatory properties that provide protection against APAP-induced hepatotoxicity. Thus, omentum-derived ASCs have potential as an alternative source for cell therapy, and may be is an effective therapeutic strategy for APAP-induced liver failure in clinical practice.

Abbreviations

APAP: acetaminophen; GSH: glutathione; ROS: reactive oxygen species; ASC: adipose tissue-derived stem cell; ALF: acute liver failure; SOD: superoxide dismutase; GPx: glutathione peroxidase;

CYP2E1: cytochrome P450 subfamily 2E1; CYP1A2: cytochrome P450 subfamily 1A2; CYP2A5: cytochrome P450 subfamly 2A5; Nrf2: NF-E2 related factor 2; NQO1: NADPH quinone oxidoreductase; HO-1: heme oxygenase-1; MAPK: mitogen-activated protein kinase; NAPQI: N-acetyl-p-benzoquinoneimine; $O_2^{\cdot-}$: superoxide; OH·: hydroxyl radicals; MSC: mesenchymal stem cell; NAC: N-acetyl cysteine.

Competing interests
The authors declare that they have no competing interest.

Authors' contributions
YJH participated in performing the research and writing the article. PC participated in data collection. CYL participated in data analysis and interpretation. SYY participated in data collection and statistical analysis. MTL contributed funding. HSL contributed administrative, technical and logistical support. YMW participated in the research concept and design, critical revision of the article and the final approval of the article. All authors read and approved the final manuscript.

Acknowledgments
This study was supported by a grant from the National Science Council NSC 101-3114-B-002-003.

Author details
[1]Institute of Biotechnology, College of Bioresources and Agriculture, National Taiwan University, Taipei, Taiwan. [2]Department of Surgery, National Taiwan University Hospital, Taipei, Taiwan. [3]Department of Surgery, National Taiwan University Hospital Yun-Lin Branch, Yunlin, Taiwan. [4]Department of Medicine Education & Bioethics Graduate Institute of Medical Education, Bioethics National Taiwan University College of Medicine, Taipei, Taiwan. [5]Department of Internal Medicine, National Taiwan University Hospital and National Taiwan University College of Medicine, Taipei, Taiwan. [6]Department of Surgery, National Taiwan University College of Medicine, Taipei, Taiwan.

Received: 6 July 2015 Accepted: 12 January 2016

References
1. Larsen A. Acetominophen hepatoxicity. Clin Liver Dis. 2007;11:525–48.
2. James LP, Mayeux PR, Hinson JA. Acetaminophen-induced hepatotoxicity. Drug Metab Dispos. 2003;31:1499–506.
3. Jorge LP, Gonsebatt ME. The role of antioxidants and antioxidant-related enzymes in protective responses to environmentally induced oxidative stress. Mutat Res. 2009;674:137–47.
4. Caplan AI, Bruder SP. Mesenchymal stem cells: building blocks for molecular medicine in the 21st century. Trends Mol Med. 2001;7:259–64.
5. Banas A, Teratani T, Yamamoto Y, Tokuhara M, Takeshita F, Osaki M, et al. IFATS collection: in vivo therapeutic potential of human adipose tissue mesenchymal stem cells after transplantation into mice with liver injury. Stem Cells. 2008;26:2705–12.
6. Chen YT, Sun CK, Lin YC, Chang LT, Chen YL, Tsai TH, et al. Adipose-derived mesenchymal stem cell protects kidneys against ischemia-reperfusion injury through suppressing oxidative stress and inflammatory reaction. J Transl Med. 2011;9:51.
7. Salomone F, Barbagallo I, Puzzo L, Piazza C, Li VG. Efficacy of adipose tissue-mesenchymal stem cell transplantation in rats with acetaminophen liver injury. Stem Cell Res. 2013;11:1037–44.
8. Wu YM, Joseph B, Gupta S. Immunosuppression using the mTOR inhibition mechanism affects replacement of rat liver with transplanted cells. Hepatology. 2006;44:410–9.
9. Sotiropoulou P, Perez SA, Salagianni M, Baxevanis CV, Papamichail M. Characterization of the optimal culture conditions for clinical scale production of human mesenchymal stem cells. Stem Cells. 2006;24:462–71.
10. Lee KD, Kuo TK, Whang-Peng J. In vitro hepatic differentiation of human mesenchymal stem cells. Hepatology. 2004;40:1275–84.
11. Liu ZX, Han D, Gunawan B, Kaplowitz N. Neutrophil depletion protects against murine acetaminophen hepatotoxicity. Hepatology. 2006;43:1220–30.
12. McGill MR, Jaeschke H. Metabolism and disposition of acetaminophen: recent advances in relation to hepatotoxicity and diagnosis. Pharm Res. 2013;30:2174–87.
13. Kay HY, Kim YW, Ryu H, Sung SH, Hwang SJ, Kim SG. Nrf2-mediated liver protection by sauchinone, an antioxidant lignan, from acetaminophen toxicity through the PKCδ-GSK3β pathway. Br J Pharmacol. 2011;163:1653–65.
14. Lee SS, Buters JT, Pineau T, Fernandez-Salguero P, Gonzalez FJ. Role of CYP2E1 in the hepatotoxicity of acetaminophen. J Biol Chem. 1996;271:12063–7.
15. Abdelmegeed MA, Moon KH, Chen C, Gonzalez FJ, Song BJ. Role of cytochrome P450 2E1 in protein nitration and ubiquitin-mediated degradation during acetaminophen toxicity. Biochem Pharmacol. 2010;79:57–66.
16. Reid AB, Kurten RC, McCullough SS, Brock RW, Hinson JA. Mechanisms of acetaminophen-induced hepatotoxicity: role of oxidative stress and mitochondrial permeability transition in freshly isolated mouse hepatocytes. J Pharmacol Exp Ther. 2005;312:509–16.
17. Gum SI, Cho MK. Recent updates on acetaminophen hepatotoxicity: the role of nrf2 in hepatoprotection. Toxicol Res. 2013;29:165–72.
18. Chan K, Han XD, Kan YW. An important function of Nrf2 in combating oxidative stress: detoxification of acetaminophen. Proc Natl Acad Sci U S A. 2001;98:4611–6.
19. Song H, Cha MJ, Song BW. Reactive oxygen species inhibit adhesion of mesenchymal stem cells implanted into ischemic myocardium via interference of focal adhesion complex. Stem Cells. 2010;28:555–63.
20. Kuo TK, Hung SP, Chuang CH. Stem cell therapy for liver disease: parameters governing the success of using bone marrow mesenchymal stem cells. Gastroenterology. 2008;134:2111–21.
21. Cho KA, Woo SY, Seoh JY, Han HS, Ryu KH. Mesenchymal stem cells restore CCl4-induced liver injury by an antioxidative process. Cell Biol Int. 2012;36:1267–74.
22. Liu Z, Meng F, Li C, Zhou X, He Y, Mrsny RJ, et al. Human umbilical cord mesenchymal stromal cells rescue mice from acetaminophen-induced acute liver failure. Cytotherapy. 2014;16:1207–19.
23. Kim HJ, Nel AE. The role of phase II antioxidant enzymes in protecting memory T cells from spontaneous apoptosis in young and old mice. J Immunol. 2005;175:2948–59.
24. Harrill AH, Watkins PB, Su S, Ross PK, Harbourt DE, Stylianou IM, et al. Mouse population-guided resequencing reveals that variants in CD44 contribute to acetaminophen-induced liver injury in humans. Genome Res. 2009;19:1507–15.
25. Yang R, Miki K, He X, Killeen ME, Fink MP. Prolonged treatment with N-acetylcystine delays liver recovery from acetaminophen hepatotoxicity. Crit Care. 2009;13:R55.
26. Heard KJ. Acetylcysteine for acetaminophen poisoning. N Engl J Med. 2008;359:285–92.
27. Nakagawa H, Maeda S, Hikiba Y. Deletion of apoptosis signal-regulating kinase 1 attenuates acetaminophen-induced liver injury by inhibiting c-Jun N-terminal kinase activation. Gastroenterology. 2008;135:1311–21.
28. Yagi H, Soto-Gutierrez A, Parekkadan B, Kitagawa Y, Tompkins RG, Kobayashi N, et al. Mesenchymal stem cells: mechanisms of immunomodulation and homing. Cell Transplant. 2010;19:667–79.
29. Sart S, Ma T, Li Y. Preconditioning stem cells for in vivo delivery. Biores Open Access. 2014;3:137–49.
30. Nakagawa H, Maeda S. Molecular mechanisms of liver injury and hepatocarcinogenesis: focusing on the role of stress-activated MAPK. Patholog Res Int. 2012;2012:172894.
31. Ayroldi E, Cannarile L, Migliorati G, Nocentini G, Delfino DV, Riccardi C. Mechanisms of the anti-inflammatory effects of glucocorticoids: genomic and nongenomic interference with MAPK signaling pathways. FASEB J. 2012;26:4805–20.